SERIAL NO. SSC-57

Second

PROGRESS REPORT

(Project SR-118)

on

CRACKING OF SIMPLE STRUCTURAL GEOMETRIES:

Investigation of Welded Ship Details

by

S. T. Carpenter and R. F. Linsenmeyer
SWARTHMORE COLLEGE

Under Bureau of Ships Contract NObs-50250
(BuShips Project NS-731-034)

for

SHIP STRUCTURE COMMITTEE

Convened by
The Secretary of the Treasury

Member Agencies—Ship Structure Committee

Bureau of Ships, Dept. of Navy
Military Sea Transportation Service, Dept. of Navy
United States Coast Guard, Treasury Dept.
Maritime Administration, Dept. of Commerce
American Bureau of Shipping

Address Correspondence To:

Secretary
Ship Structure Committee
U. S. Coast Guard Headquarters
Washington 25, D. C.

JUNE 15, 1953

SERIAL NO. SSC-57
BuShips Project NS-731-034

SHIP STRUCTURE COMMITTEE

MEMBER AGENCIES:

BUREAU OF SHIPS, DEPT. OF NAVY

MILITARY SEA TRANSPORTATION SERVICE. DEPT. OF NAVY

UNITED STATES COAST GUARD, TREASURY DEPT.

MARITIME ADMINISTRATION. DEPT. OF COMMERCE

AMERICAN BUREAU OF SHIPPING

1 June 1953

Dear Sir:

    As part of its research program related to the improvement of hull structures of ships, the Ship Structure Committee is sponsoring an investigation on the "Cracking of Simple Structural Geometries" at Swarthmore College. Herewith is a copy of the Second Progress Report, SSC-57, of the investigation entitled "Cracking of Simple Structural Geometries; Investigation of Welded Ship Details" by S. T. Carpenter and R. F. Linsenmeyer.

    Any questions, comments, criticism or other matters pertaining to the Report should be addressed to the Secretary, Ship Structure Committee.

    This Report is being distributed to those individuals and agencies associated with and interested in the work of the Ship Structure Committee.

Yours sincerely,

K. K. COWART
Rear Admiral, U. S. Coast Guard
Chairman, Ship Structure
      Committee

Second

PROGRESS REPORT
(Project SR-118)

on

CRACKING OF SIMPLE STRUCTURAL GEOMETRIES:

Investigation of Welded Ship Details

by

S. T. Carpenter and R. F. Linsenmeyer

under

Department of the Navy
Bureau of Ships
Contract NObs-50250

with

Swarthmore College

Bureau of Ships Project NS-731-034

for

SHIP STRUCTURE COMMITTEE

TABLE OF CONTENTS

ABSTRACT

This progress report presents the results of an investigation of the effect of geometry on strength and transition temperature of certain structural details found in welded ships. The detail geometries investigated were those which are currently used in ship structural design, or certain proposed modifications to existing design. These include the structural geometries found at the ends of welded, free ended stiffeners and longitudinals, and the transition details between the sheer strake and fashion plate. The specimens were of 3/4-inch thick project steel D_N or ABS class B steel.

For the tests in which free end stiffeners and longitudinals were involved, variations in the contour of the free end were investigated. It was found that cutting the end of a stiffener or a longitudinal to a radius was definitely beneficial. The chief benefits were in the lowering of transition temperature when the ends of these structural members were cut back from a square ended condition. Strength was not affected to any critical extent by varying the end geometry. The results emphasize the importance of avoiding abrupt structural transitions from one component to another. As smooth a transition as may be practicable gives the best results.

LIST OF FIGURES

LIST OF FIGURES (Continued)

LIST OF TABLES

iv

CRACKING OF SIMPLE STRUCTURAL GEOMETRIES
INVESTIGATION OF WELDED SHIP DETAILS

INTRODUCTION

A report[1] of fractures in welded ships indicated that over
half of the fracture origins were in the immediate vicinity of
welded structural discontinuities. Classifications of these
welded discontinuities have included abrupt termination of stif-
feners, longitudinals, bilge keels, and the geometry at the junc-
tion of fashion plate and the sheer strake. Fractures have been
initiated by notch effects attributed to structural geometry,
welding defects, or a combination of the two.

The purpose of the program outlined in this report has been
to evaluate the efficacy of certain welded structural details as
to tensile strength, energy absorption, and transition tempera-
ture. The welded specimens were intended to simulate existing
ship details or possible modifications of present practice.

The fabricated specimens simulate certain types of welded
details. Specimens of Type YW, Fig. 1, were intended to repre-
sent details similar to the transition details often found at
the faired termination of the fashion plate at the sheer strake.
Specimens of Type Z, Fig. 4, represent details similar to those
found at the free ends of welded components, such as stiffeners,
interrupted longitudinals, and bilge keel endings.

NOTE:

ALL EDGES FLAME-
CUT

WELDS MADE USING
E-6010 ROD

4'-0"

15"

10½"

13½"

¾"

MAIN AND
SIDE PLATES BEVELED

TYPE YW-1

⅜" FILLET WELD
(4 PLACES)

¾"

SIDE PLATES
BEVELED

TYPE YW-2.

SIDE PLATES
BEVELED

TYPE YW-3
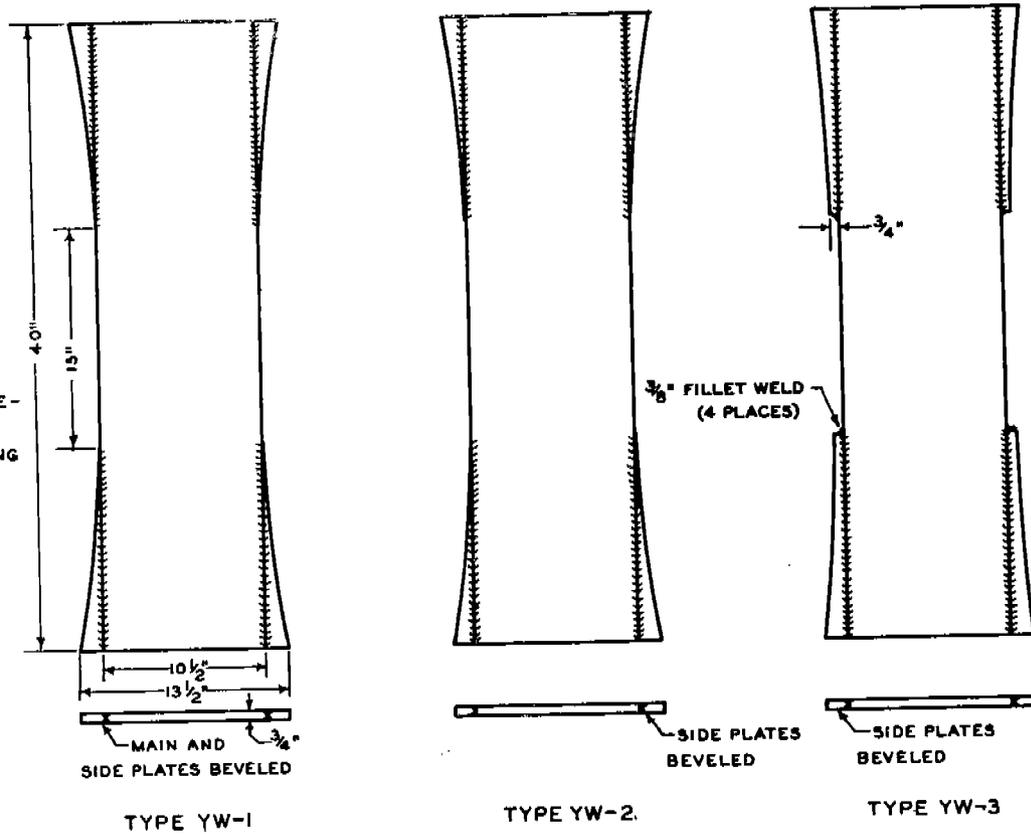
FIG. I   SPECIMENS WITH LONGITUDINAL WELDMENT

SWARTHMORE COLLEGE

3/16   4" X ½" SPLICE PLATE   (4 PLACES)

¾"

5½"

5"

5½"

12"

45°

5/16" FILLET WELD

BUTT WELD

40"

20"

20"

SECTION A-A

14"

1½"

1⅛"

80°

A

A

4½" D.

5/16" FILLET WELD

8"

3"

16"

12"

20"

11"
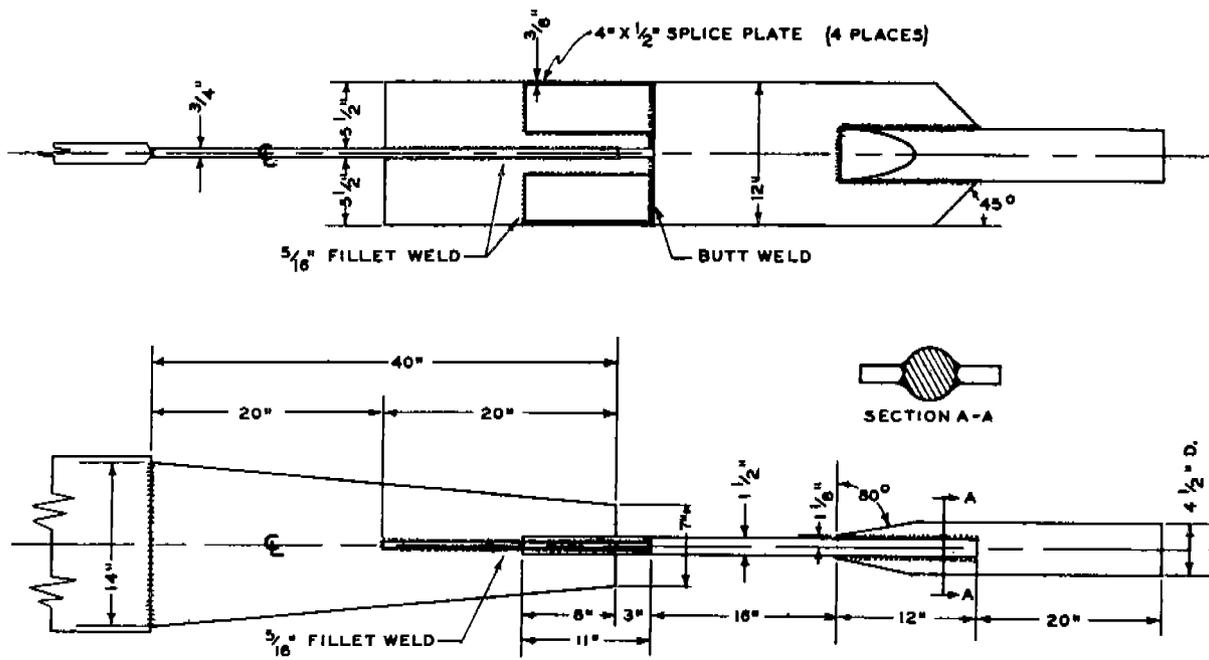
FIG. 2

TYPE DN-Z3

SPECIMEN ARRANGEMENT

SCALE: 3/32" = 1"

SWARTHMORE COLLEGE
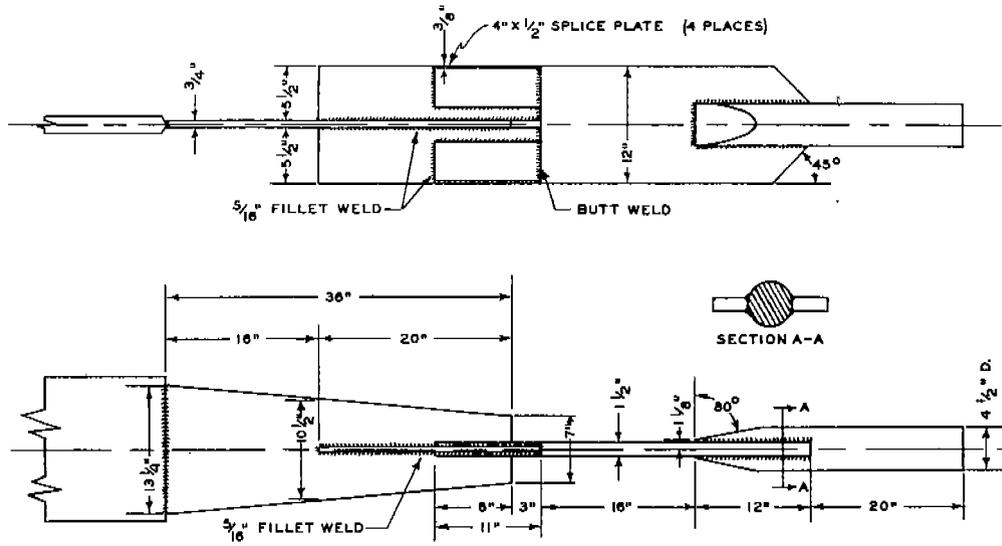
FIG. 3

TYPE ABS-B-Z3

SPECIMEN ARRANGEMENT

NOTE:

ALL EDGES FLAME-CUT

WELDS MADE USING E-6010 ROD

SCALE: $\frac{3}{32}$" = 1"

SWARTHMORE COLLEGE

TYPE ZB

TYPE ZBM

TYPE ZCI
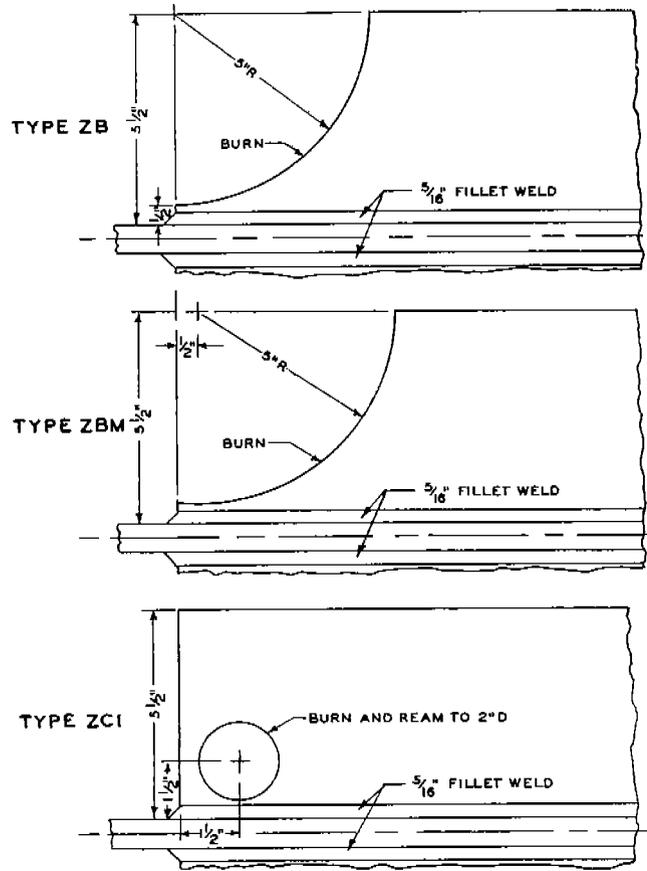
NOTE: ALL EDGES FLAME-CUT . . WELDS MADE USING E-6010 ROD

FIG. 4   END DETAIL VARIATIONS FOR TYPE
"Z" SPECIMENS

SWARTHMORE COLLEGE

The specimens were prepared by flame cutting and connected by welding. Both the flame cutting and welding techniques utilized in specimen fabrication represent the quality of workmanship to be expected in average shipyard practice. Machine guided flame cutting was employed on all straight cuts while radius cuts were hand guided. All welds were made manually using E6010 electrodes.

GENERAL PROGRAM

The specimens, while intended to simulate ship details, were of necessity simplified to a symmetrical form convenient for tensile testing. This procedure has probably tended to oversimplify the general conditions found on ships but the specimens are thought to duplicate the critical conditions representing structural and welding notch effects.

The fabricated specimens are of two general types described below:

Type YW:

The particular objective of the Type YW series was to investigate the effects on fracture of welding and plate fairing at the termination of a fashion plate where it fairs into the sheer strake. The Type YW specimens were tested with three variations as shown in Fig. 1. The side plates were assumed to simulate the fashion plates and the main plate assumed to simulate the sheer strake.

Type YW-1, with both the side and main plates beveled in preparation for welding, represents the original specimen design. Type YW-2, where only the side plates were beveled, was a modification of Type YW-1 and may be more representative of standard practice. For both types the welds were made using run-off plates. The side plates were faired by flame cutting after welding with the cuts intersecting the butt welds. Thus, the plate and weld metal at the faired terminations had heat effects of both welding and flame cutting, as well as the surface roughness associated with cutting.

Type YW-3 had the side plates beveled, but instead of fairing the side plates into the main plate, a square 3/4-in. end offset of side plates from the main plate was established. A 3/8-in. fillet weld was made across this offset. This specimen was designed to compare the effects of an abrupt transition of the side and main plates with the faired transitions of Types YW-1 and YW-2.

All specimens of the Type YW series were fabricated using 3/4-in. thick D_N steel. The main plates of the specimens were $10\frac{1}{2}$ in. wide and 40 in. long. Each of the four side plates was 3 in. wide and $12\frac{1}{2}$ in. long before flame cutting to the final contours as previously described and shown in Fig. 1. The specimens were fabricated using E6010 welding rod.

Type Z:

The purpose of tests of Type Z specimens was to ascertain the effects on fracture of certain details and geometry occurring

at the ends of abruptly terminated welded structural members.
Specimens in this category represent free ended stiffeners, inter-
rupted longitudinals, and bilge keel endings. The scope of the
Type Z specimens was limited to end variations found either to be
actually in service or to certain variations which held promise
of practical adaptability for modifying ships now in service or in
new designs.

The general design of the Type Z specimens finally adopted is
given in Figs. 2 to 5, inclusive. Figs. 2 and 3 signify the typi-
cal specimen and loading arrangements for all end variations but
specifically show the flat bar end condition termed Type Z-3, where
the flat bars are square ended. The tensile loading was applied
through the flat bars at one end and through the main plates at the
other end. The tapered 3/4-in. thick main plate provided a reduced
width and area to assure that a large part of the load introduced
through the flat bars would be retained by the bars until the free
ends, thus providing for a localization of strain on the end weld.

A single specimen intended to simulate a bilge keel ending
detail was designed as shown in Fig. 6. The 3/4-in. main plate of
ABS-B steel was cut to the same geometry as the main plates of the
Type Z specimens as previously described. The 1/2-in. side bars,
however, were replaced by structural Tee sections which were modi-
fied as shown in Fig. 6 to meet the requirements of the specimen
design. The Tee sections were cut from a standard 12-in. I-beam
weighing 50 lbs. per ft. The resulting Tee sections had flange

TYPE ZC2

BURN AND REAM TO 2" D

FLAME CUT

5/16" FILLET WELD

1½"

TYPE ZD

5½"

45°

5/16" FILLET WELD

½"

TYPE ZE

5½"

BURN AND REAM TO 2" D

5/16" FILLET WELD

1½"
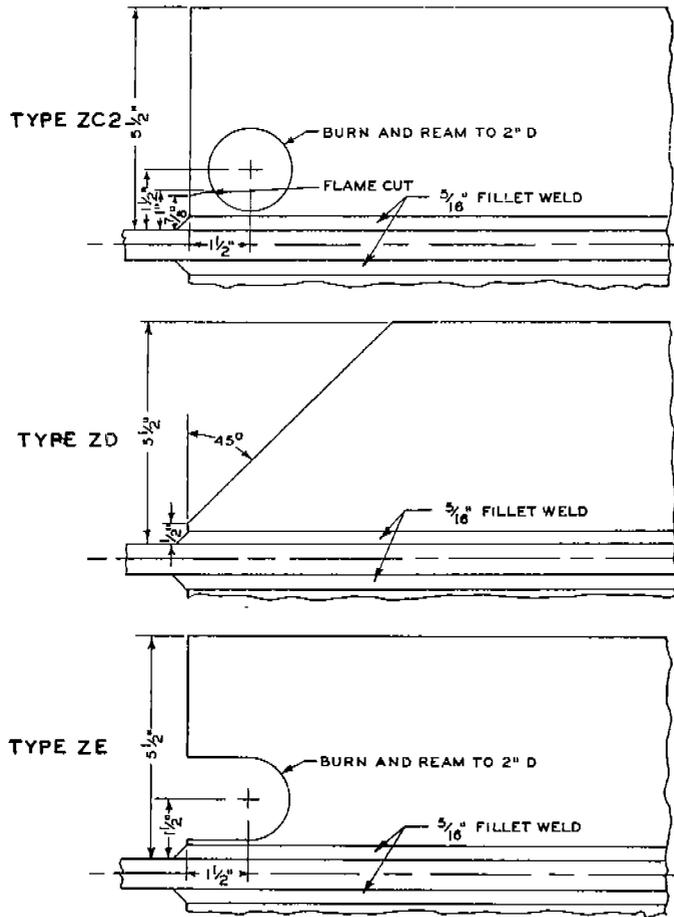
NOTE: ALL EDGES FLAME-CUT... WELDS MADE USING E-6010 ROD

FIG. 5   END DETAIL VARIATIONS FOR TYPE
"Z" SPECIMENS

SWARTHMORE COLLEGE

¾"

4"   6"R

8"   3½"

45°

5/16" FILLET WELD

BUTT WELD

MADE FROM STANDARD 12"X 5½" (50 LB) I BEAM
CUT IN HALF ALONG THE WEB

36"

16"   20"

3"

13¼"

4½" D

4½"

80°

5"

23"   32"   12"   20"
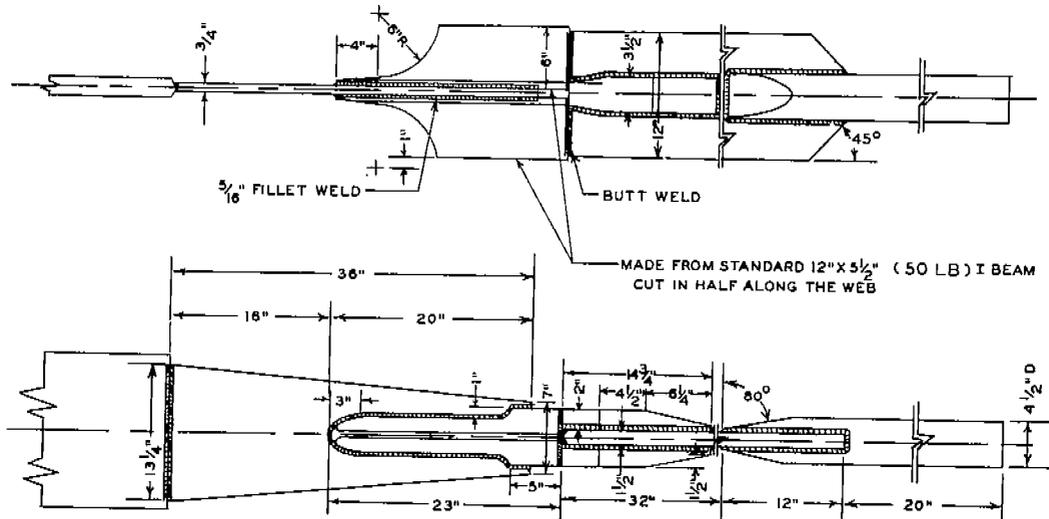
FIG. 6

TYPE ABS-B-ZT2

SPECIMEN ARRANGEMENT

SCALE: 3/32" = 1"

SWARTHMORE COLLEGE

widths of 5.477 in. and depths of 6 in. The flange widths of the Tees were reduced to 4 in., and the ends were cut back on a 5-in. radius.

Specimens of Type Z program were fabricated using a tapered 3/4-in. thick main plate of either D_N project steel or ABS grade B steel. The flat bars were of 1/2-in. thick D_N project steel or D project steel which was subsequently normalized. The tapered main plates maintained a 10½-in. width at the intersection with the flat bars and were 40 in. long for D_N steel or 36 in. long for ABS-B steel as shown in Figs. 2 and 3. The flat bars were 5½ in. wide and 24 in. long, with 20 in. of the total length being attached to the main plates with 5/16-in. fillet welds. The flat bars were reinforced over an 11-in. length to avoid the possibility of fracture at the ends of the tapered main plates (see Figs. 2 and 3).

The flat bars were cut to the end contours shown in Figs. 4 and 5 after the specimens had been fabricated. Specimens of type Z-3 are those which had no further change of end contour and were tested in the square ended condition.

Specimens of Type ZB are those which had the flat bar end contours flame cut to a 5-in. radius. One modification, Type ZB, placed the center of the radius at the end of the flat bar, while the other, Type ZBM, placed the center of the radius 1/2 in. from the end of the flat bar. These end details are shown in Fig. 4.

Specimens of Type ZC-1 are those which had a 2-in. diameter hole flame cut in the flat bars near the juncture with the tapered

main plate. Type ZC-2 specimens had continuity of metal around the holes interrupted by flame cuts from the holes to the free ends of the flat bars. These types are shown in Figs. 4 and 5.

Type ZE specimens represent a further modification of the Type ZC specimen, having parallel flame cuts to the free ends of the flat bars from the extremities of the diameter of the 2-in. hole. Type ZE is pictured in Fig. 5.

Type ZD specimens have the flat bars cut back at a 45° angle as shown in Fig. 5.

The combinations of steel used in the fabrication of specimens are tabulated in Table I and discussed in greater detail in Appendix C.

A subsequent section of the report is devoted to the unloading characteristics of the flat bars, but it is sufficient to state that about 50% of the total load is retained at a section 10 in. from the free ends. The critical section of the main plate at the ends of the flat bars is $10\frac{1}{2}$ in. wide and is, of course, subjected to the total load.

MATERIALS

Insufficient steel of any given grade was available to carry out all phases of the test program. All Type YW specimens were fabricated from "D_N"* steel. The Type Z specimens were

---

*Code designation of "D_N" identifies this steel as a fully killed normalized steel and as one of the original pedigreed steels which has been used in many other investigations. Refer to reference No. 3 in Bibliography for complete description of the pedigreed steels.

TABLE I

Classification of Test Specimens

Type of Specimen	Specimen Geom. Shown in Figure	No. of Specimens Tested	Combinations of Types of Steel		Remarks
			Main Plate 3/4" thick	Flat Bars 1/2" thick	
YW-1	1	6	D_N	none	Simulating fashion plate welding
YW-2	1	2	D_N	none	Simulating fashion plate welding
YW-3	1	3	D_N	none	Simulating fashion plate welding
Z-3	2	4	D_N	D_N	Square ended cut-offs on flat bars
Z-3	2	1	D_N	D'_N	Square ended cut-offs on flat bars
Z-3	3	7	ABS-B	D_N	Square ended cut-offs on flat bars
Z-3	3	2	ABS-B	D'_N	Square ended cut-offs on flat bars
Z-B	2 and 4	3	D_N	D_N	End of flat bars cut to 5" radius
Z-B	3 and 4	3	ABS-B	D_N	End of flat bars cut to 5" radius
Z-B	3 and 4	1	ABS-B	D'_N	End of flat bars cut to 5" radius
Z-BM	3 and 5	5	ABS-B	D'_N	Modified type Z-B (see sketch)
Z-C1	2 and 4	2	D_N	D_N	Square flat bar cut off, 2" burned hole
Z-C2	2 and 4	3	D_N	D_N	Square flat bar cut off, 2" burned hole with relief
Z-C2	3 and 4	3	ABS-B	D_N	Square flat bar cut off, 2" burned hole with relief
Z-C2	3 and 4	2	ABS-B	D'_N	Square flat bar cut off, 2" burned hole with relief
Z-D	3 and 5	3	ABS-B	D_N	45° cut off on flat bars
Z-D	3 and 5	2	ABS-B	D'_N	45° cut off on flat bars
Z-E	3 and 5	5	ABS-B	D_N	U-shaped cutout (see sketch)
Z-E	3 and 5	1	ABS-B	D'_N	U-shaped cutout (see sketch)
Z-T	6		ABS-B	tee bar ASTM-A7	Simulating bilge keel ending

first made using "D_N" steel, and when the supply was exhausted, steel of American Bureau of Shipping Grade B (to be designated as ABS-B) was used. All of the above steel was of nominal 3/4-in. thickness and used for main plates. For the Type Z specimens the 1/2-in. thick flat bars were made of "D_N" and of "D'_N" steels. The latter steel will be described subsequently. The structural tees used in the simulated bilge keel tests were of the ASTM-A7 type, while the main plates for these specimens were of ABS-B steel.

The steel designated as "D'_N" represents the steel obtained by normalizing a 1/2-in. thick plate of "D" steel. This steel was normalized by Lukens Steel at a temperature of 1650 °F. Although standard normalizing procedures were used at the mill, the physical tests indicate that "D'_N" is different from the original "D_N" steel. The chemical composition of the "D" plate used in obtaining "D'_N" steel was assumed to be close to the standard of "D_N" steel heretofore used.

The chemical composition of the various steels used is given in tabular form:

Chemical Composition, %

| Type of Steel	C	Mn	Si	Al	Ni	S
D_N and D'_N	0.19	0.54	0.19	0.019	0.15	--
ABS-B	0.16	0.67	0.02	--	0.05	0.027

The physical properties, as determined using tensile tests, are as follows:

Type of Steel	Specimen Cross-Section	Physical Properties (in rolling direction)		Elongation in 2", %
		Maximum Strength psi	Yield Strength psi	
D_N (3/4" thick)	.505" dia.	62,600	36,300	36.5
D_N (1/2" thick)	1/2" square	59,300	37,100	42.5
D'_N (1/2" thick)	1/2" square	65,800	47,200	37.5
ABS-B (3/4" thick)	.505" dia.	60,300	34,300	40.0

The type or combinations of the various types of steel used in a given specimen is shown in Table I and is discussed in Appendix "D".

The notch sensitive uniformity of 6-ft. by 10-ft. plates of steel was checked by using 1-in. by 3/4-in. edge notched specimens as shown in Figs. 7 and 8. A series of these specimens was made from the remnants of each of the plates used in the program and as tested in tension in a temperature range of -50°F to +130°F. The specimens were loaded to 15,000 lbs. in one minute and the temperature read at that load. The reduction in specimen thickness at the notch was measured after fracture. These reductions plotted as ordinates with temperatures as abscissas are shown in Figs. 7 and 8. With due allowance for scatter, the plates of ABS-B steel appear to be similar in notch sensitive characteristics, and the plates of D_N steel also appear to be similar in notch sensitivity.

FIG. 7
CONTROL TESTS
DN STEEL

SWARTHMORE COLLEGE

FIG. 8
CONTROL TESTS
ABS-B STEEL

SWARTHMORE COLLEGE

FIG. 9 3/4" ON PLATE LAYOUT
CODE C.G.
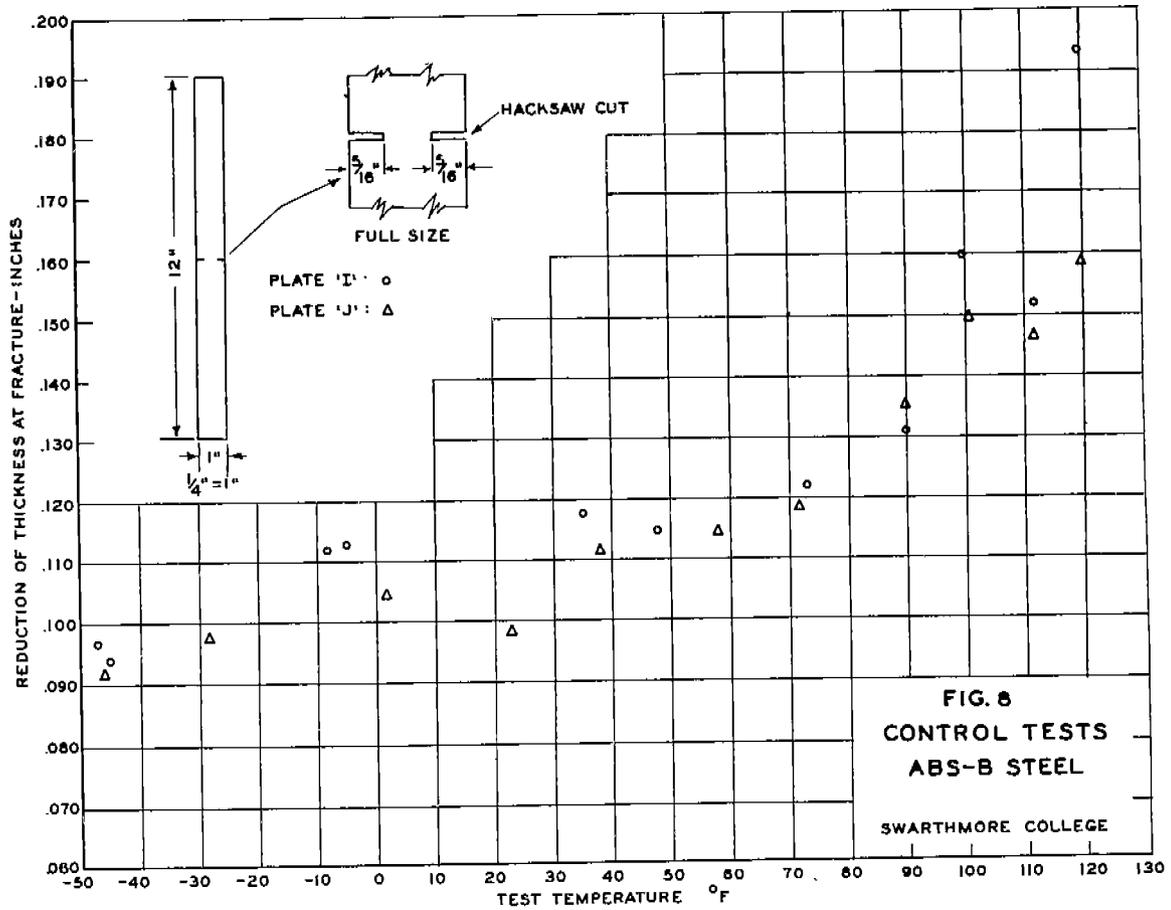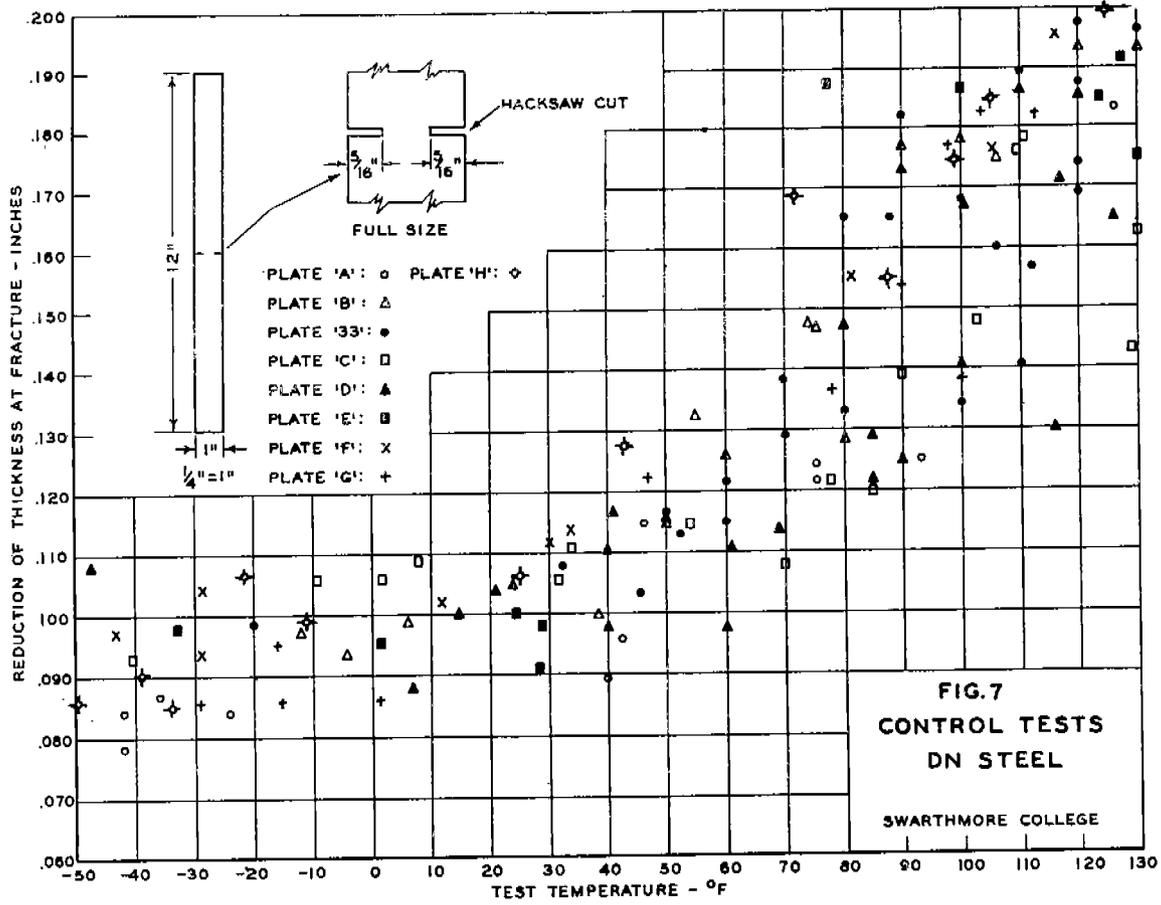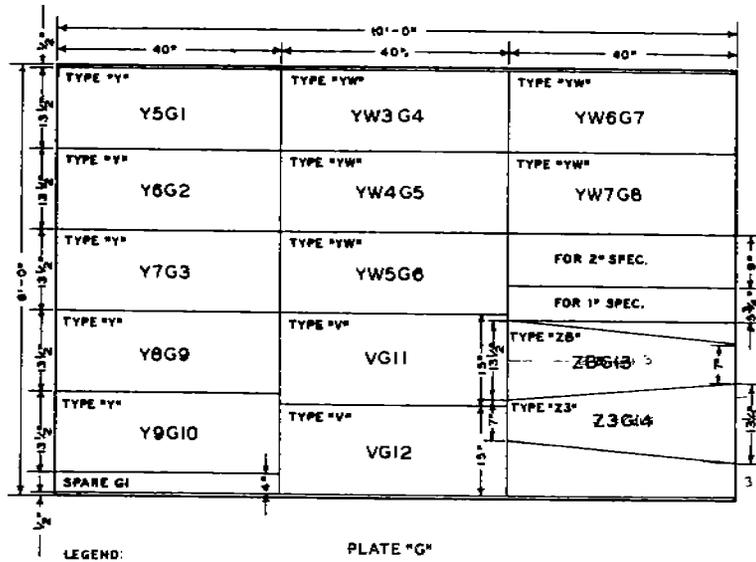
PLATE "G"

LEGEND:
SPECIMEN SIZE: AS INDICATED
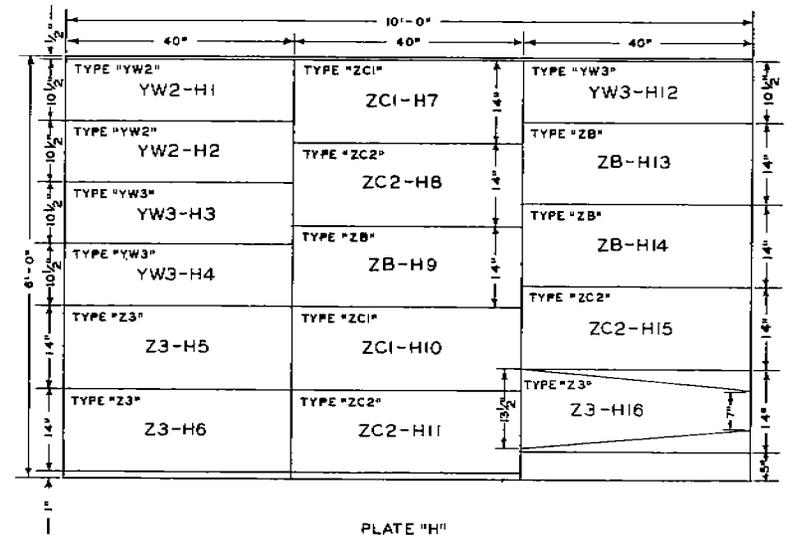
**FIG.10** 3/4" ON PLATE LAYOUT
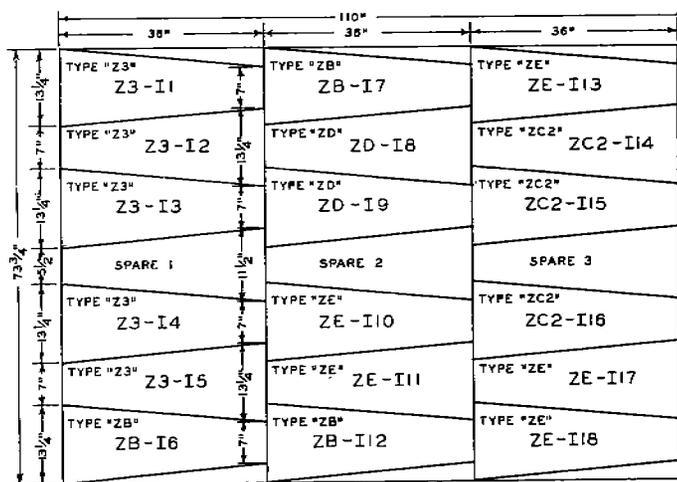
PLATE "H"

PLATE "I"

NOTE: ALLOW APPROX. 1/8" BETWEEN
SPECIMENS FOR BURN WASTE

FIG.11 3/4" ABS-B PLATE LAYOUT
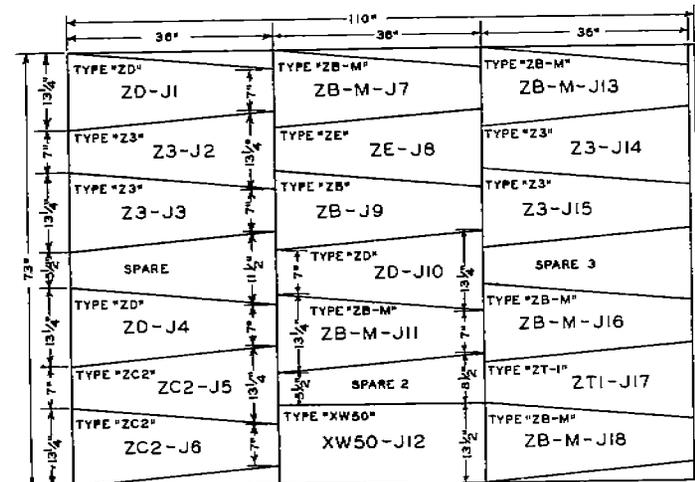

PLATE "J"

NOTE: ALLOW APPROX. 1/8" BETWEEN
SPECIMENS FOR BURN WASTE.

DIMENSIONS OF PLATES IN THIRD COLUMN
ARE THE SAME AND ARE IN THE SAME
ORDER AS THOSE IN FIRST COLUMN.

FIG.12 3/4" ABS-B PLATE LAYOUT

SWARTHMORE COLLEGE

All welds were made using E6010 welding electrodes. The manufacturer of this electrode indicates that the chemical analysis of the electrode is: C = 0.05 to .10%, Mn = 0.50 to 0.65%, and Si = 0.10 to 0.30%. The manufacturer also indicates that the physical properties of the weld metal should be as follows: tensile strength--65,000 to 77,000 lb. per sq. in.; yield point--54,000 to 60,000 lb. per sq. in.; elongation in 2-in.--22 to 30%.

INSTRUMENTATION

The elongation of each specimen was measured with increasing load over the entire specimen length. A spool type extensometer, sensitive to 0.005 in., was employed for this purpose with the terminal points of the extensometer located on the pulling heads. Since the pulling heads had a much greater cross-sectional area than the specimen, the elongations registered on the extensometer were attributed in their entirety to the elongation of the specimen.

Specimens of the YW series were further instrumented by using the Swarthmore SR-4 clip gage over a 16-in. gage length spanning the reduced width portion of the specimen. Four such gages were attached on one face of the plate. Fig. 13 is a photograph of a typical installation of Swarthmore clip gages and spool extensometer.

The specimens were surrounded by an insulated temperature control chamber which had double glazed plexiglass windows. The specimen was free to elongate without being restrained by the chamber.
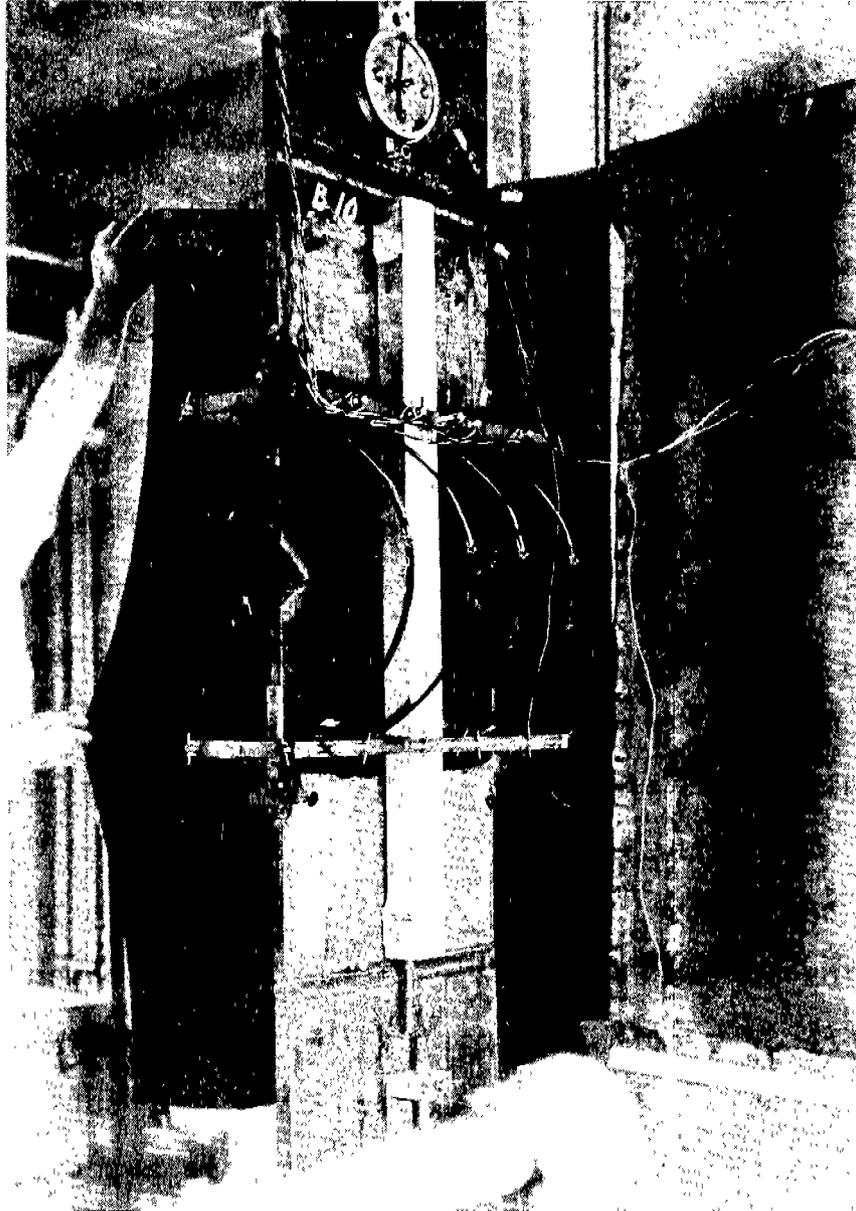
Fig. 13 - Clip Gages and Spool Extensometer Installation

The specimens were cooled to the testing temperature by air which was circulated through a closed system consisting of the chamber, insulated hose connections, and an insulated box containing dry ice. The specimen temperature at the beginning of each test was maintained until fracture. Fig. 14 is a photograph of a Type Z specimen in the temperature control chamber.

The temperatures of the specimens were determined by the use of copper-constantan thermocouples inserted into holes drilled with a #60 drill 1/8-in. into the plate and were located in the main plate and the flat bars. The thermocouples were insulated from the air in the chamber by a plastic asphaltic cement.

The specimens were tested in a 600,000-lb. capacity Baldwin Southwark testing machine.

The first specimen of Type Z-3 was tested with SR-4 electric strain gages cemented to one flat bar to determine the elastic stress distribution within the plate and the direction of the principal stresses. The gages were located in the positions shown in Fig. 15.

TEST DATA

The test data are recorded in the tables of Appendix A. The data include test temperatures, maximum and fracture loads, character of fractures, total specimen elongations at maximum and fracture loads, and energy absorption to maximum and fracture loads.
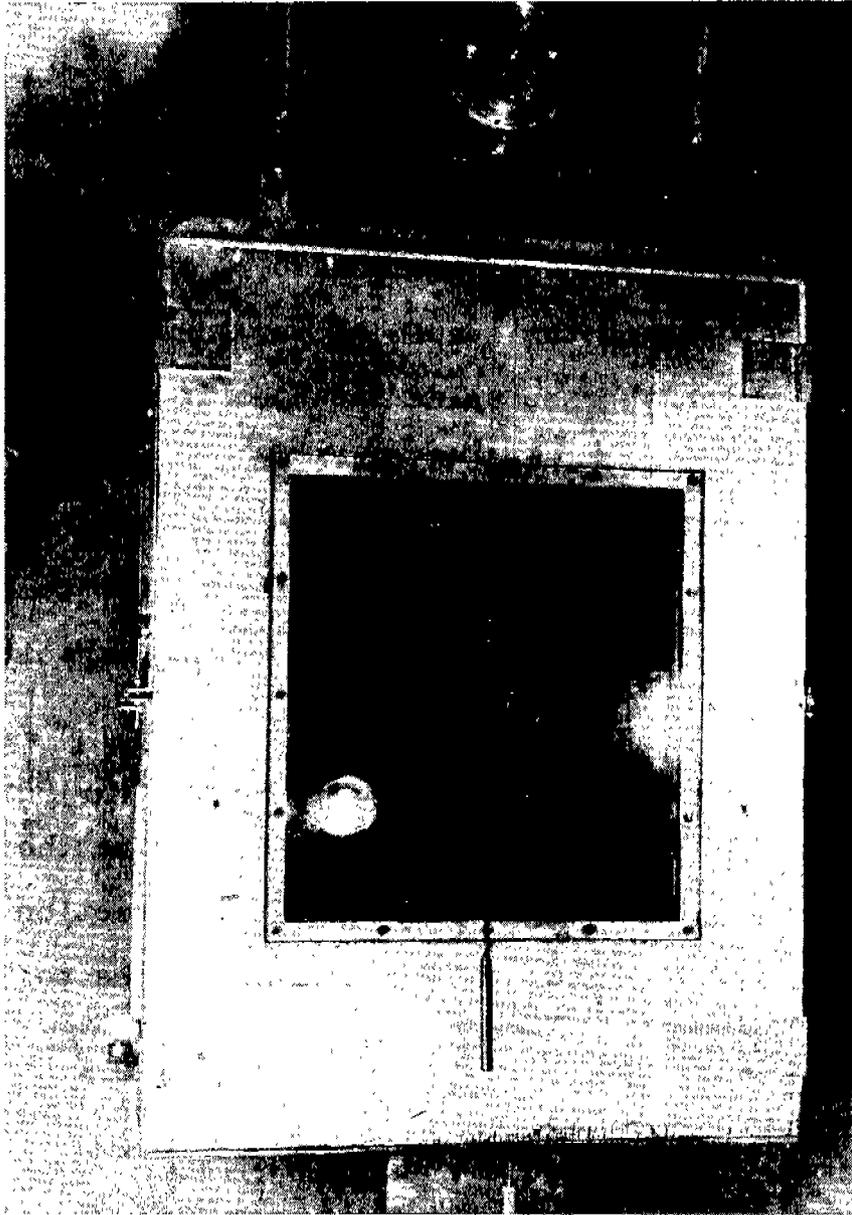
Fig. 14 - Specimen in Temperature Control Chamber
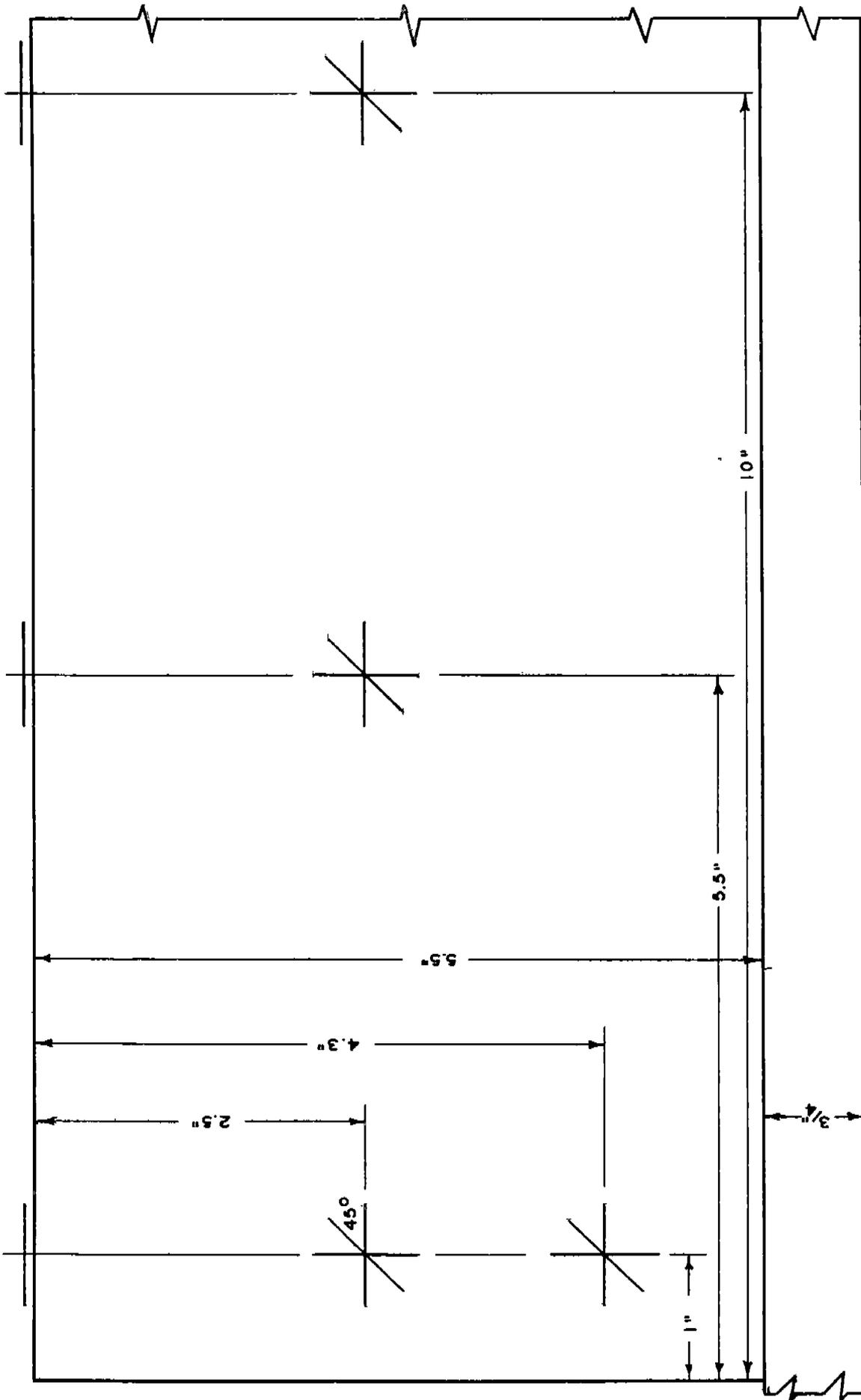
FIG. 15   STRAIN GAGE LOCATIONS - SPECIMEN DN-Z3-H6

SWARTHMORE COLLEGE

The energies to maximum and fracture loads were computed from the areas under the load vs. elongation curves shown in Appendix B.

The character of the fracture is given in terms of the percentage of the fracture surface exhibiting a shear type of fracture. The remainder of the fracture surface was of the cleavage type. The shear type of fracture is characterized by a silky, fine grained appearance with all fracture surfaces being inclined at approximately 45° to the plane of the plate.

DISCUSSION OF TEST RESULTS
TYPE YW SPECIMENS

Ultimate Load

Welded specimens of Types YW-1 and YW-2 had the same external geometry as the specimens of the unwelded Type Y series previously reported.[2] The results of the Type Y series, unwelded and unnotched specimens, were used as a base of comparison for previously made edge notched specimens, and hence are useful here for comparative purposes. The results for Type Y are plotted on Figs. 16A and 16B. The maximum loads for specimens of the Types YW-1 and YW-2 series appear to be directly comparable to the maximum loads exhibited by specimens of the Type Y series at the same test temperatures. The maximum tensile loads for specimens of each of these three series are plotted in Fig. 16. Plate beveling and longitudinal welding had little effect on strength when compared with the Type Y series which had no weldment.
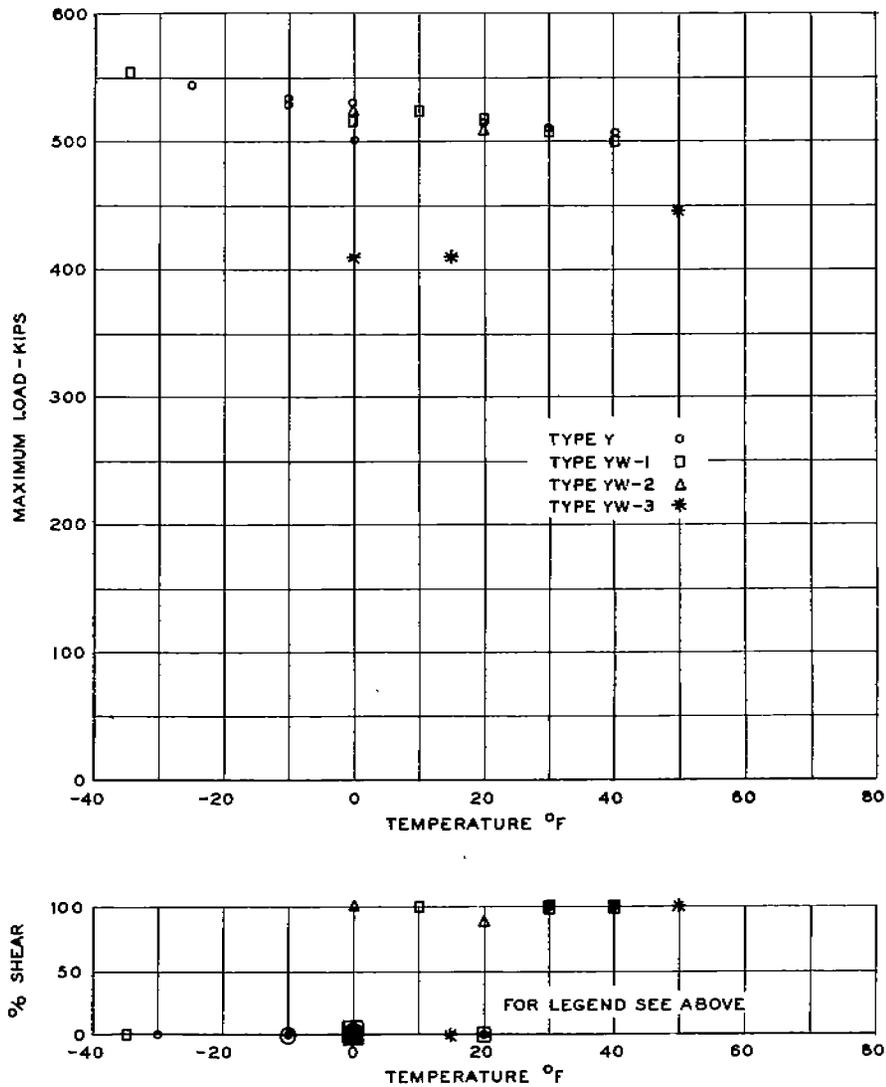
FIG.16A SUMMARY – MAXIMUM LOAD AND PERCENT SHEAR
VS. TEMPERATURE
TYPE Y SPECIMENS
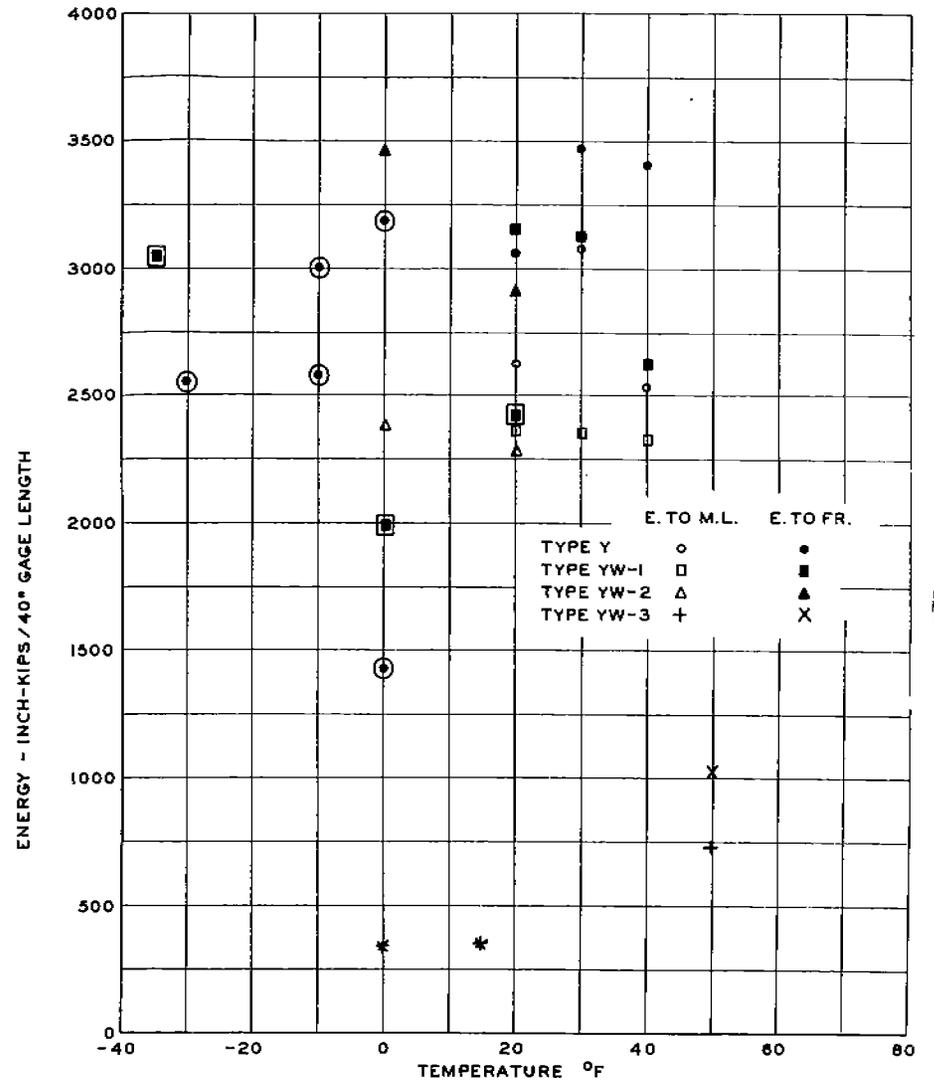
FIG.16B SUMMARY – ENERGIES TO MAXIMUM LOAD AND
FRACTURE VS. TEMPERATURE
TYPE Y SPECIMENS

Specimens of the YW-1 and YW-2 series exhibited the trend shown by the Type Y series with respect to maximum loads. Maximum loads generally increased as test temperatures were lowered. An exception to the general increase in maximum load values for the Type YW-1 specimens appears to occur around the transition temperature where a lower maximum load was noted than at higher and lower temperatures. The tendency toward increasing loads with decreasing temperatures was noted in 3/4-in. square unnotched tensile coupons;[2] however, the 3/4-in. square coupons did not exhibit a drop off in load value, nor did they show a transition from shear to cleavage modes of fracture in the range of test temperatures.

The 5/16-in. fillet welds and the 3/4-in. offsets at the ends of the side plates of the YW-3 specimens had decidedly detrimental effects on strength. Two specimens tested at 0°F and +15°F exhibited maximum loads which were approximately 100 kips lower than the YW-1 and YW-2 specimens tested at about the same temperatures.

The effects of plate beveling, which established the cross-sectional form of the longitudinal weldment, were apparently of little significance in limiting values of maximum load. Abrupt changes in external specimen geometry, however, combined with fillet welds at the point of offset, appeared to be more important factors in limiting the maximum load.

Energy to Maximum Load

Relationships between energy to maximum load, measured over the specimen length of 40 in., and test temperature for specimens of Types YW-1, YW-2, and YW-3 are shown in Fig. 16B. The results for unwelded specimens of Type Y,[2] having the same geometry as Types YW-1 and YW-2, are also plotted in Fig. 16B. The scatter of the limited data makes the interpretation of the results difficult.

The energy to maximum load for welded specimens of Types YW-1 and YW-2 generally have slightly lower values at most test temperatures than the energies reported for unwelded Type Y. The exceptions occur at 0° F and at -35°F, where a single specimen of Type YW-1 with a cleavage fracture, had an energy to maximum load which was higher than that for any other specimen. The phenomenon of high energy values at low temperatures accompanied by cleavage fracture has previously been reported by the investigators.[2] A close grouping of the energy values for the three geometrically similar types occurs at the approximate transition temperature, +20°F, and the greatest dispersion of energy values occurs just below the transition temperature zone at 0°F.

Due to limited tests of Type YW-2, no conclusive comparisons can be made with Type YW-1. It appears, however, that the effects of welding and plate beveling reduces the energy absorbing capacity by only a small amount when results are compared with unwelded specimens of the same external geometry.

The three specimens of Type YW-3, with a 5/16-in. fillet weld and a 3/4-in. offset at the end of the side plates, had values of energy to maximum load which fell far below the energy values for the Types YW-1, YW-2, and Y at the same test temperatures. The energy absorbing capacity of specimens of Type YW-3 appears to be about 20% of that of YW-1 and YW-2.

It is therefore apparent, given a free choice of details, that an abrupt change in geometry as exemplified by the details of Type YW-3 should be avoided. Type YW-3 is definitely inferior in both load and energy capacity.

Energy to Fracture

A graphical representation of values of energy to fracture of specimens of Types YW-1, YW-2, and YW-3 is given in Fig. 16B. Energy to fracture values for the previously reported geometrically similar series of Type Y is also shown.

Values of energy to fracture must be viewed considering the type of fracture, i.e., shear or cleavage. Specimens in shear always attain a higher energy value at fracture load than that at maximum load, while specimens failing in complete cleavage are assumed to have the same energy as at maximum load. The tenacity of the shear type of fracture is well known, and energy to fracture exemplifies this feature.

For Types YW-1, YW-2, and Y, it would appear that the energies to fracture are roughly equivalent at all test temperatures. In contrast, specimens of Type YW-3 exhibited energies to fracture

which were less than 20% of the energy values for specimens of Types YW-1 and YW-2. As was the case with maximum load and energy to maximum load, external specimen geometry again seems to be the more important parameter in limiting the amount of energy absorbed to fracture.

Transition Temperatures

The criteria used to evaluate transition temperature for specimens of the YW series were based on fracture appearance, energy to maximum load, and energy to fracture. The estimated transition temperatures for each of the criteria are shown in Table II.

The transition temperatures as represented by fracture appearance are the temperatures taken from sketched curves (not shown) of per cent shear vs. temperature based on data as shown in Fig. 16 and represent the temperature at which a 50% shear fracture would be expected.

Transition temperatures based on values of energy to maximum load or to fracture were taken from sketched curves of energies vs. temperatures based on data shown in Figs. 16A and 16B. Transition temperatures represent the temperatures at the points on the sketched curves where the ordinates approximately represented the average of high and low values of energy.

The two tests of specimens of Type YW-2 at 0°F and +20°F indicated 100% shear fractures, thus making it impossible to evaluate the transition temperature for Type YW-2 except to state

that it is lower than 0°F. Type YW-1 specimens indicated a transition temperature at about 25°F based on fracture appearance and +10°F based on energy.

The higher transition temperature for Type YW-1 may be attributed to a difference in severity of the weld notch at the end of the butt weld. For Type YW-1 the part of the butt weld lying in the main plate groove ends abruptly, whereas for Type YW-2 where only the side plate was beveled a less severe weld notch was created. The fracture in all YW-1 specimens initiated through the weld termination; but for the two specimens of Type YW-2, fracture occurred above the termination for the test at +20°F and in the main plate, several inches below the termination for the test at 0°F. This change in location of fracture, coupled with the fact that both fractures were of the shear type, lends confirmation to the lesser severity of localized effects for YW-2.

Specimens of Type YW-3, due to the increased severity of localized effects at the offset, show a higher transition temperature than for YW-1 or YW-2. With only three tests of Type YW-3, it is possible to establish only an approximate value of the transition temperature at about 35°F.

TABLE II.

Transition Temperatures
Type YW and Y Specimens
D$_N$ Steel

	Transition Temperature, °F		
Type of Specimen	Based on Fracture Appearance	Based on Energy to max. load	Based on Energy to Fracture
Y	25°	indeterminate	indeterminate
YW-1	25°	10°	15°
YW-2	lower than 0°	lower than 0°	lower than 0°
YW-3	35°	indeterminate	35°

DISCUSSION OF TEST RESULTS
FULL-SIZE
TYPE Z SPECIMENS

The large number of variations of end details for the Type
Z specimens, with different materials, makes it advisable first
to discuss each type separately before a general comparison is
made. It is realized that specimen notation is complex, hence
an effort has been made to make this section as explanatory as
possible.

Type Z-3

Type Z-3 specimens, with square ended flat bars, were tested
with four variations in material. (See Table I). More tests were
made of this type than any other, due to the desire to make this
type a firm base for comparing other types. The two primary base
series used main plates of D_N and ABS-B steels with flat bars of
D_N steel. To effect a tie-in with subsequent data, the same main
plate material was used with D'_N flat bars for a small number of
specimens.

The data are given in the Tables of Appendix A and summarized
in Fig. 24.

The specimens generally fractured at the toe of the fillet
weld in either the shear or cleavage mode. For several specimens
failure initiated through the end fillet welds exposing the end of
the flat bar to full view. These typical fractures are shown in
Figs. 25 to 28, inclusive.

The maximum load, for specimens failing in 100% shear on the
fractured cross-section 10 1/2 in. in width and 3/4-in. nominal
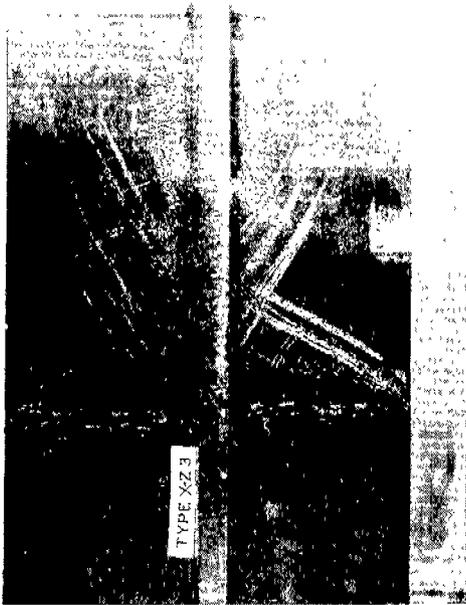
Fig. 17 - Scaling Pattern of Specimen XZ-3

Fig. 18 - Scaling Pattern of Specimen XZ-B
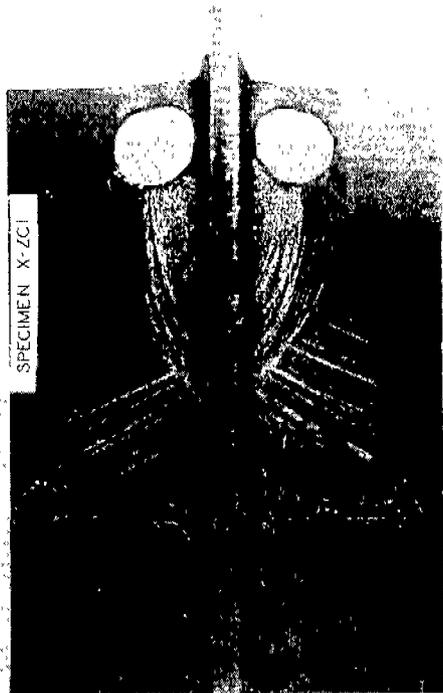
Fig. 19 - Scaling Pattern of Specimen XZ-C1

Fig. 20 - Scaling Pattern of Specimen XZ-C2
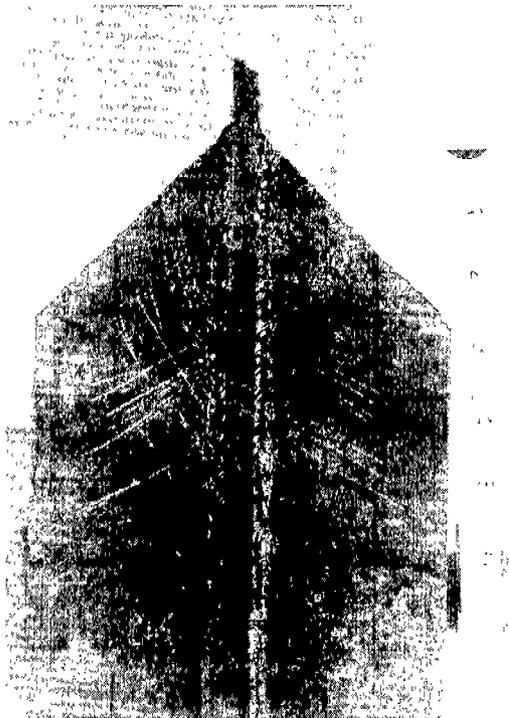
Fig. 21 - Scaling Pattern of Specimen XZ-D

Fig. 17

XZ-B
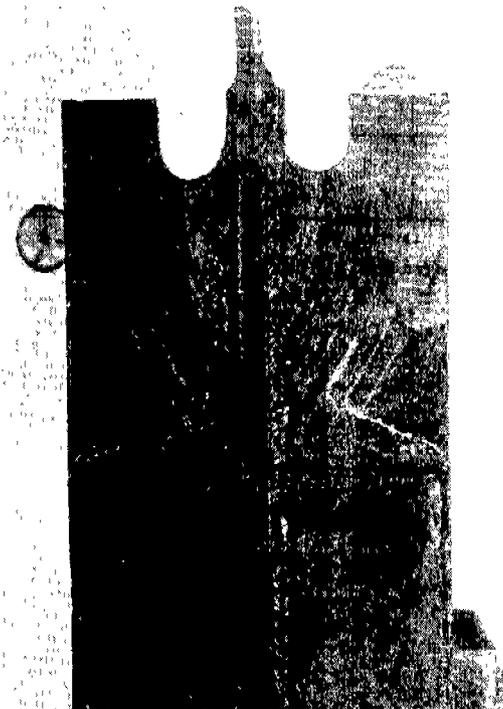
Fig. 22 - Scaling Pattern of Specimen XZ-E
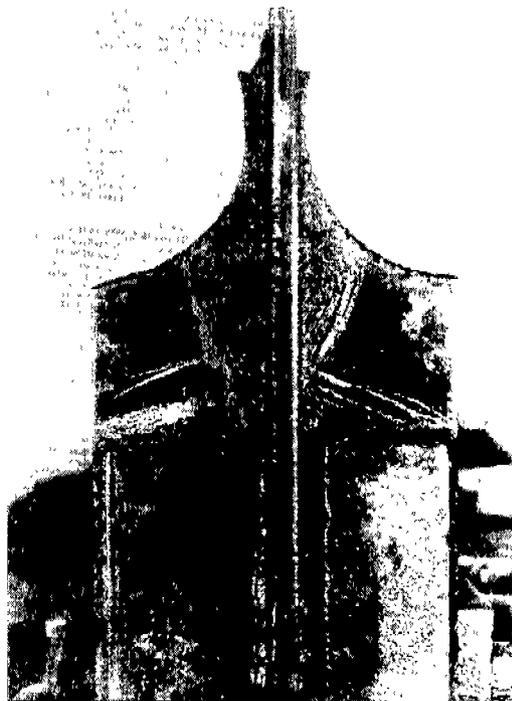
Fig. 23 - Scaling Pattern of Specimen XZ-BM

MAX. LOAD
VS. TEMP.
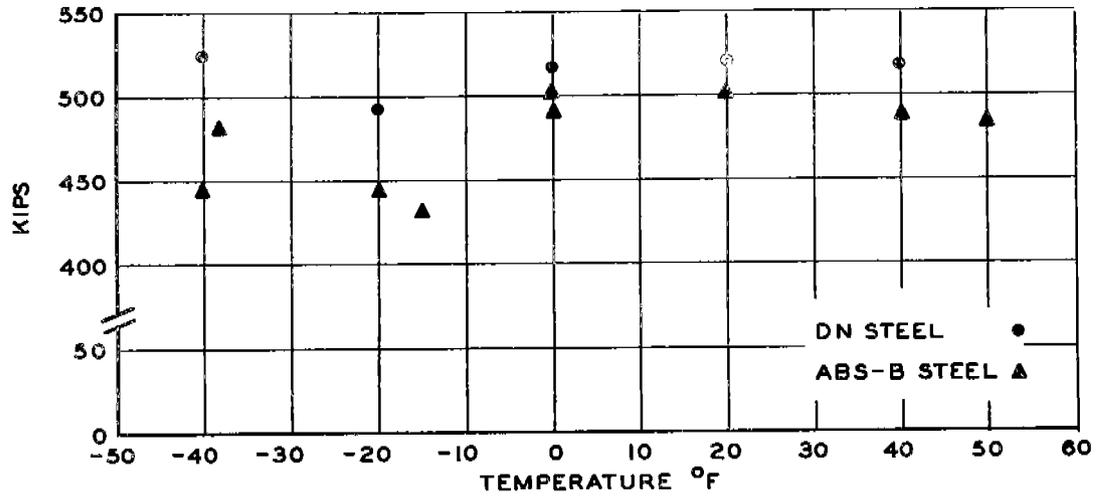
ENERGY
VS. TEMP.
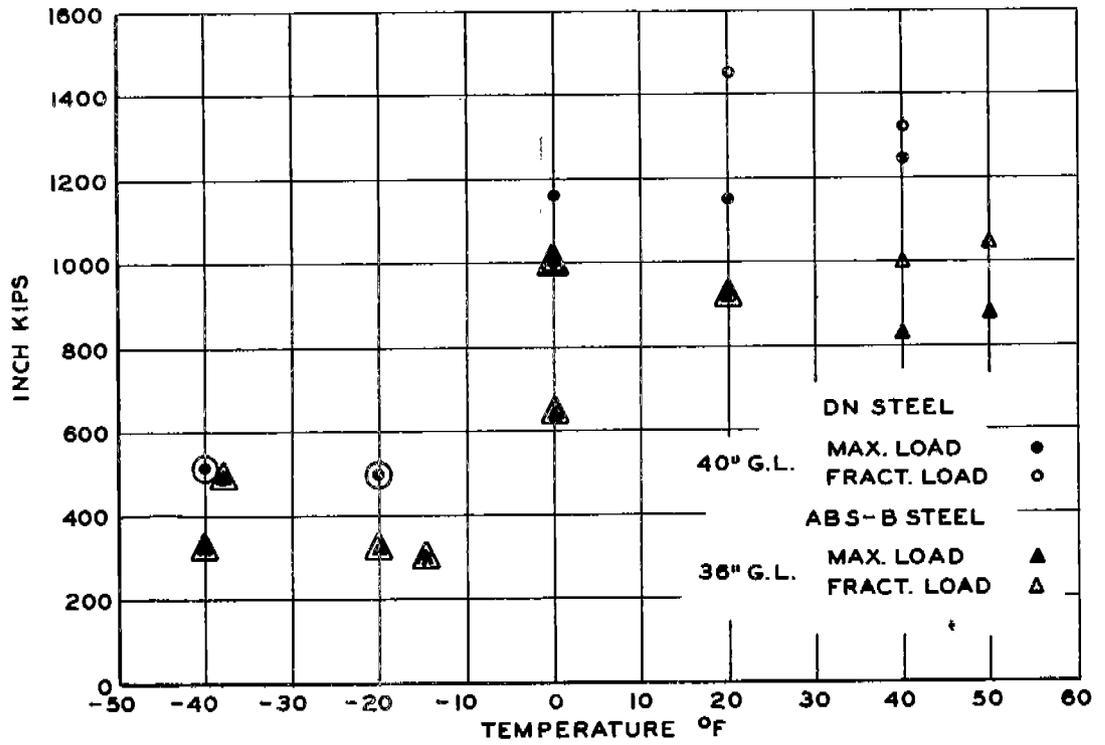
PERCENT
SHEAR
VS. TEMP.
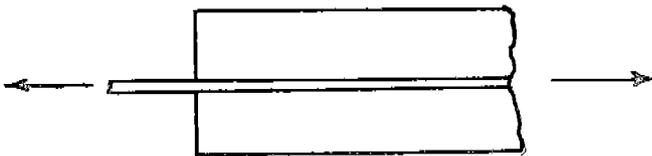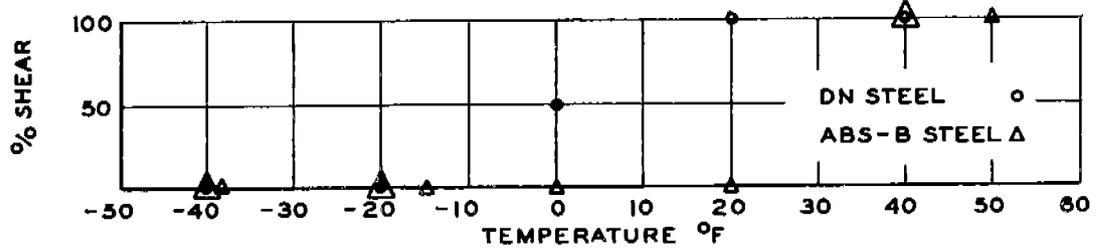
FIG. 24

SUMMARY

TYPE Z3 SPECIMENS

SWARTHMORE COLLEGE
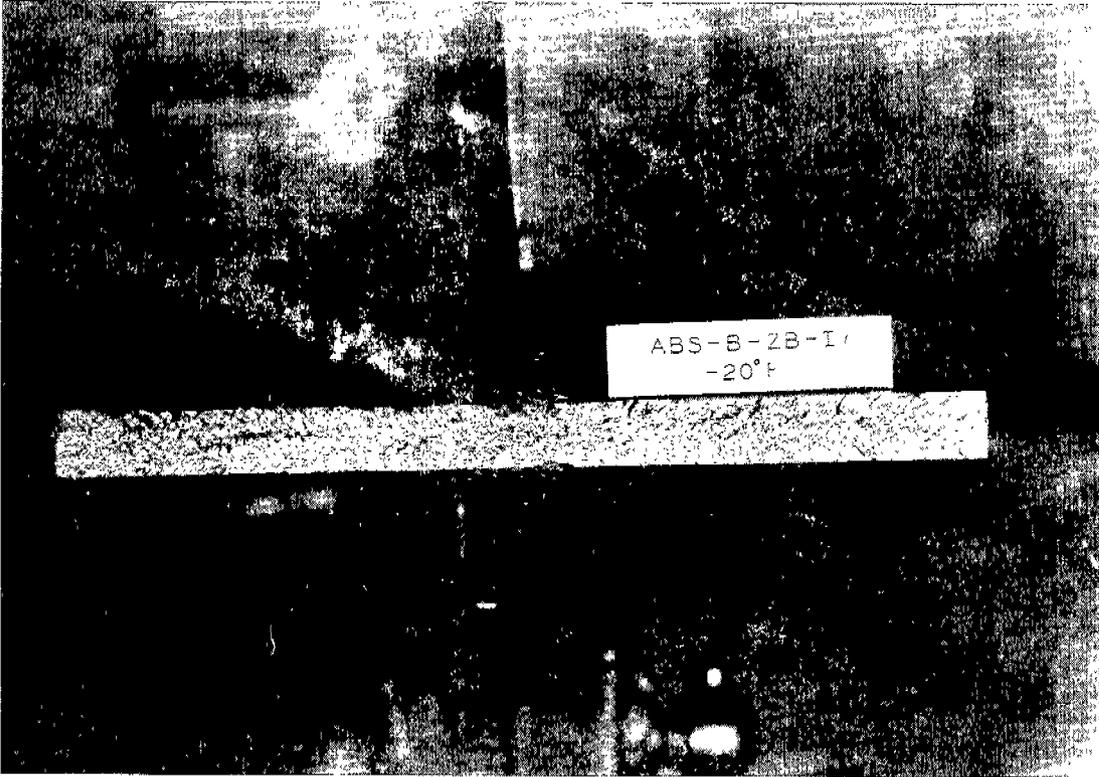
Fig. 26 — Cleavage Fracture at Toe of End Fillet Weld
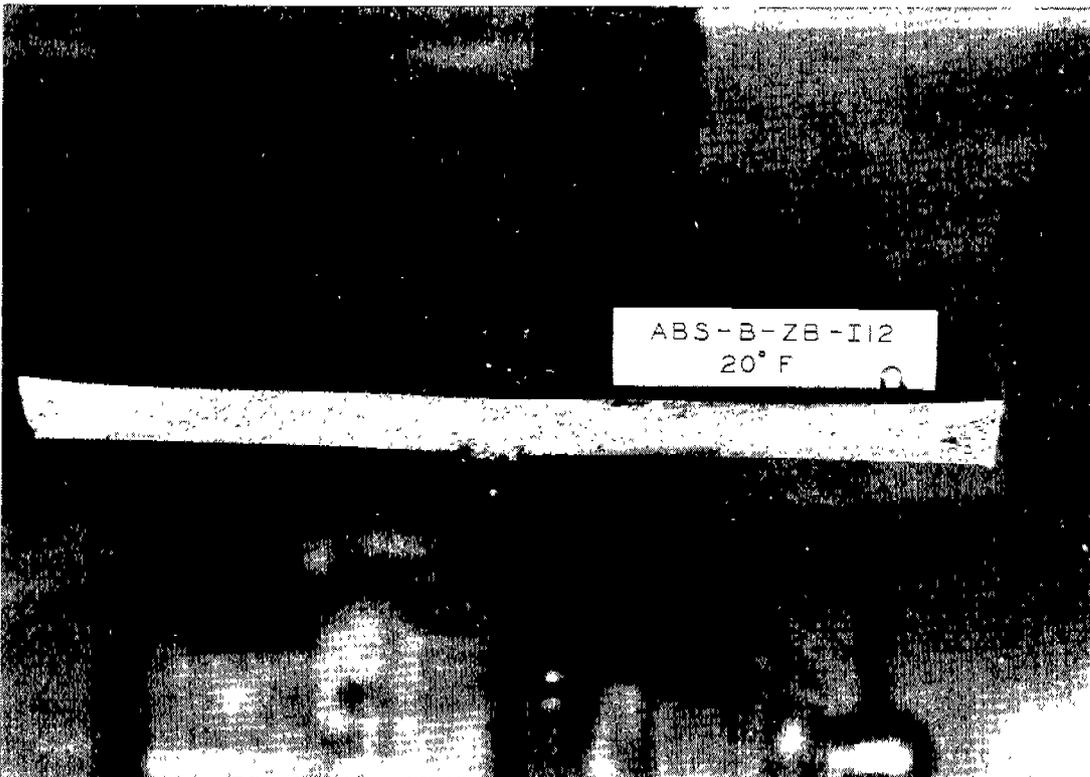
Fig. 25 — Shear Fracture at Toe of End Fillet Weld
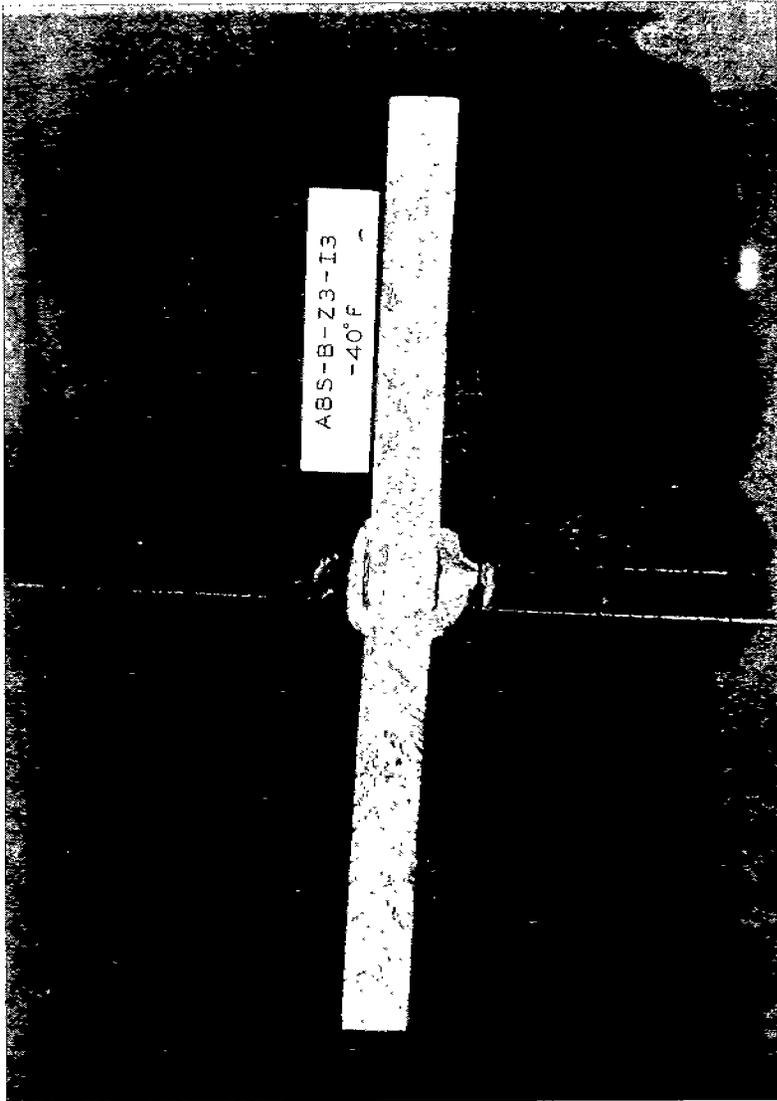
Fig. 27 - Cleavage Fracture through End Fillet Weld
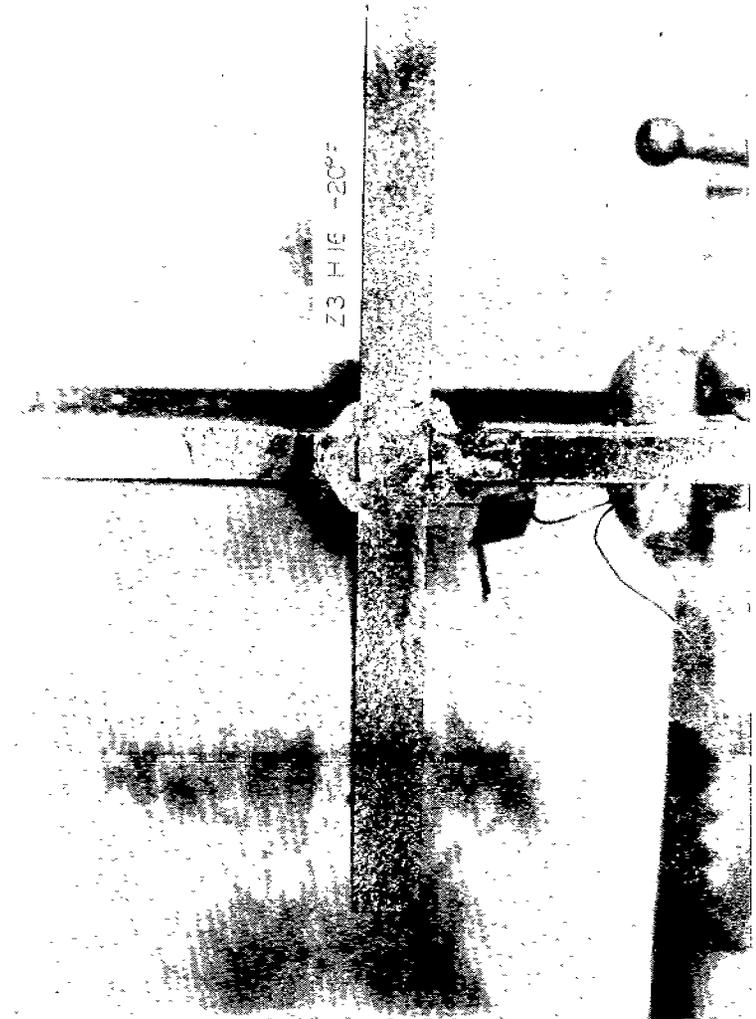
Fig. 28 - Cleavage Fracture at Flat Bar Surface

thickness, averaged 517 kips for the D_N steel and 485 kips for ABS-B steel with D_N flat bars. These maximum loads bear essentially the same ratio to one another as the tensile strength ratio for two steels found by tests on 0.505-in. diameter bars. The maximum loads for the D_N steel were fairly uniform with varying temperature, whereas the maximum load for ABS-B steel was not. For this steel, for temperatures about 40 to 50° below the transition temperature, the maximum loads were about 10% less for cleavage fracture than for shear fractures.

With respect to energy to maximum load and fractures, specimens of D_N steel are slightly better, although not significantly so if differences in gage lengths are reconciled. (40 in. for D_N and 36 in. for ABS-B plates). The energy remains at a high level for the ABS-B steel for cleavage fracture until the temperature is about 40° below the transition temperature based on appearance. (See Fig. 24).

The single point transition temperatures, in °F, determined by the criteria expressed heretofore on page 17, are as follows for Type Z-3:

TABLE III

Transition Temperatures--Type Z-3

Type of Steel Main Plate	Based on Appearance of Fracture	Based on Energy to Maximum Load
D_N	0°F	-4°F
ABS-B	+30°	-8°

The transition temperatures for D_N steel by the two criteria are consistent; however, since energy remained high for a few tests using ABS-B steel where cleavage fractures occurred, the two criteria establish widely different transition temperatures for ABS-B steel.

Type Z-3--Flat Bar Stresses

In an effort to evaluate the stress distribution in the flat bars, one specimen of Type Z-3 was instrumented with SR-4 strain gages. The gage locations are shown in Fig. 15.

From the strain gage readings, the magnitudes and directions of the principal stresses at each of the gage locations were computed and are shown in Figs. 29 and 30 for the total loads on the specimen of 150 kips and 350 kips.

From the principal stresses of Figs. 29 and 30, the stress components parallel to the main plate and normal to the main plate were calculated and are shown in Figs. 31 and 32. From these data the total load carried by the flat bars for specimen loads of 150 kips and 350 kips were computed and are shown as percentages of the total specimen load on the ordinate of the curves of Fig. 33. Distance from the free end was plotted as the absissa.

For a total specimen load of 150 kips in the elastic range of loading the percentage of the total load carried by the flat bars is directly proportional to the distance from the free ends. When this curve is extended to the 100% of total specimen load
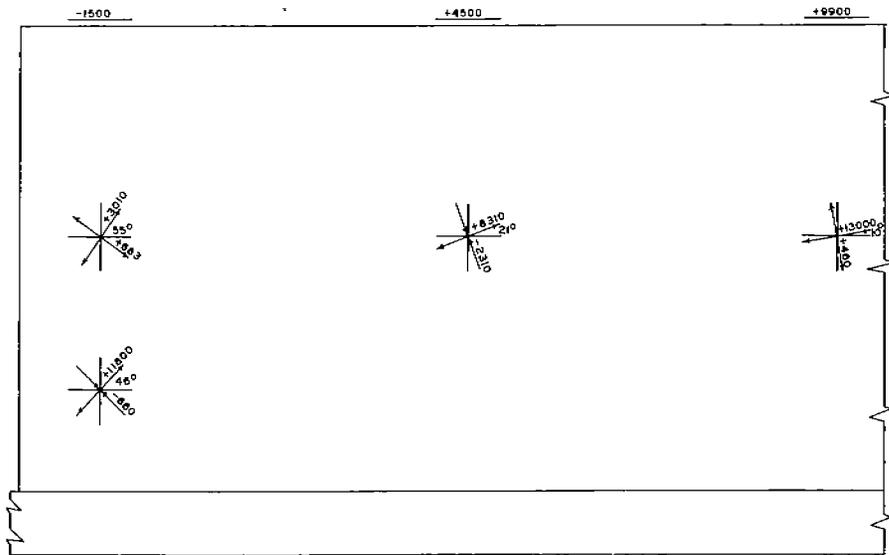
FIG. 29   PRINCIPAL   STRESSES AT 150 KIPS
SPECIMEN DN-Z3-H6
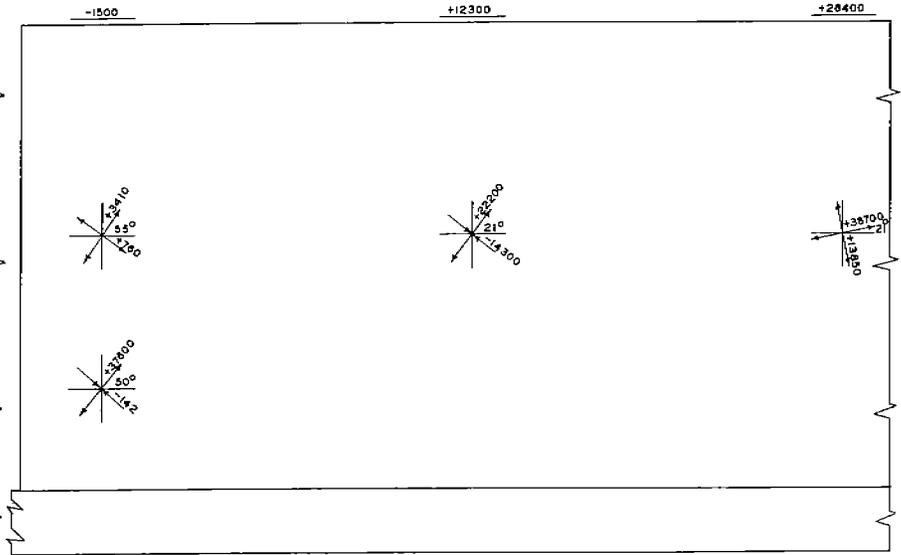
FIG. 30   PRINCIPAL   STRESSES AT 350 KIPS
SPECIMEN DN-Z3-H6
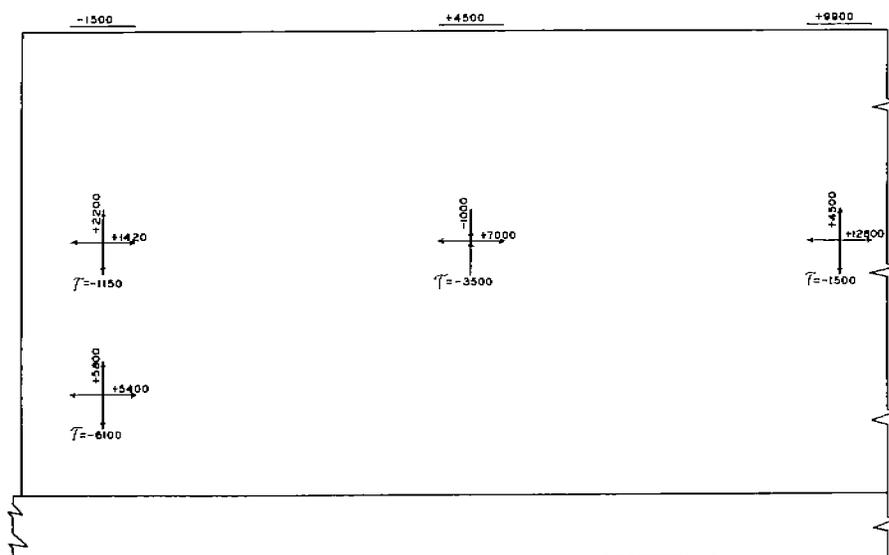
FIG. 31   STRESS COMPONENTS AT 150 KIPS
SPECIMEN DN-Z3-H6
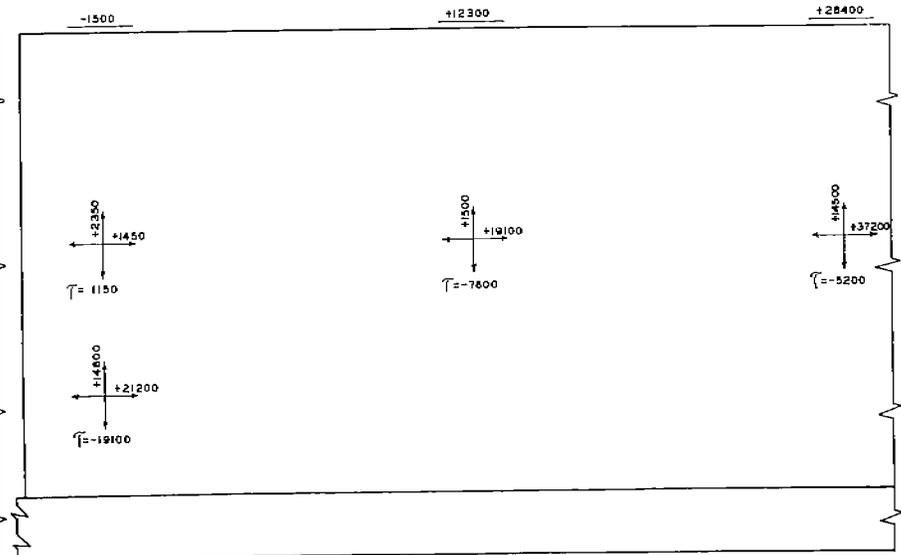
FIG. 32   STRESS COMPONENTS AT 350 KIPS
SPECIMEN DN-Z3-H6

value, the distance from the free ends as shown by the absissa is 20 inches, which is to be expected since the main plate terminates 20 inches from the free ends of the flat bars. (See Fig. 2). The transfer of load from the flat bars to the main plate is accomplished through shear along the fillet welds on either side of the flat bars. From the 150-kip curve of Fig. 33, it would appear that these shearing stresses are uniformly distributed along the side fillet welds to the main plate in the elastic range of loading.

At a total specimen load of 350 kips, parts of the main plate have reached yield point stresses, and the percentages of the total load carried by the flat bars as computed from the stresses of Fig. 32 are as shown by the 350-kip curve of Fig. 33. The shearing stresses, rather than being uniformly distributed as in the elastic range of loading, tend to increase in intensity near the end fillet weld at the free ends of the flat bars.

Type Z-B

The flat bars of the Type Z-B specimens had their free ends flame cut to a 5-in. radius in contrast to the square cut-offs of Type Z-3. The data are given in the Tables of Appendix A, and the summary of all data is shown graphically in Fig. 34.

The tests are few in number and permit only general observation and inferences to be made. However, the few tests give a background to compare results with Type Z-3. Quantitatively
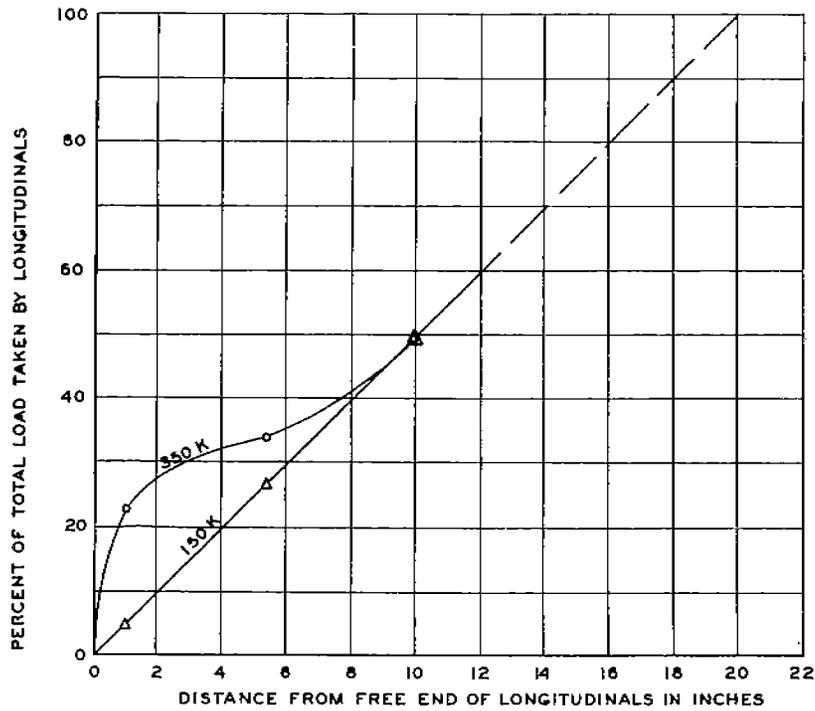
FIG. 33   UNLOADING CHARACTERISTICS OF LONGITUD-
INALS
SPECIMEN DN-Z3-H6

MAX. LOAD
VS. TEMP.

ENERGY
VS. TEMP.

PERCENT
SHEAR
VS. TEMP.
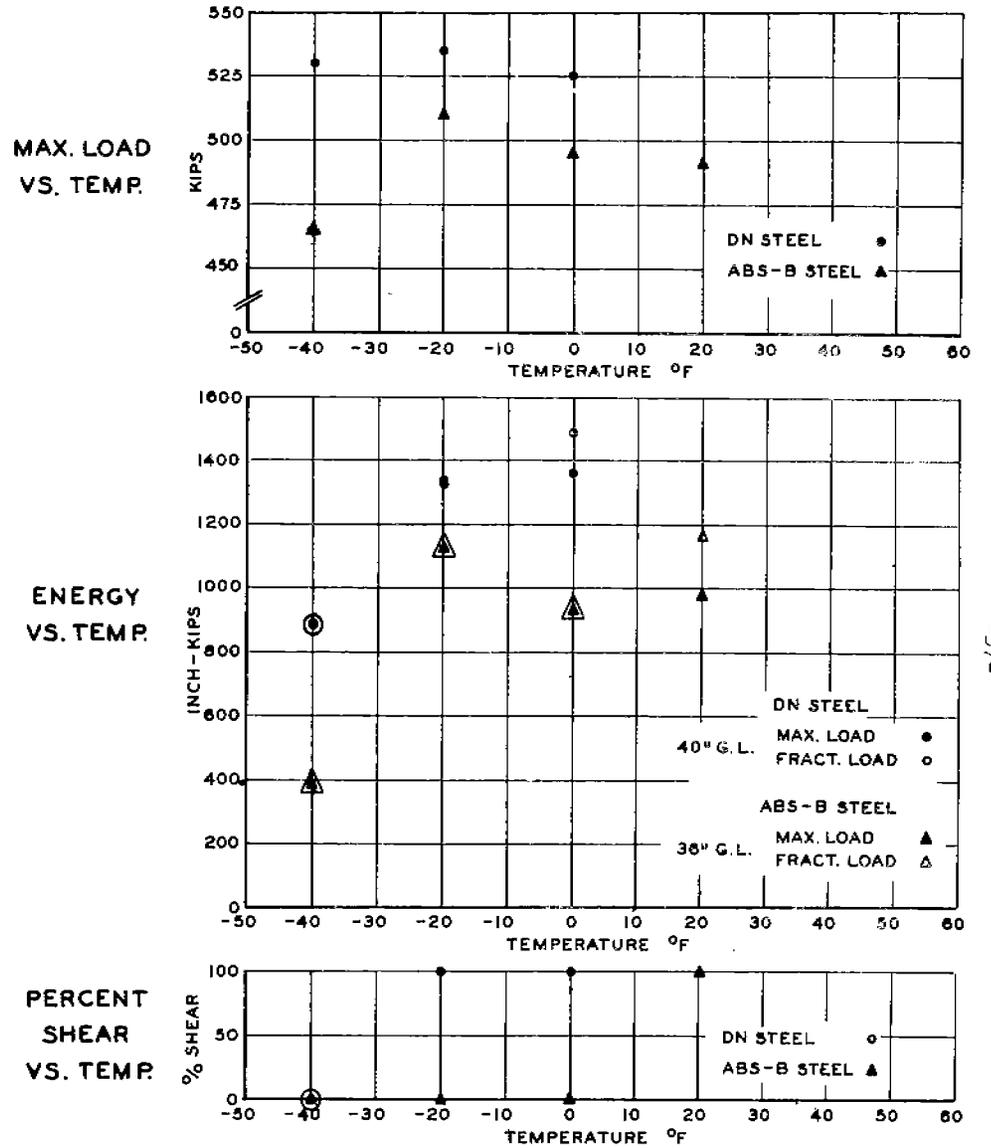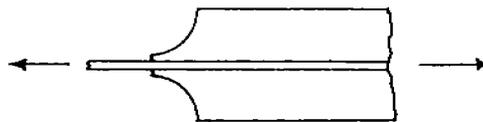
FIG. 34
SUMMARY
TYPE ZB SPECIMENS

there appears to be a small improvement in average load capacity for both D_N and ABS-B steel. Energywise an overall improvement or increase is noted compared with Type Z-3, with high energy for fracture in the cleavage mode for ABS-B steel when temperatures are 10 to 30°F below transition temperature determined from appearance of fracture.

Transition temperatures show the most significant change of any physical property relative to Type Z-3. Due to limited data, the transition temperature was established on the basis of fracture appearance only. The transition temperatures are: for D_N steel, -30°F; and for ABS-B steel, +10°F. These temperatures are 30° and 20°, respectively, below the Type Z-3 results. Since one expects transition temperature to be affected by localization of strains in the region of the end weld, it appears that the end relief afforded by Type Z-B is effective in reducing local triaxiality.

Type Z-BM

Type Z-BM is a modification of Type Z-B. (See Fig. 4). It was suggested that this detail would be a better detail for modifying existing ships than Type Z-B.

As will be seen by reference to the data in Table VI-A of Appendix A and Fig. 35 summarizing these data, no significant changes are noted in comparison with Type Z-B except that the transition temperature is approximately 25°F, a rise of 15°F compared with Type Z-B; but since the data reports only one

Left figure (Fig. 35)

MAX. LOAD
VS. TEMP.

KIPS

575
550
525
500
475

-50 -40 -30 -20 -10 0 10 20 30 40 50 60 70
TEMPERATURE °F

ENERGY
VS. TEMP.

INCH-KIPS

1600
1400
1200
1000
800
600
400
200

ENERGY TO MAX. LOAD ▲
ENERGY TO FRACTURE △

-50 -40 -30 -20 -10 0 10 20 30 40 50 60 70
TEMPERATURE °F

PERCENT
SHEAR
VS. TEMP.

% SHEAR

100
50
0

-50 -40 -30 -20 -10 0 10 20 30 40 50 60 70
TEMPERATURE °F
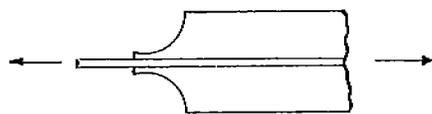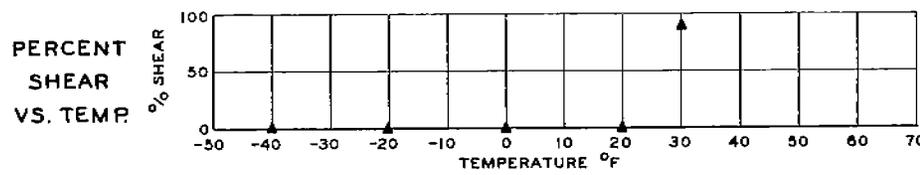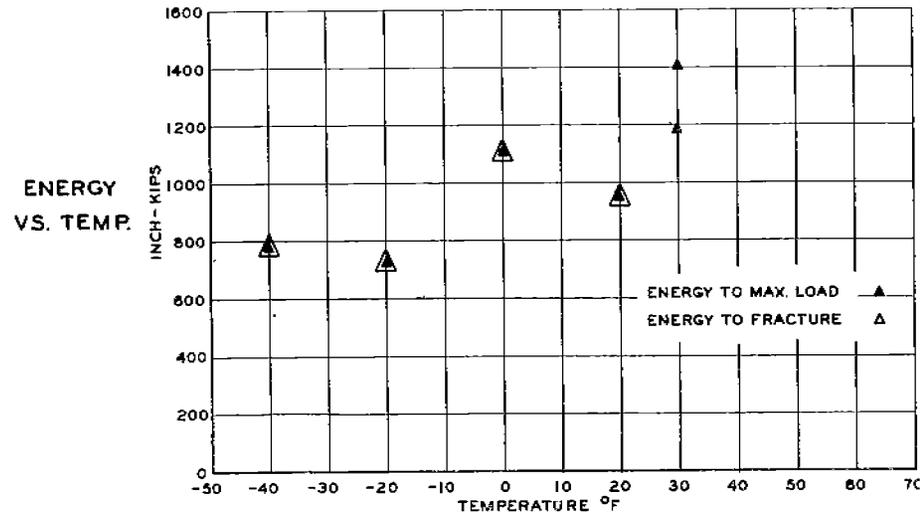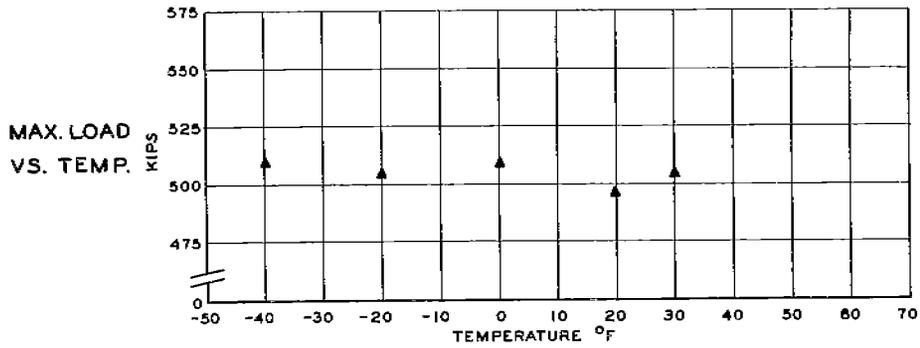
FIG. 35   SUMMARY
TYPE ZBM SPECIMENS
ABS-B STEEL

SWARTHMORE COLLEGE

Right figure (Fig. 36)

MAX. LOAD
VS TEMP.

KIPS

550
525
500
475
450

DN STEEL •
ABS-B STEEL ▲

-50 -40 -30 -20 -10 0 10 20 30 40 50
TEMPERATURE °F

ENERGY
VS. TEMP.

INCH-KIPS

1600
1400
1200
1000
800
600
400
200

DN STEEL
40" G.L.   TO MAX. LOAD •
           TO FRACT. LOAD ○
ABS-B STEEL
36" G.L.   TO MAX. LOAD ▲
           TO FRACT. LOAD △

-50 -40 -30 -20 -10 0 10 20 30 40 50
TEMPERATURE °F

PERCENT
SHEAR
VS. TEMP.

% SHEAR

100
50
0

DN STEEL •
ABS-B STEEL ▲

-50 -40 -30 -20 -10 0 10 20 30 40 50
TEMPERATURE °F

FIG. 36
SUMMARY
TYPE ZC2 SPECIMENS

SWARTHMORE COLLEGE

-39-

specimen having more than 0% shear, no firm conclusion is warranted.

Types Z-C1 and Z-C2

Figs. 4 and 5 show the end details for Types Z-C1 and Z-C2. Each type had a 2-in. diameter hole burned in the flat bar at the square end. For Z-C2 a straight flame cut was made from the free end of bar to intersect the hole. Thus two degrees of end restraint are introduced, with Type Z-C2 expected to place less load on the end weld, as is clearly indicated in the photographs of Figs. 19 and 20. The data for Type Z-C1 and Z-C2 are given in Table III-A of Appendix A. Fig. 36 summarizes these data for Type Z-C2. No plot is presented for Type Z-C1 since only two tests were made.

It is believed that the two types, Z-C1 and Z-C2, are about equal in load capacity for a given steel. With respect to energy to maximum load, Type Z-C1 is slightly inferior to Type Z-C2. In any event, the absorbed energies are in the same range as that found for Type Z-3.

In view of the slight differences noted above in strength and energy absorption, it is of the utmost significance to note that the transition temperatures show wide differences. They are summarized in Table IV.

TABLE IV

Transition Temperatures--Types Z-C1 and Z-C2 Specimens

Types of Specimen	Type of Steel Main Plate	Transition Temperatures, °F Based on Appearance of Fracture
Z-C1	D_N	-10°
Z-C2	D_N	-28°
Z-C2	ABS-B	Approx. +30° *

*Based on only one specimen failing in more than 0% shear

With D_N main plates Type Z-C2 has the lower transition temperature. This is an indication that less localization or triaxiality exists at the end weld, apparently due to the destroying of the continuity of metal around the hole. Observations related to this, for the exploratory Z series specimens, confirm the present findings. Type Z-C2 with main plates of ABS-B steel has a transition temperature much higher than when D_N steel was used. The effect of different steel follows the trend for other end variations.

Finally, the comparison of transition temperatures with the base series of Type Z-3 indicates an expectancy of lower transition temperatures for D_N steel plates. For ABS-B steel nothing positive can be reported about the relief afforded by the end details of Type ZC-2 since the transition temperature based on limited tests was approximately equal to that of Type Z-3.

Type Z-D

The ends of the flat bars for Type Z-D specimens were cut

off on a 45° angle. The data for five tests, all exhibiting cleavage fracture, are given in Appendix A and plotted in Figure 37.

The average maximum load of Type Z-D for cleavage fracture, with main plates of ABS-B steel, was slightly lower than the maximum load for Type Z-3 for cleavage fracture. Energy absorption of the plates is slightly lower for Z-D than for Z-3.

The transition temperature could not be determined from the limited data but is above +40°F. With this temperature unknown it is difficult to assess the value of cutting off the end bars on the 45° angle. This end modification is apparently poorer in this respect than the end variations discussed before. This statement must, however, be qualified by pointing out that several specimens had D'_N steel flat bars. The D'_N steel had a higher yield stress than D_N steel; consequently, the test made at +40°F and showing cleavage fracture may be misleading.

Type Z-E

The Type Z-E specimen was introduced into the program after the results of Types Z-C1 and Z-C2 had indicated that Z-C2 had a lower transition temperature apparently due to the destroying of continuity of the 2-in. diameter hole. This led to investigating the effects of a U-shaped cut-out, which was expected to possess the same characteristics as Z-C2. Refer to Fig. 5 for the end details. The data are given in Appendix A and also plotted in Fig. 38. It should be noted that the main plates were of ABS-B steel.

MAX. LOAD
VS. TEMP.

KIPS

500
475
450
25
0
-50 -40 -30 -20 -10 0 10 20 30 40 50
TEMPERATURE °F

ENERGY
VS. TEMP.

INCH - KIPS

600
500
400
300
200
100
0
-50 -40 -30 -20 -10 0 10 20 30 40 50
TEMPERATURE °F

ABS—B STEEL

36" G.L.   MAX. LOAD ▲
             FRACT. LOAD △

PERCENT
SHEAR
VS. TEMP.

% SHEAR

100
50
-50 -40 -30 -20 -10 0 10 20 30 40 50
TEMPERATURE °F
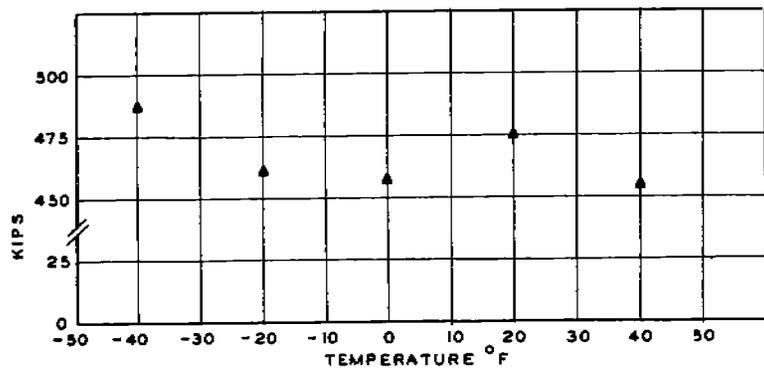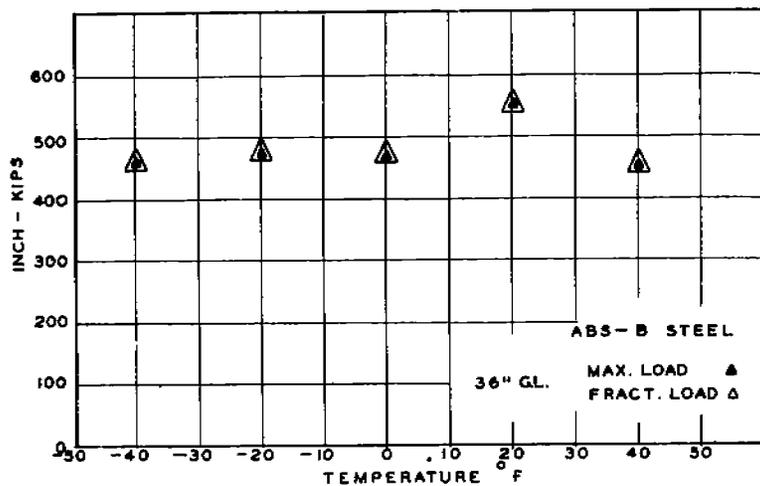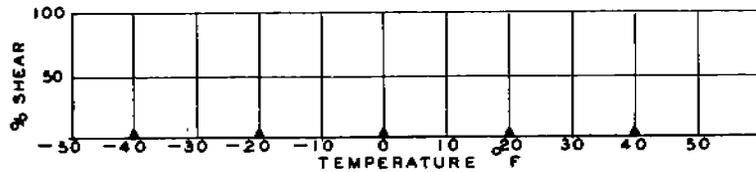
NOTE : TYPE ZD SPECIMENS
WERE NOT TESTED
USING DN STEEL

FIG. 37

SUMMARY
TYPE ZD SPECIMENS

SWARTHMORE COLLEGE

MAX. LOAD
VS. TEMP.

KIPS

550
500
475
450
25
0
-50 -40 -30 -20 -10 0 10 20 30 40 50 60
TEMPERATURE °F

ENERGY
VS. TEMP.

INCH-KIPS

1600
1400
1200
1000
800
600
400
200
0
-50 -40 -30 -20 -10 0 10 20 30 40 50 60
TEMPERATURE °F

ABS-B STEEL

36"G.L.   MAX. LOAD ▲
            FRACT. LOAD △

PERCENT
SHEAR
VS. TEMP.

% SHEAR

100
50
0
-50 -40 -30 -20 -10 0 10 20 30 40 50 60
TEMPERATURE °F
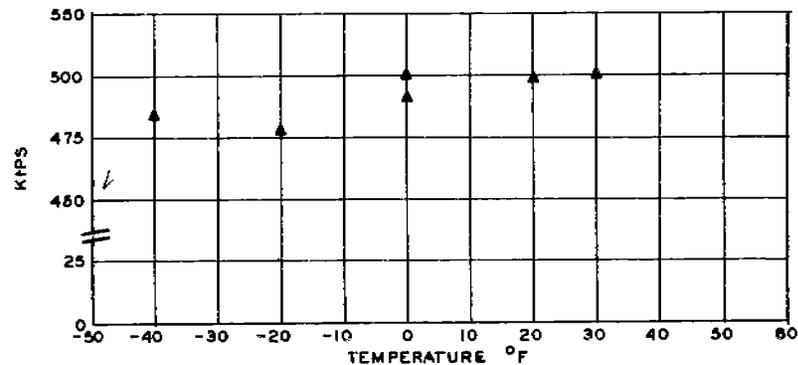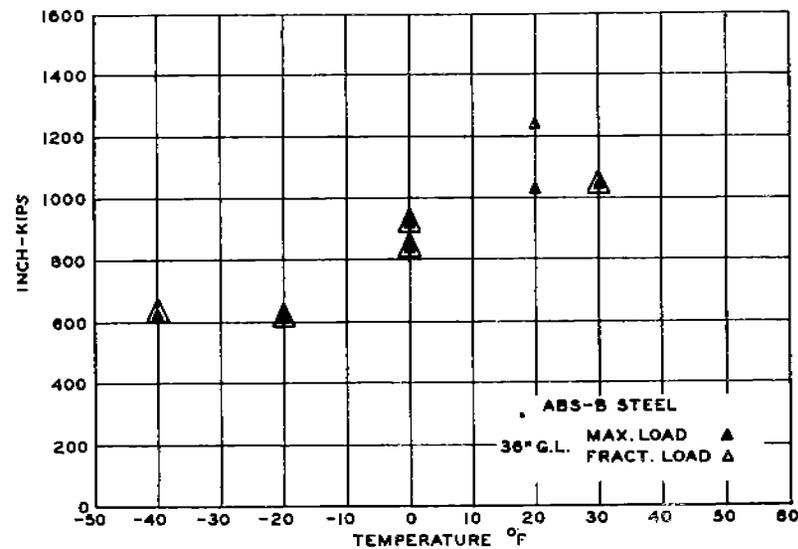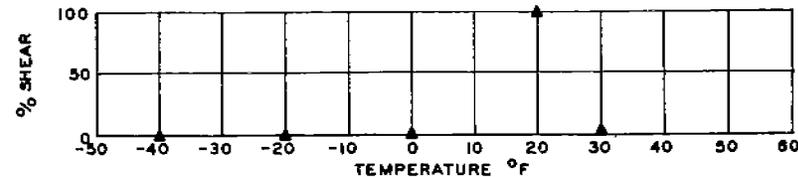
NOTE: TYPE ZE SPECIMENS
WERE NOT TESTED
USING DN STEEL
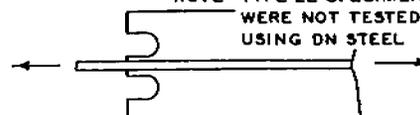
FIG. 38

SUMMARY
TYPE ZE SPECIMENS

SWARTHMORE COLLEGE

-43-

Type Z-E has approximately the same load resisting and
energy absorbing capacity as Z-C2. With respect to transition
temperature, based on appearance of the fracture, Type Z-E has
a transition temperature of +10°F. This disregards the one test
at +30°F using D'_N flat bars. The temperature of +10°F is 20°F
lower than that obtained for Type Z-C2. With the evidence at
hand the investigators can only conclude that the overall char-
acteristics of Type Z-E are certainly as good as for Z-C2, and
may be better with respect to transition temperature.

Type Z-T

The Type Z-T specimen, designed to simulate a bilge keel
ending detail, was tested at -40°F. The specimen exhibited
a cleavage fracture which initiated through the toes of the
fillet welds at the ends of the Tee sections at a load of
465 kips. The energy absorbed by the specimen to the fracture
load was 397 inch-kips. The maximum load and energy absorption
were of approximately the same order of magnitude as the Type
Z-B specimen with main plate of ABS-B at the same test tem-
perature.

OVERALL DISCUSSION

To assist in giving an overall view of the physical response
of the Type Z specimens, Table V provides in summary form values
of average maximum load, average energies to maximum load, and
transition temperature. The average loads and energies are given
separately for specimens failing in 100% shear and 0% shear. The

TABLE V

Summary of Test Results Type Z Specimens

Type of Specimen	Combinations of Types of Steel 3/4" Main Plate	Combinations of Types of Steel 1/2" Flat Bars	Average Maximum Loads, kips 100% Shear Fractures	Average Maximum Loads, kips 0% Shear Fractures	Average Energy* to Max. Load, in.-kips 100% Shear Fractures	Average Energy* to Max. Load, in.-kips 0% Shear Fractures	Transition Temperature, °F Based on Fracture Appearance	Transition Temperature, °F Based on Energy to Max. Load
Z-3	D_N	D_N	517 (2)	522 (1)	1190 (2)	518 (1)	0°	-4°
Z-3	DN	D'_N		485 (1)		500 (1)		
Z-3	ABS-B	D_N	485 (2)	475 (5)	857 (2)	616 (5)	+30°	-8°
Z-3	ABS-B	D'_N		464 (2)		465 (2)		
Z-B	D_N	D_N	533 (2)	529 (1)	1352 (2)	890 (1)	-30°	
Z-B	ABS-B	D_N	492 (1)	503 (3)	985 (1)	1040 (3)	+10°	
Z-B	ABS-B	D'_N		463 (1)		392 (1)		
Z-BM	ABS-B	D'_N	505[2] (1)	504 (4)	1195[2] (1)	899 (4)	+25° approx.	
Z-C1	D_N	D_N	524 (1)	504 (1)	1165 (1)	728 (1)	-10°	
Z-C2	D_N	D_N	523 (2)	536 (1)	1255 (2)	995 (1)	-26°	
Z-C2	ABS-B	D_N		494 (3)		893 (3) above	+20°	
Z-C2	ABS-B	D'_N		477 (1)		482 (1)	+30° approx.	
Z-D	ABS-B	D_N		460 (3)		472 (3) above	+20°	
Z-D	ABS-B	D'_N		473 (2)		486 (2) above	+40°	
Z-E	ABS-B	D_N	498 (1)	489 (4)	1032 (1)	748 (4)	+10°	
Z-E	ABS-B	D'_N		500[1] (1)		1040[1] (1) above	+30°	

(Not ascertainable)

*D_N Specimens 40" long
ABS-B Specimens 36" long

1) 5% shear
2) 90% shear

Numbers in parentheses indicate the number of specimens averaged.

transition temperatures given are based almost entirely on appearance of fracture. For most types the establishment of transition temperatures from energy curves was limited by too few data.

Transition temperature is the most discriminating characteristic for evaluating the geometry of the flat bar end conditions. The range of transition temperatures summarized in Table V emphasizes the importance of choosing the most favorable end contour on the flat bars, which were intended to simulate interrupted longitudinals and stiffeners.

The exploratory program, which disclosed strain patterns and stress directions, indicates that through changing the end geometry, the direction of stress on the end weld relative to the main plate can be altered. The endings investigated disclosed that the direction of principal stress can be changed from approximately a right angle to the face of the main plate in the case of the square cut-off, to 45° for the 45° cut-off, and to a direction parallel to the main plate with a curved ending. It is thought that this change in direction is one factor in establishing conditions for fracture in the weld and the plate directly beneath the weld.

Simultaneously with the limiting of stress direction, the end contours of the flat bars limit the total force acting on the end welds. The cutting away of material reduces the load carrying ability of the flat bar in the critical region at the

fractured cross-section. This second effect is integrated with
the stress direction; i.e., with a reduced flat bar cross-section
of a given contour, stress direction and magnitude may be con-
trolled. A favorable combination will lower transition tempera-
ture, as evidenced by the results for Type Z-B, and increase the
expectancy of ductile action in the main plate. Test results
roughly follow this reasoning but do not precisely confirm it.

For reasons stated before, the Type Z-3 (square cut-off
flat bars) was made the base for comparison purposes. For
main plates of D_N steel, end modifications of types Z-B, Z-Cl
and Z-C2 resulted in lower transition temperatures than for Z-3.
The radius contour of Type Z-B depressed the transition tempera-
ture by the greatest amount. Although the radius contour of
Type Z-B was the most beneficial, the Type Z-C2 flat bar
termination with flame cut hole was essentially equal to Type
Z-B in depressing transition temperature.

For specimens using main plates of ABS-B steel, benefits
of lower transition temperature are shown for Types Z-B and
Z-E. Type Z-C2 was equal to Type Z-3, whereas Type Z-BM was
only slightly beneficial in lowering transition temperature.
Type Z-D, with flat bars cut off at 45°, had a higher transition
temperature than the square cut-off of series Z-3. It should
be noted that the transition temperatures of all specimens
using ABS-B steel was higher than those of D_N steel for all end
variations where duplicating tests were made.

The Type Z-BM specimens, with end contour cut to a radius with a slightly upturned end, were expected to be as good, relative to transition temperature, as Type Z-B, where the upturned end was eliminated. Limited tests did not confirm this opinion. However, the differences in transition temperature may be due to the D'_N flat bars used in all Z-BM specimens.

In comparing the transition temperatures of Types Z-C1 and Z-C2 with 2-in. diameter burned holes, having main plates of D_N steel, the straight cut from end of flat bar to the circular hole as in Type Z-C2 was beneficial in lowering transition temperature. For ABS-B steel plates no direct comparisons between the two types were possible due to lack of tests of Type Z-C1. Comparing the results of Z-C2 with Type Z-3, with ABS-B steel it appears that no definite benefits accrue. Thus for D_N steel the detail of Z-C2 appears beneficial, and for ABS-B steel it does not.

The effects of various flat bar endings on maximum load (see Table V) and the graphical summaries of Figs. 39 and 40 permit certain generalizations to be made.

First, the maximum load, within the limits of reliability of test results, does not appear to be significantly affected by the end contours, although there is an indication that the end radius of Type Z-B is better than square cut-offs in this respect. Since Type Z-B is definitely preferential to Z-3 with respect to transition temperature, its improved load
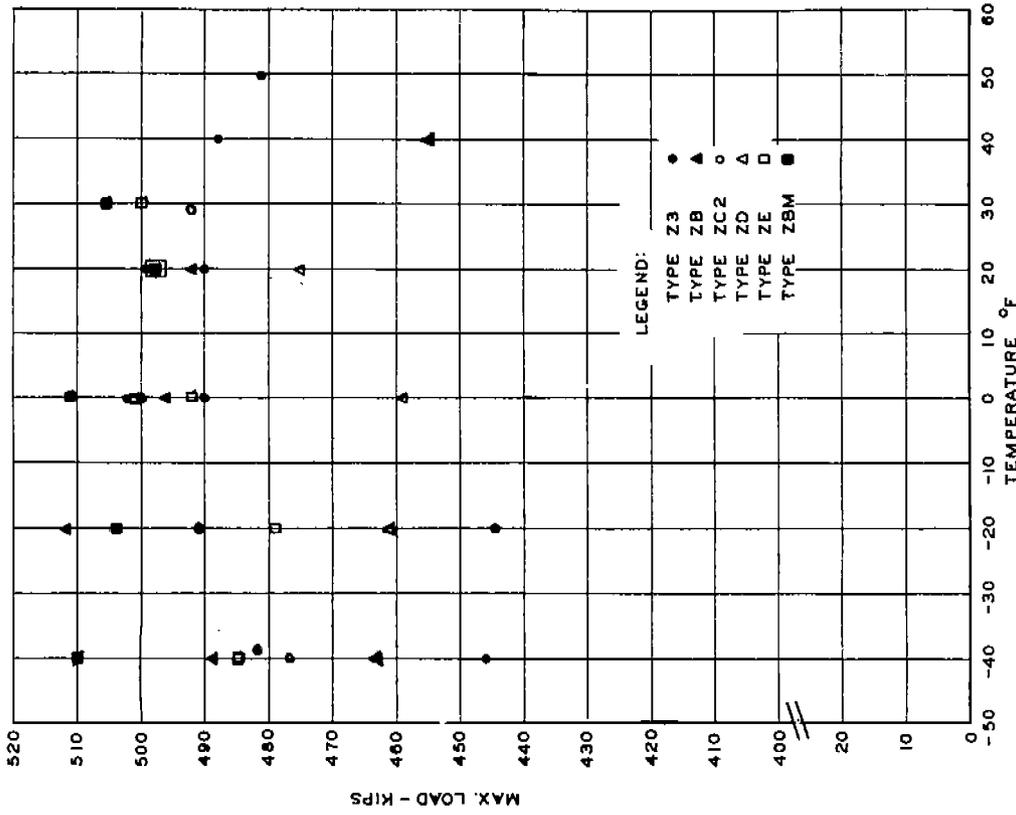
FIG.40 SUMMARY – MAXIMUM LOAD VS. TEMPERATURE
TYPE Z SPECIMENS – ABS–B STEEL
GAGE LENGTH 36"

SWARTHMORE COLLEGE
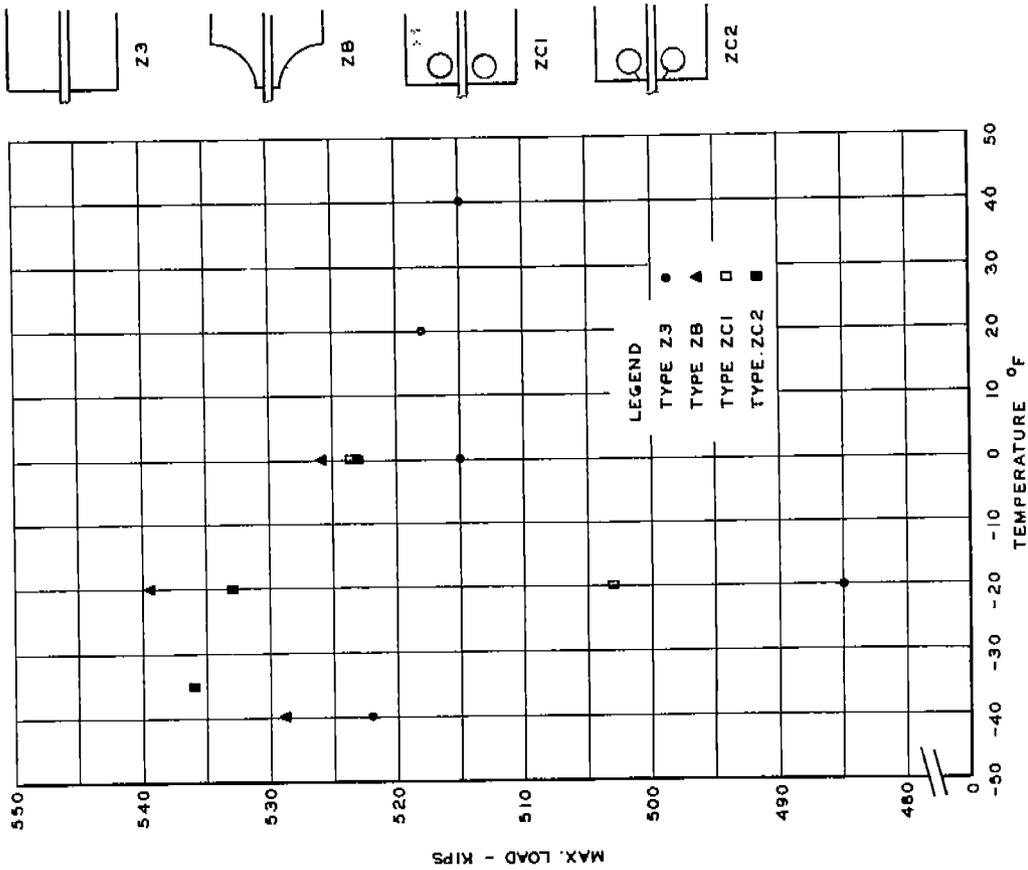
FIG.39 SUMMARY – MAXIMUM LOAD VS. TEMPER–
ATURE
TYPE Z SPECIMENS–QN STEEL
GAGE LENGTH 40"

SWARTHMORE COLLEGE

performance also provides a sound reason for favoring this detail.

Second, the average maximum loads, in general, are nearly alike for either cleavage failures or shear failures for a given type of specimen and kind of steel. Average loads as high, or often higher, for cleavage failure than for shear failure are not a new finding and have been reported before by this laboratory.[2] A close examination of the maximum load tabulations for varying temperatures (plotted in Figs. 39 and 40) revals much scatter in loads for both the shear and cleavage modes. In general, the low load values for the cleavage mode occurred at a temperature 20 to 30°F lower than the transition.

The energies to maximum load are summarized in Table V and shown in Figs. 41 and 42. For D_N steel plates, Type Z-B (radius cut ending) shows the highest energy values. This, along with the favorable trends in transition temperature and load capacity, adds further evidence to the suitability of the Z-B form. Again Z-C2 runs a close second to Z-B.

Energies to maximum load remain high for cleavage fractures at 20°F to 30°F below the transition from shear to cleavage fracture. Evidence of this may be noted for each type of specimen. The average energies for the cleavage mode are perhaps meaningless unless each test is viewed separately. As a practical matter of selecting a transition temperature based on energy, one finds that these high values act to lower the transition temperature from that based on
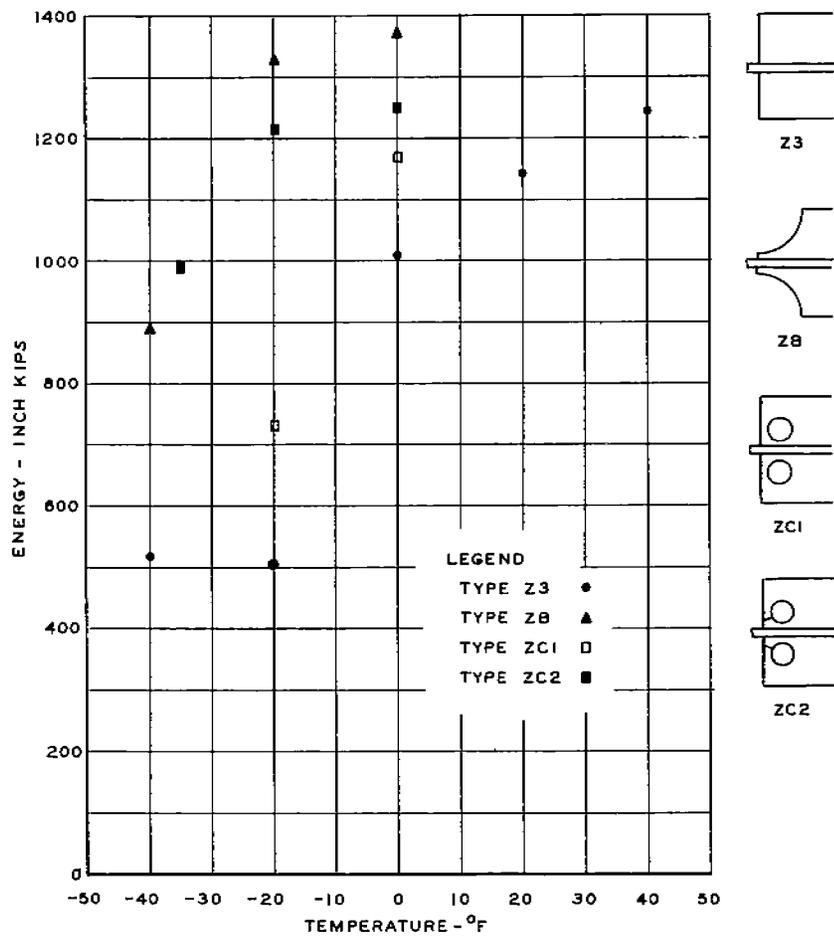
FIG.41 SUMMARY – ENERGY TO MAXIMUM LOAD
VS. TEMPERATURE
TYPE Z SPECIMENS – DN STEEL
GAGE LENGTH 40"

SWARTHMORE COLLEGE
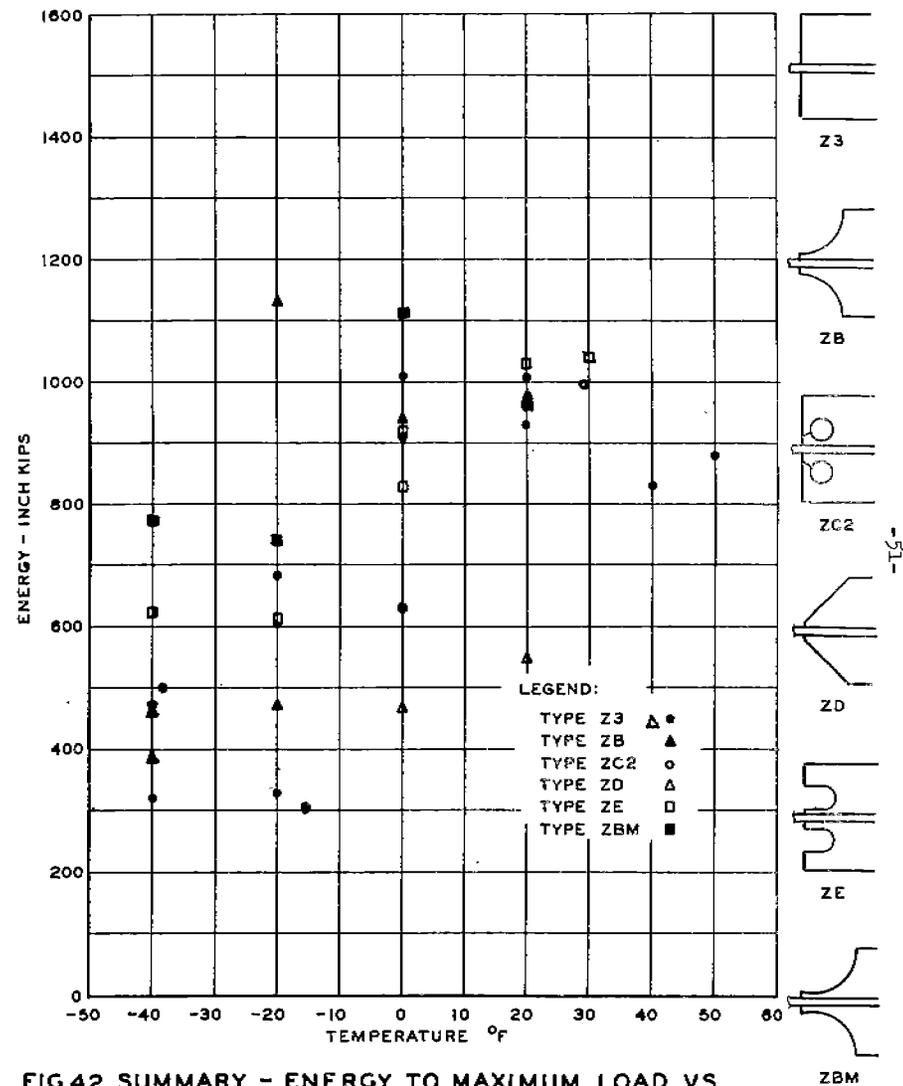
FIG.42 SUMMARY – ENERGY TO MAXIMUM LOAD VS.
TEMPERATURE
TYPE Z SPECIMENS – ABS-B STEEL
GAGE LENGTH 36"

SWARTHMORE COLLEGE

fracture appearance. For the square ended Type Z-3 of D_N steel, the transition temperature so determined is 4°F lower and for the ABS-B steel, 38°F lower than values based on fracture appearance. Thus, on an energy basis, the ABS-B steel would have a 4°F lower transition temperature than the D_N steel, whereas the ABS-B steel had a transition temperature 30°F higher than D_N steel based on fracture appearance. This is an anomaly that cannot be further investigated for other types because of limited data.

SUMMARY STATEMENTS

It often appears warranted to limit the reliability and applicability of test results by qualifying statements. If that were to be done here, it would be essential to note: (a) that the main plates of all specimens were narrow relative to the details; (b) that the edges of the main plate, representing a hull or bulkhead plate were free from lateral restraint; and (c) that limited tests were made as dictated by economy and available steel. All of these reservations would make certain conclusions relative to full-size ship details uncertain. However, since all of these conditions were appropriately noted when establishing this investigation, it is hoped that this work may point out the direction that future work should take or that the present data may be utilized in at least a qualitative manner for guiding immediate practical considerations where geometrical notches are involved.

(1) Test results confirm the long standing belief that abrupt changes in structural geometry can only have detrimental effects. While abrupt changes in structural geometry are critical, as has been clearly demonstrated by a large number of actual casualties, little has been known about the actual relief that could be furnished by modifications in geometry. The test results indicate that anything short of the most practical smooth structural transition, from one structural component to another, impairs load

capacity, energy absorption, and raises transition temperature.

(2) The structural notch effect of abrupt or gradually faired terminations of structural components, as exemplified by free ended longitudinals or stiffeners, is a result of the compounding of concentrations of stress and the direction of that stress at the termination. Favorable combinations of this compound effect tend to eliminate the structural notch. A favorable combination of the compounding effects can be attained when the stress direction at the free end of a longitudinal is as nearly parallel to the hull or bulkhead plating as possible, in conjunction with a decrease in the magnitude of this stress. The direction may be controlled by smooth contour endings and the stress magnitude reduced by a reduction in end cross-sectional area. It has been found that the most favorable combination results when the end contour of a longitudinal is cut to a radius.

(3) Transition temperature was the most important characteristic in comparing the results of variable end geometry of the Type Z specimens. Load and energy absorption were less critically affected by changes in type of endings.

(4) The study reported herein does not lend itself to a critical separation of geometrical and welding notch effects. It is essential to keep in mind that the most favorable geometric condition would be nullified by a weld of poor penetration.

(5) While it was not the overall purpose of this program to

compare the notch sensitivity of D_N and ABS-B steels, such a comparison can be made. The ABS-B steel used was definitely inferior to D_N steel on a transition temperature basis. The other characteristics of ABS-B compared with D_N, such as load capacity and energy absorption, is more favorable.

BIBLIOGRAPHY

1. Progress Summary, "Investigation of Fractured Steel Plates Removed from Welded Ships" SSC Report, Serial No. NBS-3, Dated June 1, 1951, Williams, M. L., Myerson, M. R., Kluge, G. L., and Dale, L. R.

2. First Progress Report, "Cracking of Simple Structural Geometries: The Effects of Edge Notch Geometry on Flat Steel Plates", SSC Report, Serial No. SSC-51, Dated May 12, 1952, Carpenter, S. T., and Linsenmeyer, R. F., Swarthmore College.

3. Progress Report on Correlation of Laboratory Tests with Full Scale Ship Plate Fracture Tests, Pennsylvania State College, Research Project SR-96, SSC Report, Serial No. SSC-9, March 19, 1947, by M. Gensamer, E. P. Klier, T. A. Prater, F. C. Wagner, J. O. Mack, and J. L. Fisher

ACKNOWLEDGMENTS

APPENDIX A

Tables of Basic Data

TABLE I-A

DATA SUMMARY - TYPE Z-3 Specimens

Steel	Specimen No.	Test Temp. °F	% Shear Fracture Surfaces	Maximum Load Kips	Fracture Load Kips	Energy to Max. Load Inch-Kips	Energy to Fracture Load Inch-Kips	Elongation to Max. Load Inches	Elongation to Fracture Load
D_N	H-6	40	100	515.2	510	1,245.0	1,323.5	2.75	2.90
D_N	G-14	20	100	518	205	1,141.0	1,453.5	2.55	3.2
D_N	G-13	0	50	515	325	1,007.0	1,172.0	2.30	2.65
D_N	H-5	-40	0	522	522	517.5	517.5	1.08	1.08
D_N	*H-16	-20	0	485	485	500.5	500.5	1.240	1.240
ABS-B	I-1	0	0	502	502	1,012.5	1,012.5	2.370	2.370
ABS-B	I-2	+20	0	499	499	930.0	930.0	2.180	2.180
ABS-B	I-3	-40	0	446	446	322.5	322.5	0.875	0.875
ABS-B	I-4	+40	100	488.5	50	832.5	1,070.0	2.100	2.835
ABS-B	I-5	+50	100	481.5	40	881.5	1,044.0	2.15	2.890
ABS-B	J-2	-20	0	444	444	332.5	332.5	0.935	0.935
ABS-B	J-3	-38	0	483	483	500.0	500.0	1.305	1.305
ABS-B	*J-14	0	0	490	490	626.0	626.0	1.555	1.555
ABS-B	*J-15	-15	0	437.5	437.5	303.5	303.5	0.865	0.865

TABLE II-A

DATA SUMMARY - TYPE Z-B Specimens

Steel	Specimen No.	Test Temp. °F	% Shear Fracture Surfaces	Maximum Load Kips	Fracture Load Kips	Energy to Max. Load Inch-Kips	Energy to Fracture Load Inch-Kips	Elongation to Max. Load Inches	Elongation to Fracture Load
D_N	H-9	0	100	526	519	1375	1490	3.00	3.22
D_N	H-14	-20	100	539.5	534	1330	1331	3.00	3.03
D_N	H-13	-40	0	529	529	390	890	2.035	2.035
ABS-B	I-12	+20	100	492.0	85.0	985.0	1170.0	2.375	3.000
ABS-B	I-6	0	0	496.0	496.0	945.0	945.0	2.265	2.265
ABS-B	I-7	-20	0	511.5	511.5	1136.0	1136.0	2.605	2.605
ABS-B	*I-9	-40	0	463.0	463.0	392.5	392.5	1.055	1.055

TABLE III-A

DATA SUMMARY - TYPE Z-C1 Specimens

Steel	Specimen No.	Test Temp. °F	% Shear Fracture Surfaces	Maximum Load Kips	Fracture Load Kips	Energy to Max. Load Inch-Kips	Energy to Fracture Load Inch-Kips	Elongation to Max. Load Inches	Elongation to Fracture Load
D_N	H-7	0	100	523.6	180	1,165	1,440	2.6	3.25
D_N	H-10	-20	0	503.5	503.5	728	728	1.72	1.72

TYPE Z-C2 Specimens

Steel	Specimen No.	Test Temp. °F	% Shear Fracture Surfaces	Maximum Load Kips	Fracture Load Kips	Energy to Max. Load Inch-Kips	Energy to Fracture Load Inch-Kips	Elongation to Max. Load Inches	Elongation to Fracture Load
D_N	H-8	0	100	523	515	1,255	1,515	2.75	3.25
D_N	H-15	-20	90	533.5	230	1,215	1,412	2.65	3.075
D_N	H-11	-35	0	536.5	536.5	995	995	2.20	2.20
ABS-B	I-14	+20	0	490	490	1,080	1,080	2.550	2.550
ABS-B	I-15	0	0	500	500	915	915	2.135	2.135
ABS-B	I-16	-20	0	491.5	491.5	685	685	1.685	1.685
ABS-B	*J-5	-40	0	477.0	477.0	482.5	482.5	1.260	1.260
ABS-B	*J-6	+29	50	492.0	280	997.5	1,155	2.375	2.790

*D'_N Steel Side Bars

TABLE IV-A

DATA SUMMARY — TYPE Z-D Specimens

Steel	Specimen No.	Test Temp. °F	% Shear Fracture Surfaces	Maximum Load Kips	Fracture Load Kips	Energy to Max. Load Inch-Kips	Energy to Fracture Load Inch-Kips	Elongation to Max. Load Inches	Elongation to Fracture Load
ABS-B	I-9	+20	0	475	475	555.0	555.0	1.425	1.425
ABS-B	I-8	0	0	459	459	470.0	470.0	1.250	1.250
ABS-B	J-1	-20	0	461	461	475.0	475.0	1.275	1.275
ABS-B	*J-4	-40	0	489	489	467.5	467.5	1.195	1.195
ABS-B	*J-10	+40	0	455	455	455.0	455.0	1.215	1.215

TABLE V-A

DATA SUMMARY — TYPE Z-E Specimens

Steel	Specimen No.	Test Temp. °F	% Shear Fracture Surfaces	Maximum Load Kips	Fracture Load Kips	Energy to Max. Load Inch-Kips	Energy to Fracture Load Inch-Kips	Elongation to Max. Load Inches	Elongation to Fracture Load
ABS-B	I-10	+20	100	498	75	1,032.5	1,247.5	2.400	3.100
ABS-B	I-13	-20	0	479	479	615.	615.	1.565	1.565
ABS-B	I-17	-40	0	485.5	485.5	626.	626.	1.580	1.580
ABS-B	I-11	0	5	500.5	500.5	920.	921.5	2.165	2.200
ABS-B	I-18	0	0	492	492.	832.5	832.5	2.025	2.025
ABS-B	*J-8	+30	5	500	499	1,040.0	1,040.0	2.390	2.420

TABLE VI-A

DATA SUMMARY — TYPE Z-E Specimens

Steel	Specimen No.	Test Temp. °F	% Shear Fracture Surfaces	Maximum Load Kips	Fracture Load Kips	Energy to Max. Load Inch-Kips	Energy to Fracture Load Inch-Kips	Elongation to Max. Load Inches	Elongation to Fracture Load
ABS-B	*J-11	-20	0	504		740.0	740.0	1.770	1.770
ABS-B	*J-7	0	0	510.5		1,116.0	1,116.0	2.570	2.570
ABS-B	*J-18	-40	0	510.		782.5	782.5	1.885	1.885
ABS-B	*J-13	+20	0	498		957.5	957.5	2.300	2.300
ABS-B	*J-16	+30	90	505		1,195.0	1,400.0	2.750	.3.450

*D'N Steel Side Bars

TABLE VII-A

DN Steel – Type YW1 Specimens

Flat Plate Tests – Size: 13½" wide x 3/4" thick x 40" long

Longitudinal Weldment

Spec. No.	Temp. °F.	% Shear Fracture Surfaces	Loads in Kips			Energy in Inch Kips						Elongation in Inches*			
			Visible Crack	Max.	Fract.	To Vis. Crack 16½"	40"	To Maximum Load 16½"	40"	To Fracture 16½"	40"	Max. Load 16½"	40"	Fracture 16½"	40"
G–6	40	100	–	500.5	230.0	–	–	1,480.0	2,320.0	1,760.0	2,625.0	3.240	5.135	3.890	5.875
G–5	30	100	–	507.0	140.0	–	–	1,480.0	2,353.0	2,160.0	3,118.0	3.250	5.225	5.040	6.935
G–7	20	0	–	519.0	519.0	–	–	1,525.0	2,430.0	1,525.0	2,430.0	3.270	5.275	3.27	5.275
G–8	15	100	–	525.0	458.0	–	–	1,525.0	2,345.0	2,540.0	3,165.0	3.260	5.100	5.250	6.700
G–4	0	0	–	515.5	515.5	–	–	1,205.0	1,995.0	1,205.0	1,995.0	2.675	4.370	2.675	4.370
F–10	–35	0	–	554.5	554.5	–	–	1,910.0	3,050.0	1,910.0	3,050.0	3.650	6.150	3.650	6.150

TABLE VIII-A

DN Steel – Type YW 2 Specimens

Flat Plate Tests – Size: 13½" wide x 3/4" thick x 40" long

Longitudinal Weldment

Spec. No.	Temp. °F.	% Shear Fracture Surfaces	Loads in Kips			Energy in Inch Kips						Elongation in Inches*			
			Visible Crack	Max.	Fract.	To Vis. Crack 16½"	40"	To Maximum Load 16½"	40"	To Fracture 16½"	40"	Max. Load 16¼"	40"	Fracture 16¼"	40"
H–1	20	90	–	516.2	221	–	–	1,430.0	2,285.0	1,570.0	2,915.0	3.13	5.02	3.26	6.50
H–2	0	100	–	525	235	–	–	1,580.0	2,390.0	2,725.0	3,475.0	3.36	5.16	5.60	7.95

TABLE IX-A

DN Steel – Type YW 3 Specimens

Flat Plate Tests – Size: 13½" wide x 3/4" thick x 40" long

Longitudinal Weldment

Spec. No.	Temp. °F.	% Shear Fracture Surfaces	Loads in Kips			Energy in Inch Kips						Elongation in Inches*			
			Visible Crack	Max.	Fract.	To Vis. 16½"	Crack 40"	To Maximum Load 16½"	40"	To Fracture 16½"	40"	Max. Load 16½"	40"	Fracture 16½"	40"
H–4	15	0	–	410	410	–	–	279.0	369.4	279.0	369.4	0.79	1.045	0.79	1.045
H–3	0	0	–	410	410	–	–	221.0	339.4	221.0	339.4	0.64	0.955	0.64	0.955
H–12	+50	100	–	445	334	–	–	395.0	737.5	692.0	1020.0	1.45	1.72	1.79	2.64

*Energy and elongation given for 16½" and 40" Gage Lengths

APPENDIX B

LOAD ELONGATION DIAGRAMS
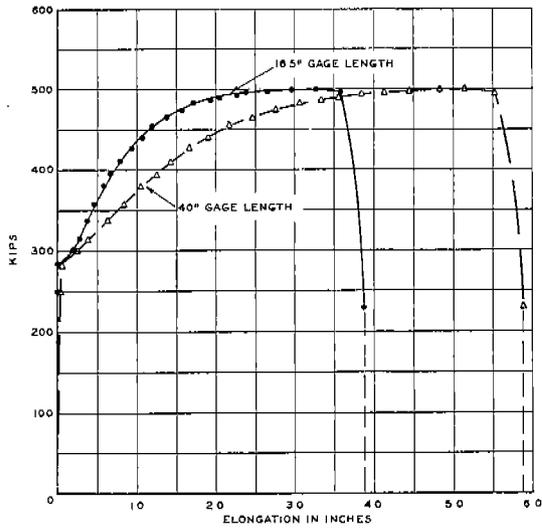
LEGEND:
SPECIMEN SIZE: 13½" X 40" X ¾"

FIG.I-B

LOAD-ELONGATION DIAGRAM
TYPE YWI SPECIMEN
DN-YWI-G6   40°F
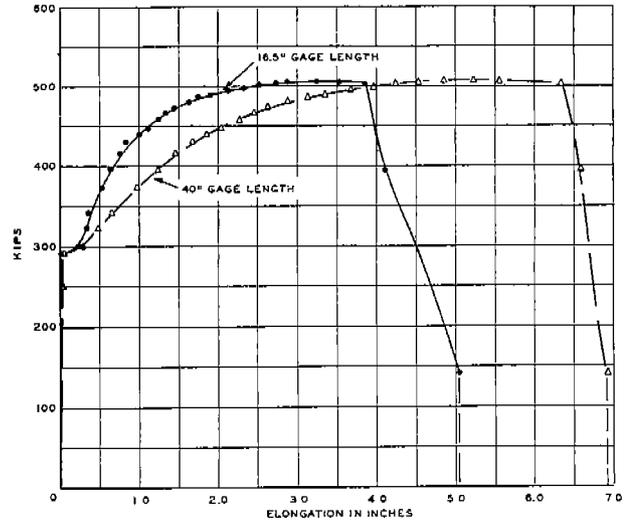
LEGEND:
SPECIMEN SIZE: 13½" X 40" X ¾"

FIG.II-B

LOAD-ELONGATION DIAGRAM
TYPE YWI SPECIMEN
DN-YWI-G5   30°F
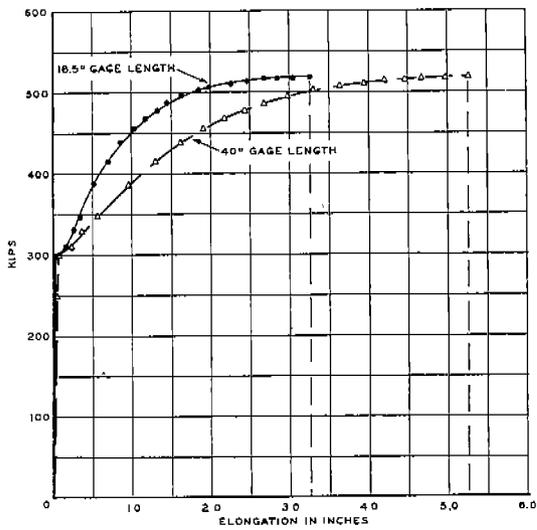
LEGEND:
SPECIMEN SIZE 13½" X 40" X ¾"

FIG.III-B

LOAD-ELONGATION DIAGRAM
TYPE YWI SPECIMEN
DN-YWI-G7   20°F

SWARTHMORE COLLEGE
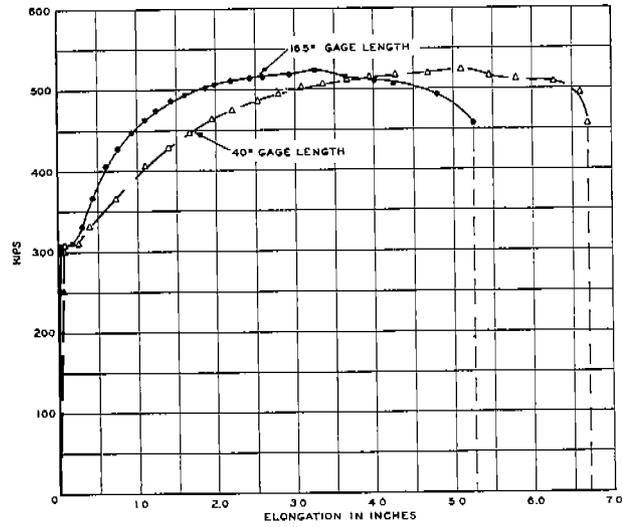
LEGEND
SPECIMEN SIZE: 13½" X 40" X ¾"

FIG.IV-B

LOAD-ELONGATION DIAGRAM
TYPE YWI SPECIMEN
DN-YWI-G8   15°F

SWARTHMORE COLLEGE
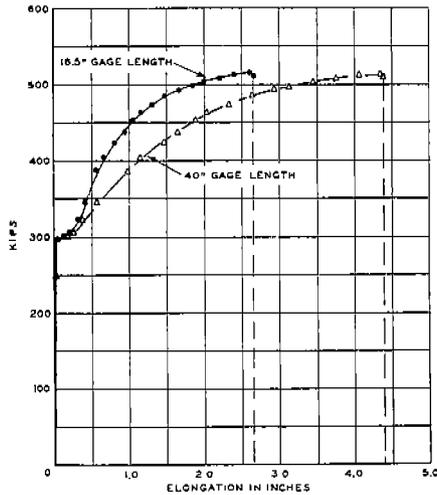
FIG. V-B
LOAD-ELONGATION DIAGRAM
TYPE YWI SPECIMEN
DN-YWI-G4   0°F
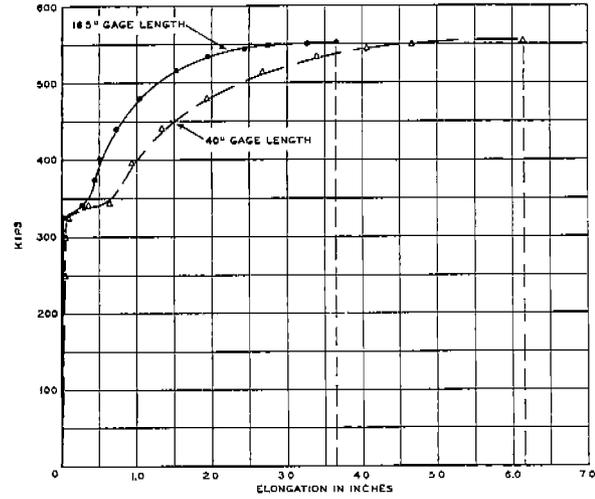
LEGEND
SPECIMEN SIZE: 13½" X 40" X ¾"

FIG. VI-B
LOAD-ELONGATION DIAGRAM
TYPE YWI SPECIMEN
DN-YWI-FIO   -35°F

LEGEND:
SPECIMEN SIZE: 13½" X 40" X ¾"
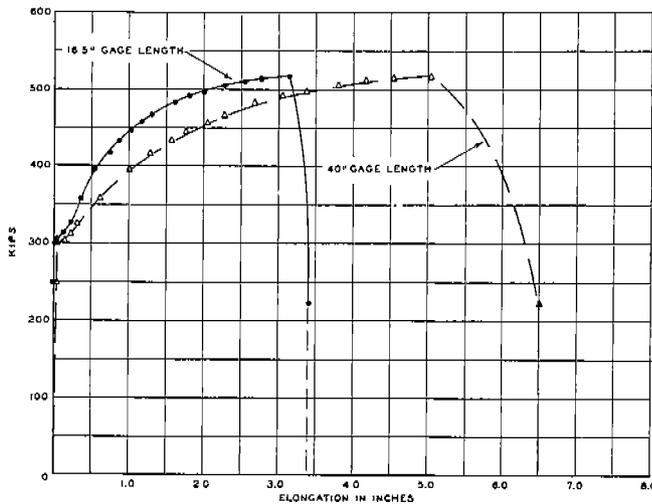
FIG. VII-B
LOAD-ELONGATION DIAGRAM
TYPE YW2 SPECIMEN
DN-YW2-HI   20°F
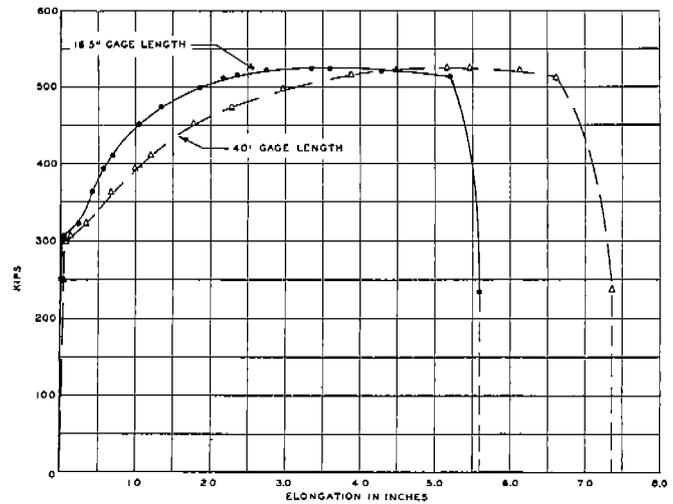
FIG. VIII-B
LOAD-ELONGATION CURVE
TYPE YW2 SPECIMEN
DN-YW2-H2   0°F
SWARTHMORE COLLEGE
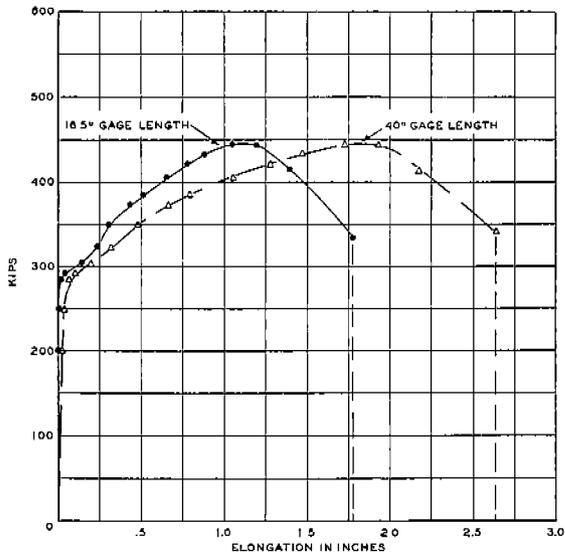
LEGEND
SPECIMEN SIZE: 13½" X 40" X ¾"

FIG. IX–B
LOAD–ELONGATION DIAGRAM
TYPE YW3 SPECIMEN
DN–YW3–H12   50°F
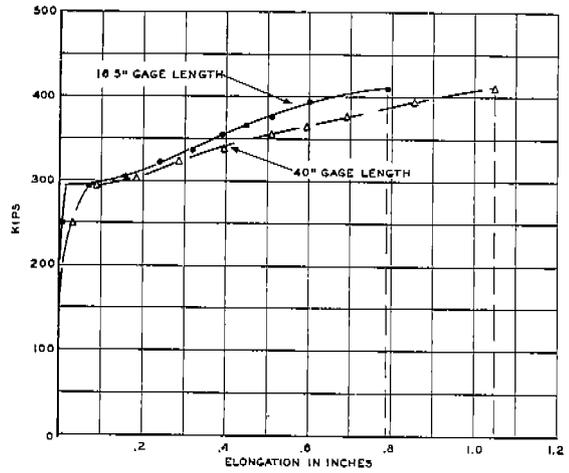
FIG. X–B
LOAD–ELONGATION DIAGRAM
TYPE YW3 SPECIMEN
DN–YW3–H4   15°F
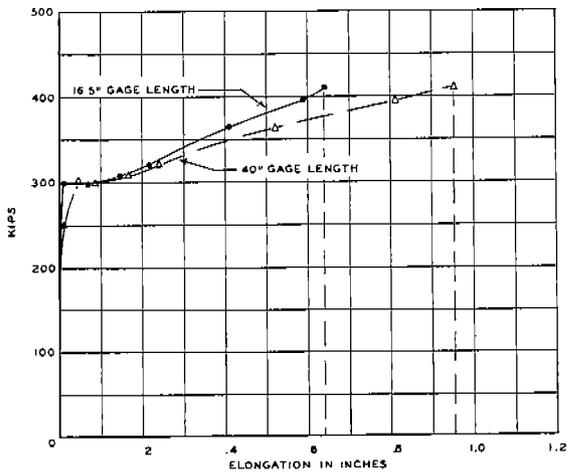
FIG. XI–B
LOAD–ELONGATION DIAGRAM
TYPE YW3 SPECIMEN
DN–YW3–H3   0°F
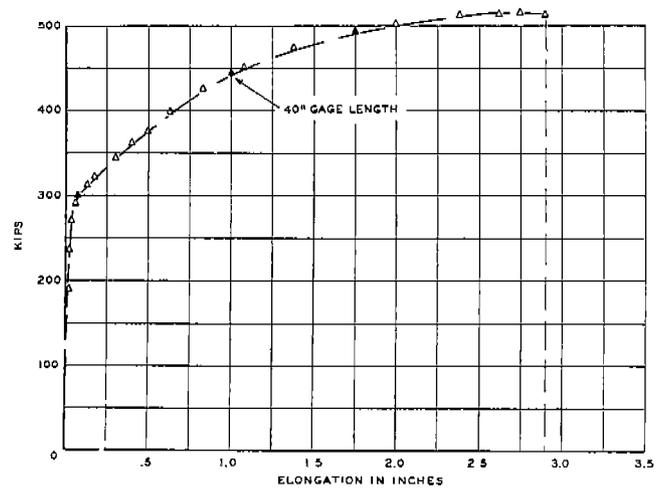
FIG. XII–B
LOAD–ELONGATION DIAGRAM
TYPE Z3 SPECIMEN
DN–Z3–H6   40°F

SWARTHMORE COLLEGE
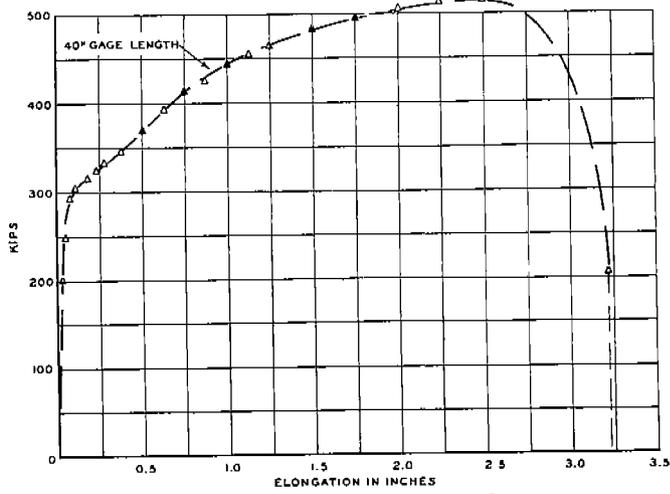
FIG. XIII-B
LOAD-ELONGATION DIAGRAM
TYPE Z3 SPECIMEN
DN-Z3-G14   20°F
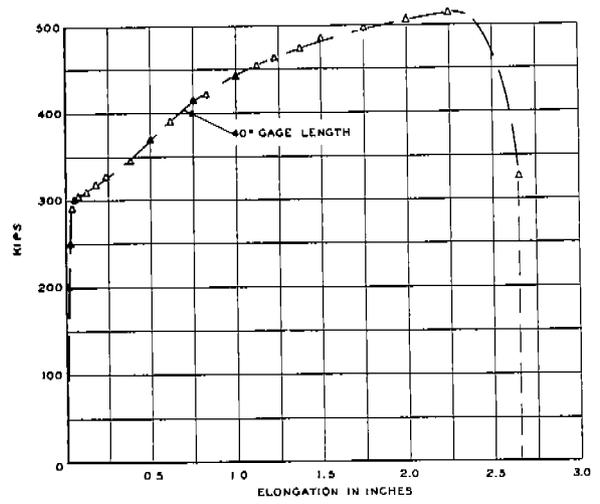
FIG. XIV-B
LOAD-ELONGATION DIAGRAM
TYPE Z3 SPECIMEN
DN-Z3-G13   0°F
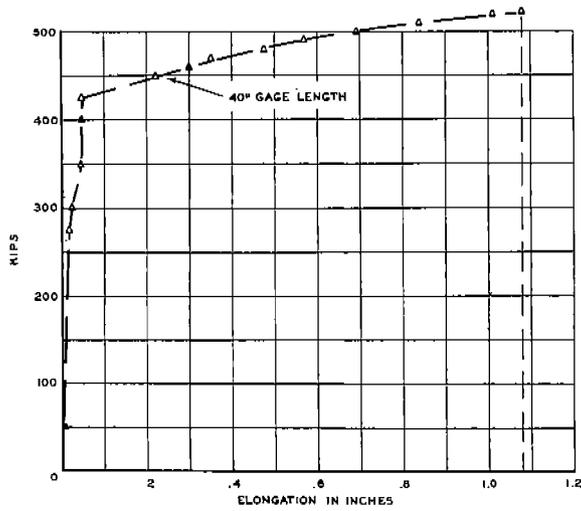
FIG. XV-B
LOAD-ELONGATION DIAGRAM
TYPE Z3 SPECIMEN
DN-Z3-H5   -40°F
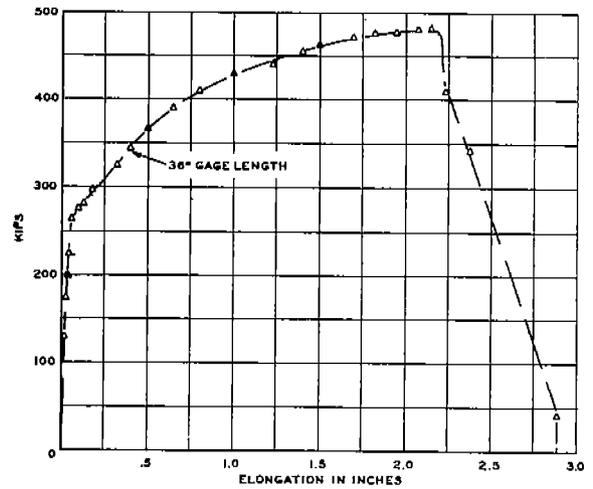
FIG. XVI-B
LOAD-ELONGATION DIAGRAM
TYPE Z3 SPECIMEN
ABS-B-Z3-I5   50°F   100% SHEAR

SWARTHMORE COLLEGE
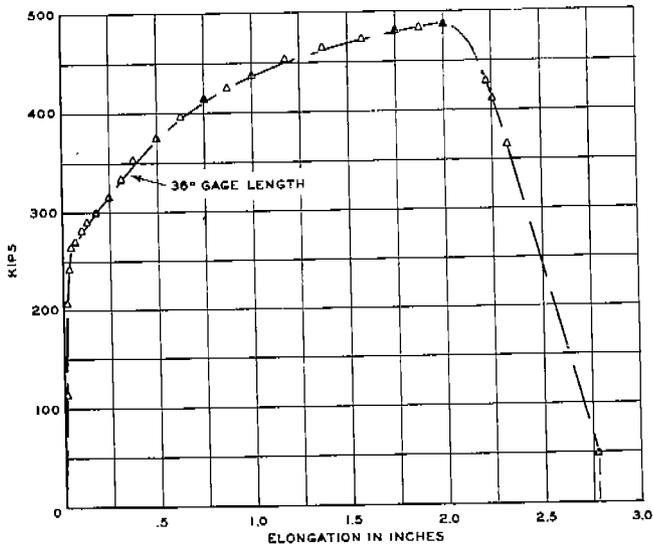
FIG. XVII-B
LOAD-ELONGATION DIAGRAM
TYPE Z3 SPECIMEN
ABS-B-Z3-I4   40°F 100% SHEAR
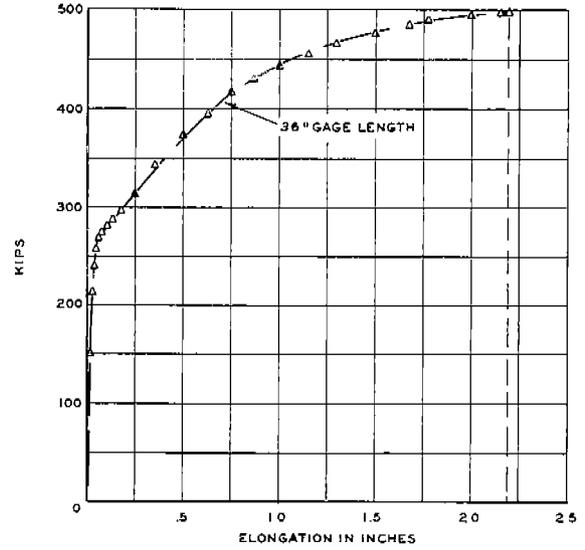
FIG. XVIII-B
LOAD-ELONGATION DIAGRAM
TYPE Z3 SPECIMEN
ABS-B-Z3-I2 20°F 0% SHEAR
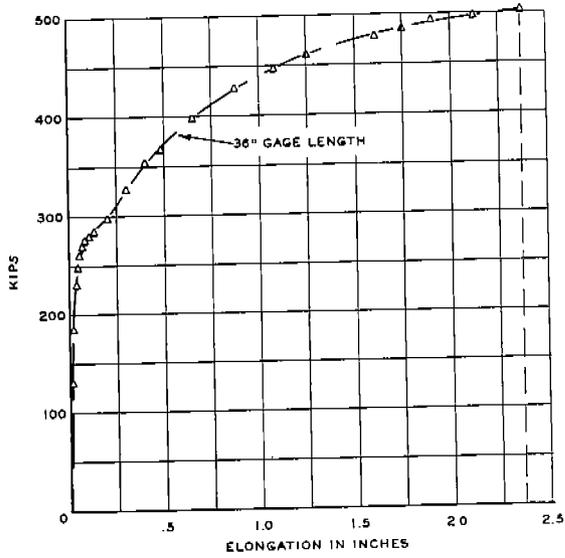
FIG. XIX-B
LOAD-ELONGATION DIAGRAM
TYPE Z3 SPECIMEN
ABS-B-Z3-I1 0°F 0% SHEAR

FIG. XX-B
LOAD-ELONGATION DIAGRAM
TYPE Z3 SPECIMEN
ABS-B-Z3-J14 0°F 0% SHEAR

SWARTHMORE COLLEGE

SWARTHMORE COLLEGE
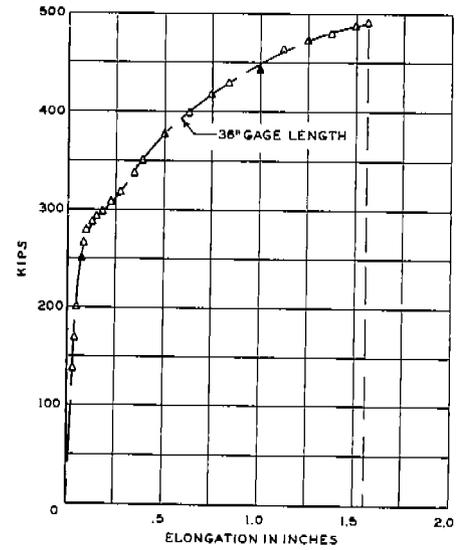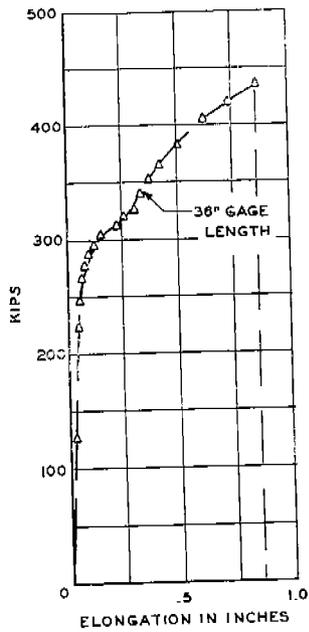
FIG. XXI-B
LOAD-ELONGATION DIAGRAM
TYPE Z3 SPECIMEN
ABS-B-Z3-J15 -15°F 0% SHEAR
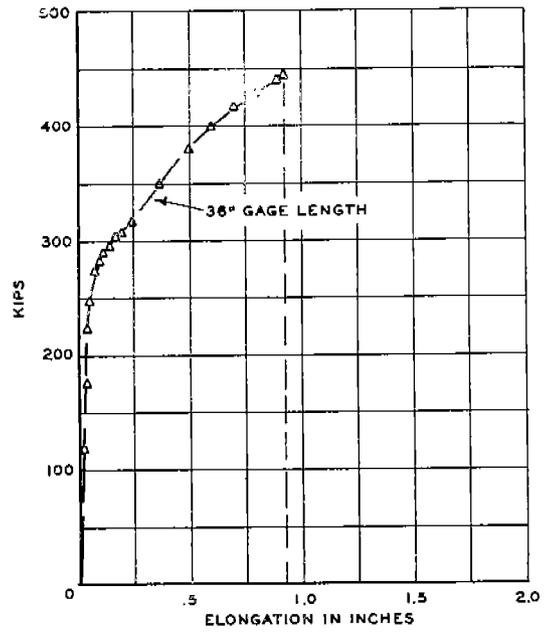
FIG. XXII-B
LOAD-ELONGATION DIAGRAM
TYPE Z3 SPECIMEN
ABS-B-Z3-J2 -20°F 0% SHEAR
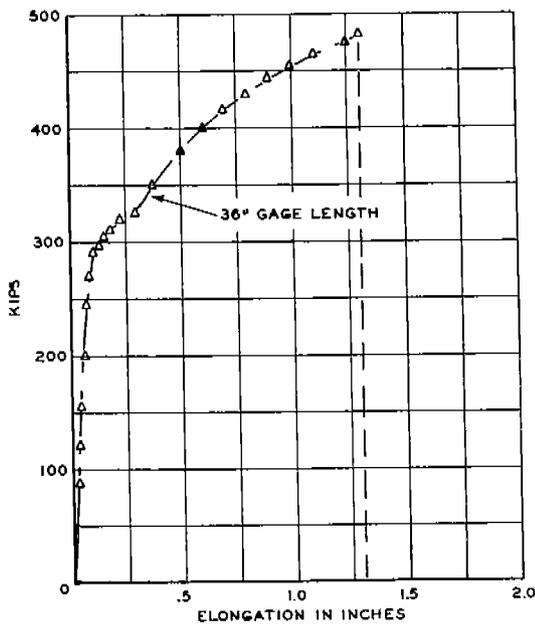
FIG. XXIII-B
LOAD-ELONGATION DIAGRAM
TYPE Z3 SPECIMEN
ABS-B-Z3-J3 -38°F 0% SHEAR
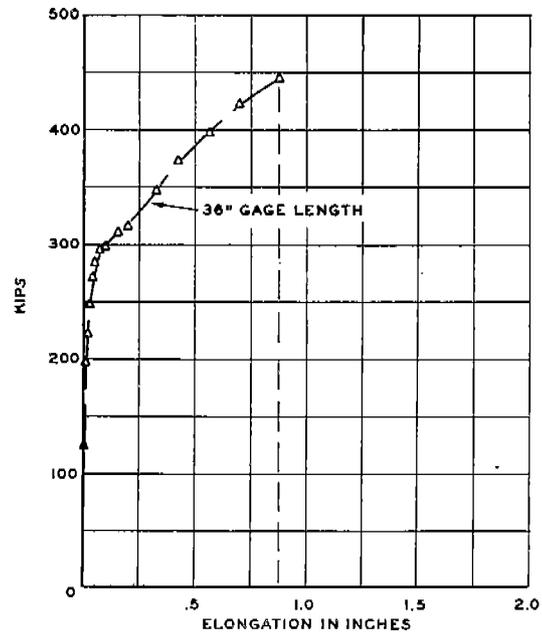
FIG. XXIV-B
LOAD-ELONGATION DIAGRAM
TYPE Z3 SPECIMEN
ABS-B-Z3-I3 -40°F 0% SHEAR
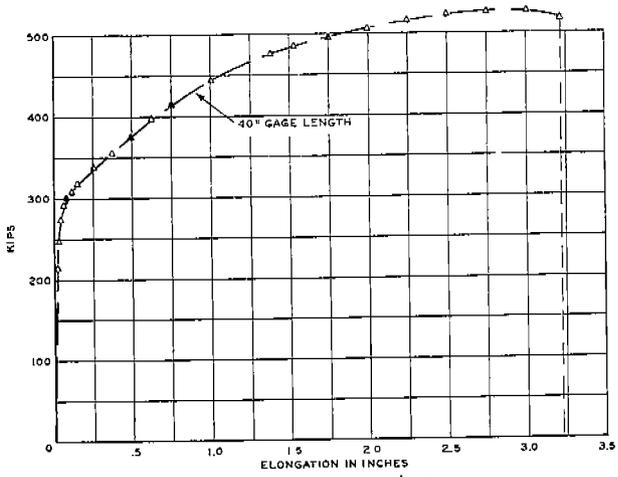
FIG. XXV-B

LOAD-ELONGATION DIAGRAM
TYPE ZB SPECIMEN
DN-ZB-H9   0°F
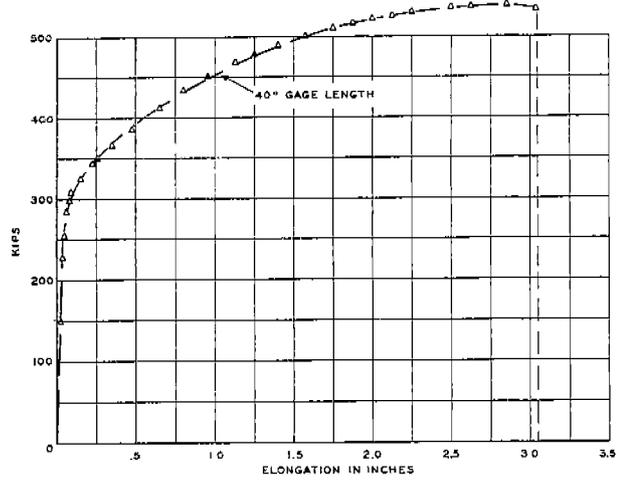
FIG. XXVI-B

LOAD-ELONGATION DIAGRAM
TYPE ZB SPECIMEN
DN-ZB-H14   -20°F
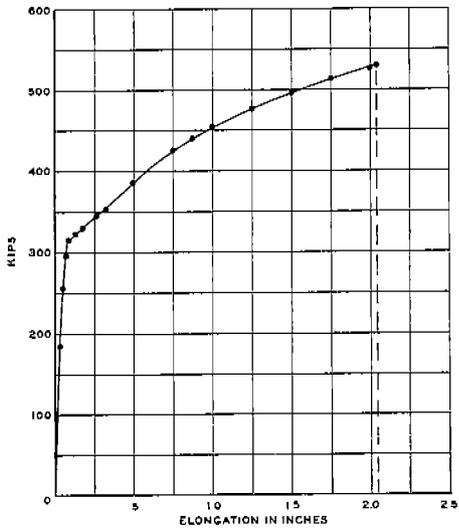
FIG. XXVII-B

LOAD-ELONGATION DIAGRAM
TYPE ZB SPECIMEN
DN-ZB-H13   -40°F   0% SHEAR

SWARTHMORE COLLEGE
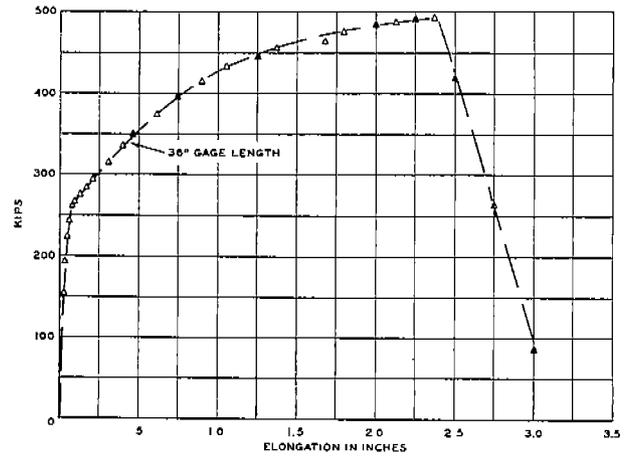
FIG. XXVIII-B

LOAD-ELONGATION DIAGRAM
TYPE ZB SPECIMEN
ABS-B-ZB-I12 20°F 100% SHEAR

SWARTHMORE COLLEGE
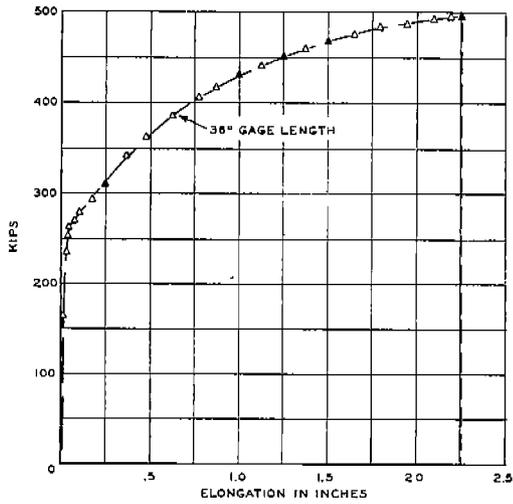
FIG. XXIX-B
LOAD-ELONGATION DIAGRAM
TYPE ZB SPECIMEN
ABS-B-ZB-I6 0°F 0% SHEAR
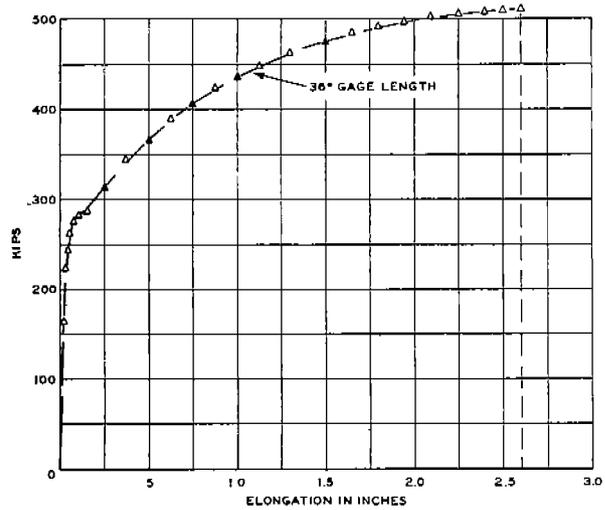
FIG. XXX-B
LOAD-ELONGATION DIAGRAM
TYPE ZB SPECIMEN
ABS-B-ZB-I7 -20°F 0% SHEAR
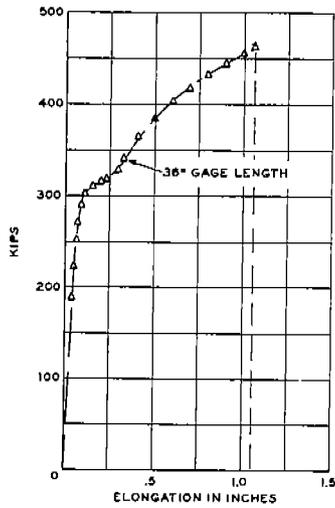
FIG. XXXI-B
LOAD-ELONGATION DIAGRAM
TYPE ZB SPECIMEN
ABS-B-ZB-I9 -40°F 0% SHEAR
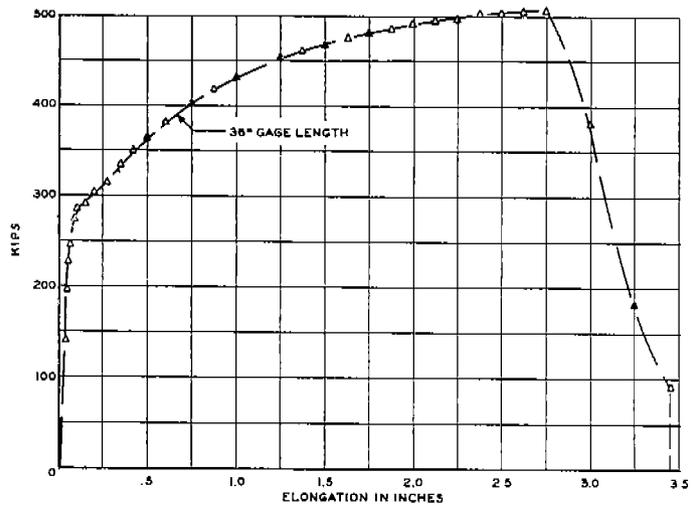
FIG. XXXII-B
LOAD-ELONGATION DIAGRAM
TYPE ZBM SPECIMEN
ABS-B-ZBM-JI6 30°F 90% SHEAR
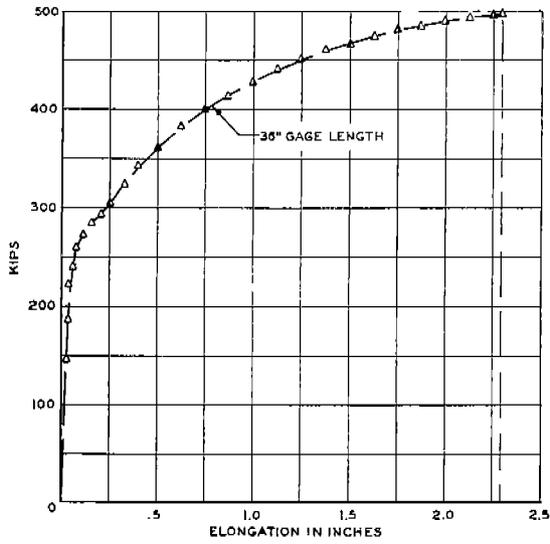
FIG. XXXIII~B
LOAD-ELONGATION DIAGRAM
TYPE ZBM SPECIMEN
ABS-B-ZBM-J13 20°F 0% SHEAR
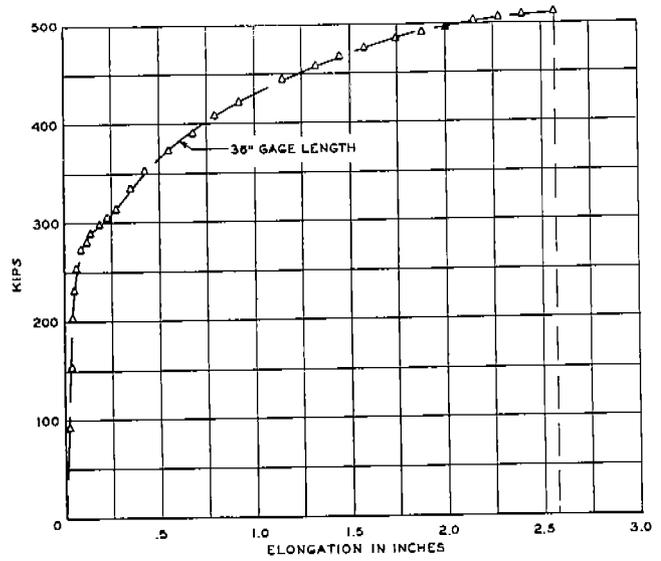
FIG. XXXIV~B
LOAD-ELONGATION DIAGRAM
TYPE ZBM SPECIMEN
ABS-B-ZBM-J7 0°F 0% SHEAR
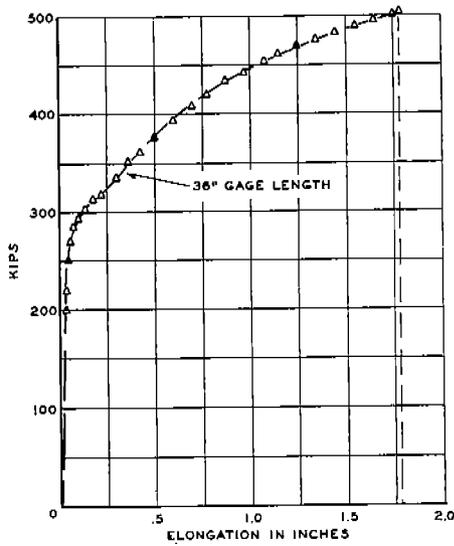
FIG. XXXV-B
LOAD-ELONGATION DIAGRAM
TYPE Z-BM SPECIMEN
ABS-B-ZB-M-J11 -20°F 0% SHEAR
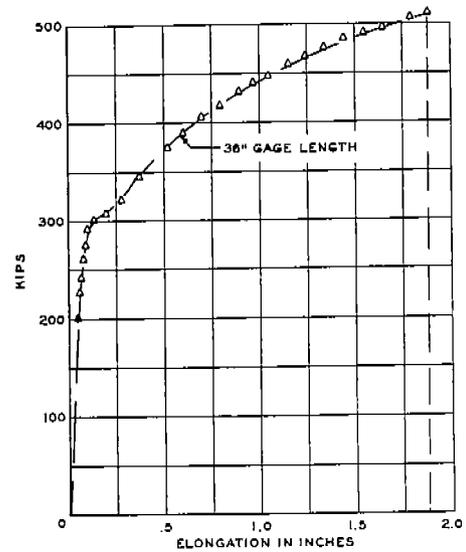
FIG. XXXVI-B
LOAD-ELONGATION DIAGRAM
TYPE ZBM SPECIMEN
ABS-B-ZBM-J18 -40°F 0% SHEAR

SWARTHMORE COLLEGE

SWARTHMORE COLLEGE
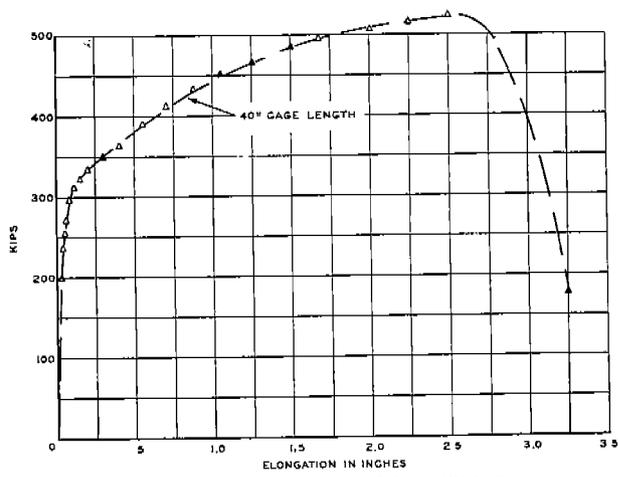
FIG. XXXVII-B
LOAD-ELONGATION DIAGRAM
TYPE ZCI SPECIMEN
DN-ZCI-H7   0°F
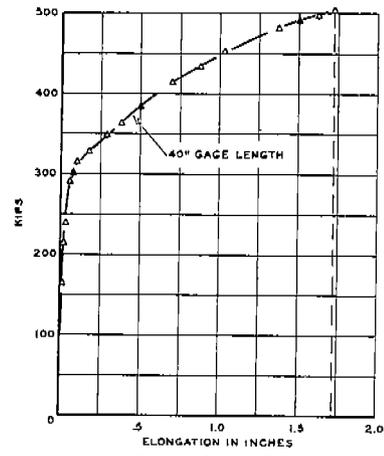
FIG. XXXVIII-B
LOAD-ELONGATION DIAGRAM
TYPE ZCI SPECIMEN
DN-ZCI-HIO -20°F
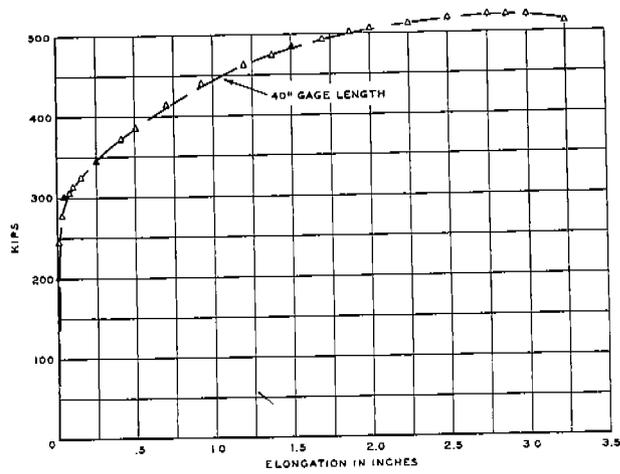
FIG. XXXIX-B
LOAD-ELONGATION DIAGRAM
TYPE ZC2 SPECIMEN
DN-ZC2-H8   0°F
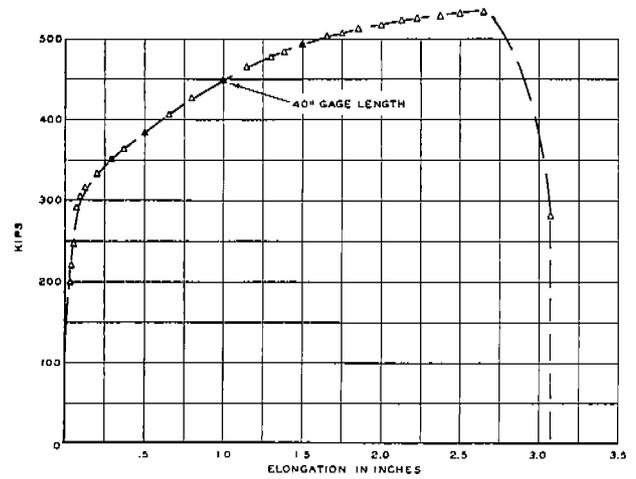
FIG. XL-B
LOAD-ELONGATION DIAGRAM
TYPE ZC2 SPECIMEN
DN-ZC2-HI5 -20°F

SWARTHMORE COLLEGE

SWARTHMORE COLLEGE
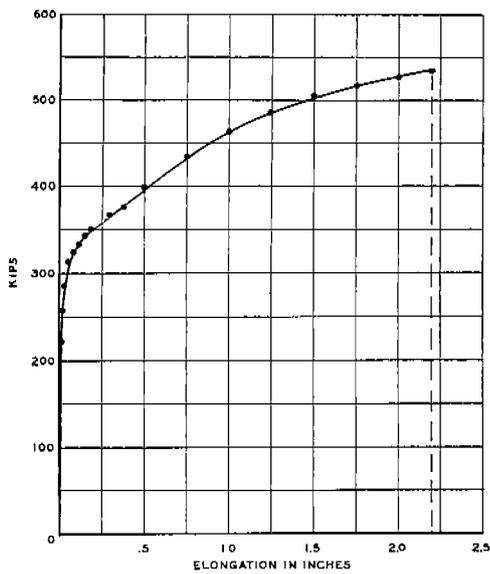
FIG. XLI-B
LOAD-ELONGATION DIAGRAM
TYPE ZC2 SPECIMEN
DN-ZC2-HII -35°F 0% SHEAR
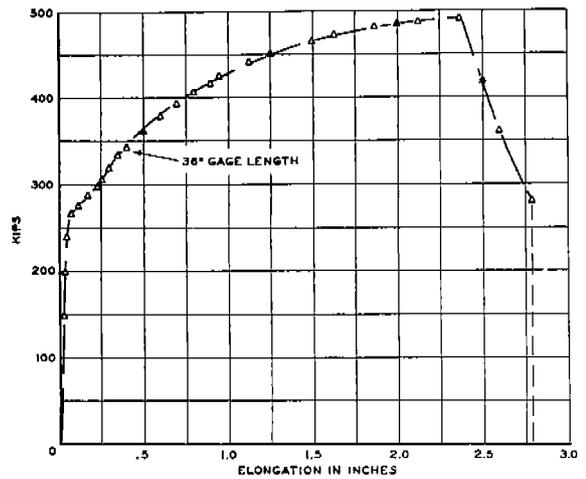
FIG. XLII-B
LOAD-ELONGATION DIAGRAM
TYPE ZC2 SPECIMEN
ABS-B-ZC2-J6 29°F 50% SHEAR
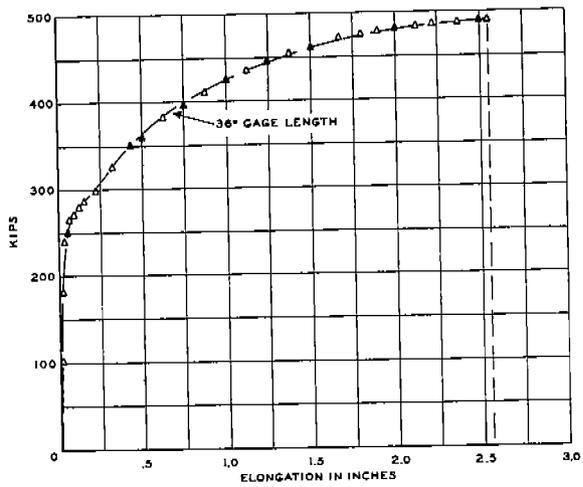
FIG. XLIII-B
LOAD-ELONGATION DIAGRAM
TYPE ZC2 SPECIMEN
ABS-B-ZC2-I14 20°F 0% SHEAR
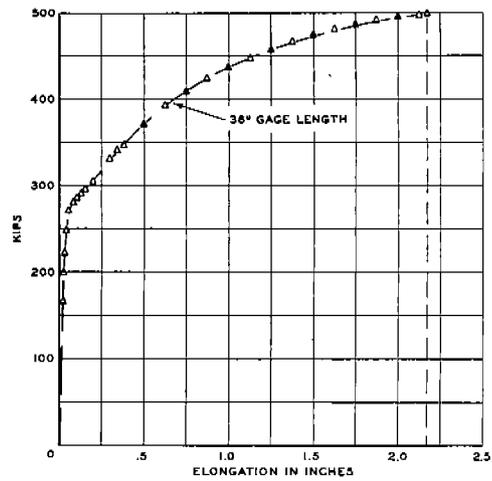
FIG. XLIV-B
LOAD-ELONGATION DIAGRAM
TYPE ZC2 SPECIMEN
ABS-B-ZC2-I15 0°F 0% SHEAR
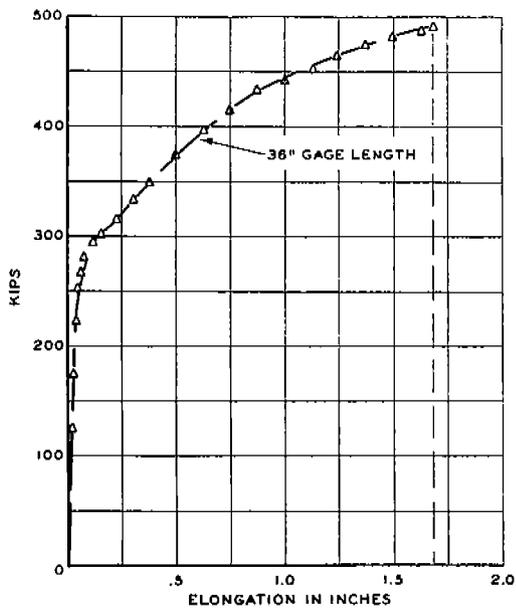
FIG. XLV-B
LOAD-ELONGATION DIAGRAM
TYPE ZC2 SPECIMEN
ABS-B-ZC2-I16 -20°F 0% SHEAR
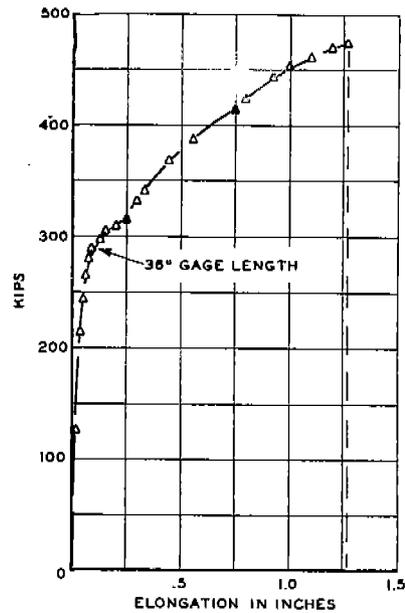
FIG. XLVI-B
LOAD-ELONGATION DIAGRAM
TYPE ZC2 SPECIMEN
ABS-B-ZC2-J5 -40°F 0% SHEAR
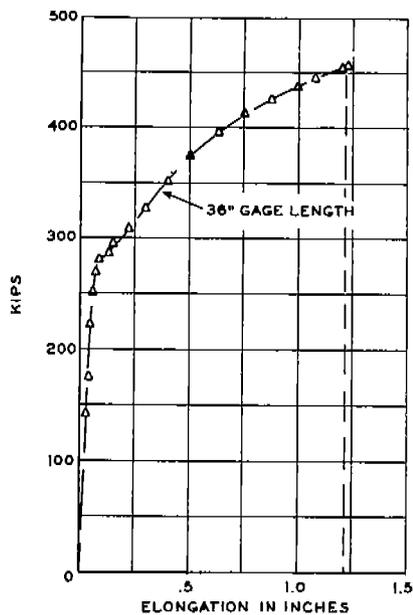
FIG. XLVII-B
LOAD-ELONGATION DIAGRAM
TYPE ZD SPECIMEN
ABS-B-ZD-J10 40°F 0% SHEAR
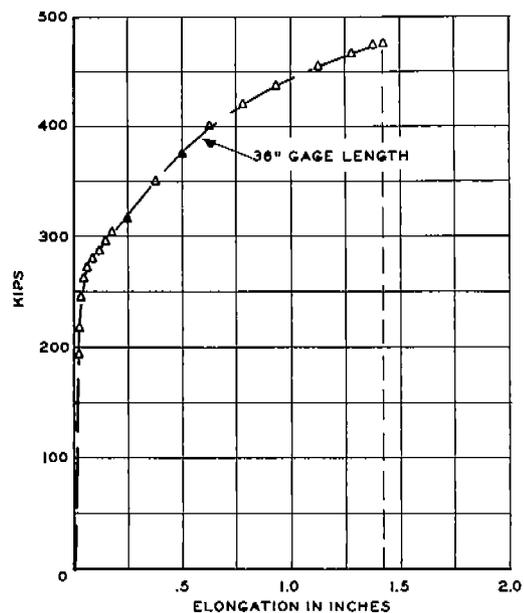
FIG. XLVIII-B
LOAD-ELONGATION DIAGRAM
TYPE ZD SPECIMEN
ABS-B-ZD-I9 20°F 0% SHEAR
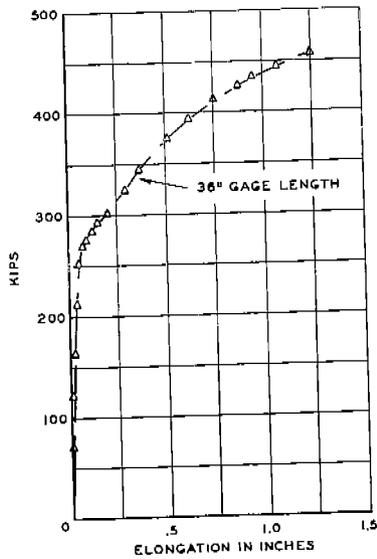
FIG. XLIX - B

LOAD - ELONGATION DIAGRAM
TYPE ZD SPECIMEN
ABS - B - ZD - I8 0°F 0% SHEAR
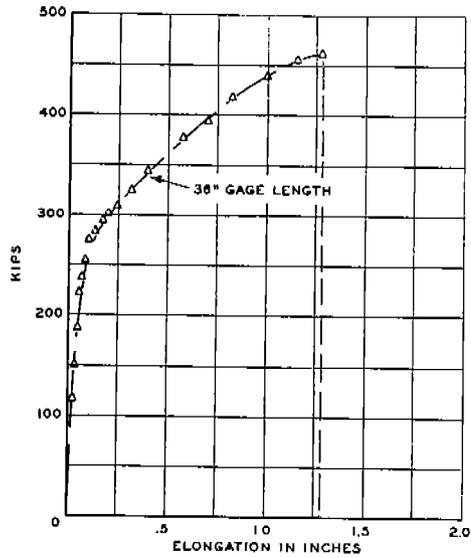
FIG. L - B

LOAD - ELONGATION DIAGRAM
TYPE ZD SPECIMEN
ABS - B - ZD - JI -20°F 0% SHEAR
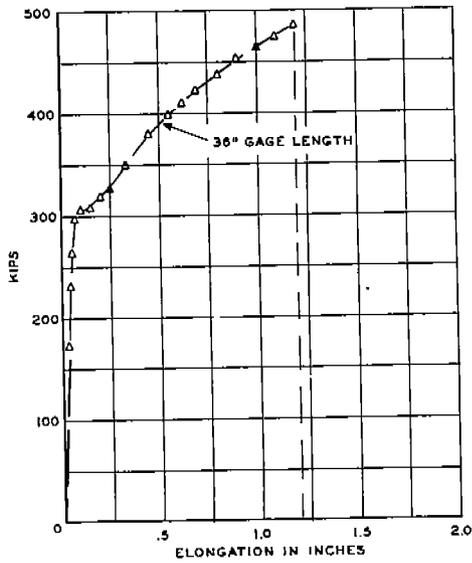
FIG. LI - B

LOAD - ELONGATION DIAGRAM
TYPE ZD SPECIMEN
ABS - B - ZD - J4 -40°F 0% SHEAR
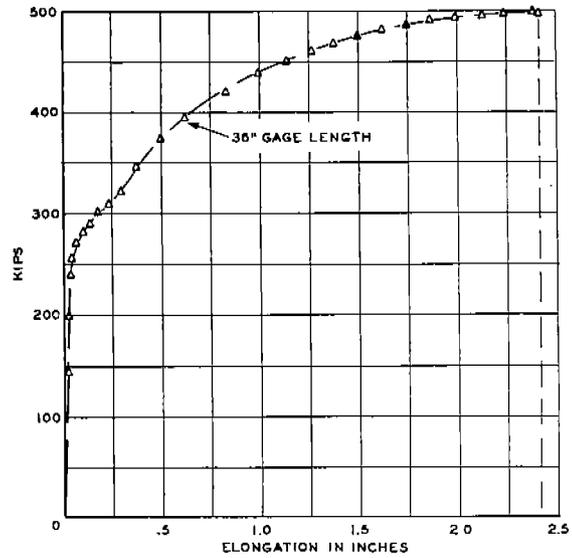
FIG. LII - B

LOAD - ELONGATION DIAGRAM
TYPE ZE SPECIMEN
ABS - B - ZE - J8 30°F 5% SHEAR

SWARTHMORE COLLEGE
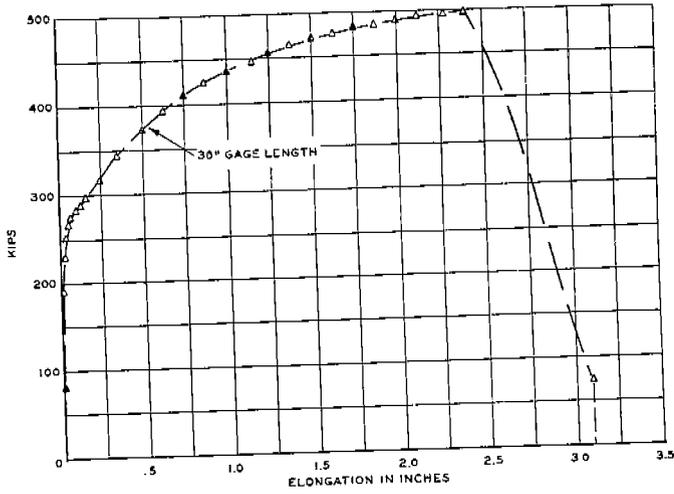
FIG. LIII-B
LOAD-ELONGATION DIAGRAM
TYPE ZE SPECIMEN
ABS-B-ZE-I10 20°F 100% SHEAR
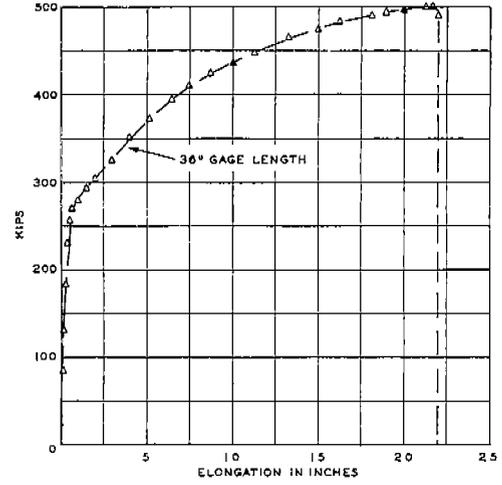
FIG. LIV-B
LOAD ELONGATION DIAGRAM
TYPE ZE SPECIMEN
ABS-B-ZE-I11 0°F 5% SHEAR
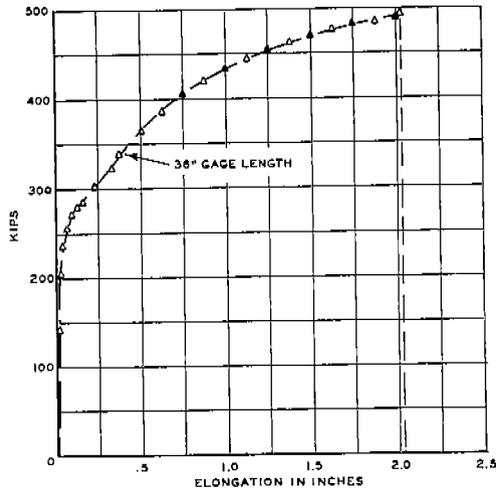
FIG. LV-B
LOAD-ELONGATION DIAGRAM
TYPE ZE SPECIMEN
ABS-B-ZE-I18 0°F 0% SHEAR
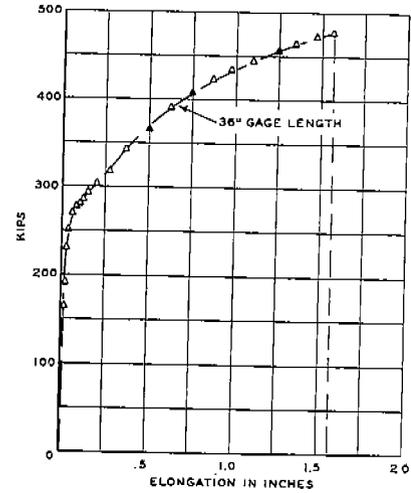
FIG. LVI-B
LOAD-ELONGATION DIAGRAM
TYPE ZE SPECIMEN
ABS-B-ZE-I13 -20°F 0% SHEAR
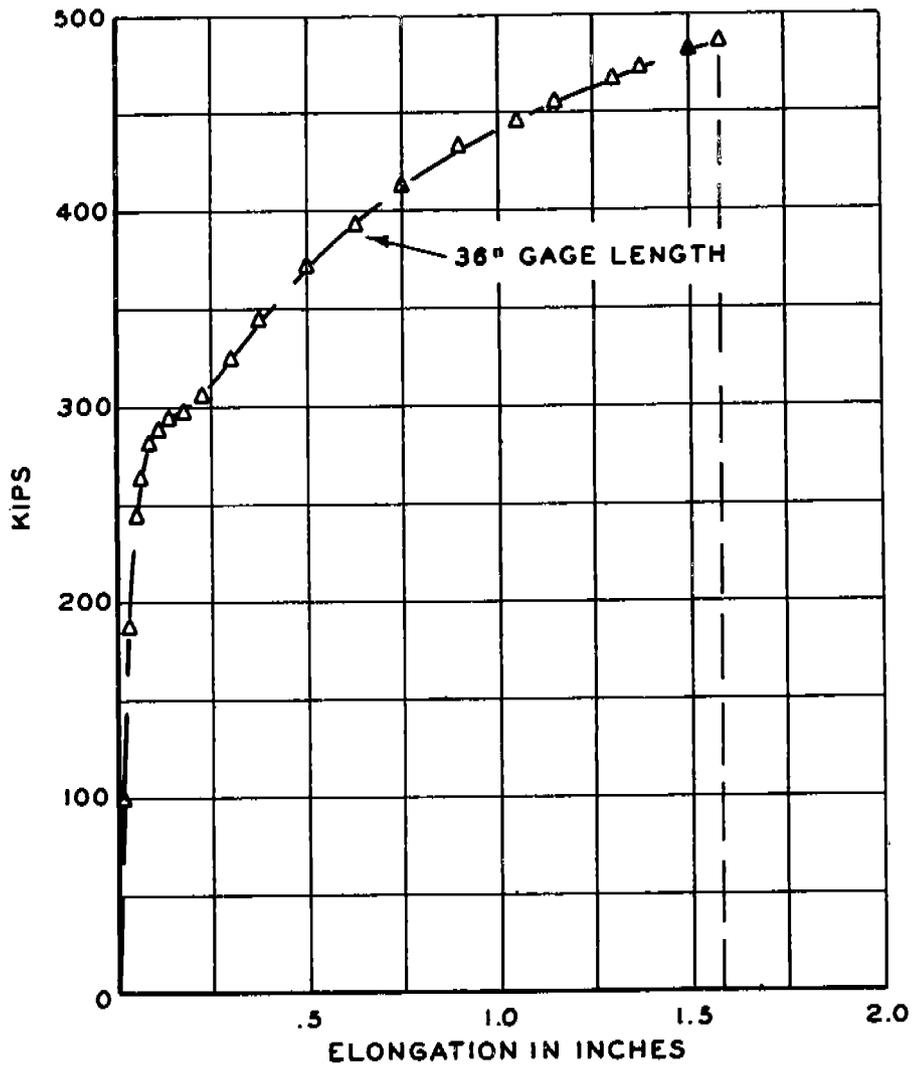
FIG. LVII-B
LOAD-ELONGATION DIAGRAM
TYPE ZE SPECIMEN
ABS-B-ZE-II7 -40°F 0% SHEAR

SWARTHMORE COLLEGE

APPENDIX C

SPECIMENS AND SPECIMEN FABRICATION

The general specimen Types, YW and Z, have been described before and drawings have been presented which show the geometry involved. However, due to the great number of variations in geometry and materials used, Table I classifies the test specimens in a more explicit manner.

Specimens of the YW series were fabricated by flame cutting the main plate, 10 1/2 in. by 40 in. by 3/4 in., and four side plates, 1 1/2 in. by 12 1/2 in. by 3/4 in. Specimens of the YW-1 series were further prepared by flame cutting double bevels on the 10 1/2-in. by 40-in. plate from the end for a distance of 12 1/2 in. along the sides, and flame cutting double bevels on one edge of each of the side plates; while specimens of the YW-2 and YW-3 series had only the side plates beveled. The side plates were then welded to the main plate, and the specimen faired by flame cutting tangent to the main plate. The side plates of specimens of Type YW-3 were cut tangent to the main plate, but a 3/4-in. shoulder remained between the side plate and the main plate. Fig. 1 shows the specimen geometries and fabrication technique.

Specimens of Type Z-3 (See Figs. 2 and 3) were designed to represent a square cut-off of an interrupted longitudinal or stiffener. It was thought that the restraint at the ends of the

flat bars would represent the most severe end conditions possible.
Other specimens of the Z series attempted to relieve the end re-
straint through changing the geometry at the ends of the flat bars.
Type Z-3 specimens were fabricated with four combinations of steel
plates. (Refer to Table I). The first series of Type Z-3 speci-
mens used 3/4-in. thick D_N steel for the main plates and 1/2-in.
thick D_N steel for the flat bars. The main plates were 40 in.
long and 10 1/2 in. wide at the ends of the flat bars. (See Fig 2.)
The second combination tested incorporated 3/4-in. thick ABS-B
steel for the main plates and 1/2-in. thick D_N steel for the flat
bars. The main plates were 36 in. long and were 10 1/2 in. wide
at the ends of the flat bars. (See Fig. 3.) The third combination
used 3/4-in. thick ABS-B steel of the same dimensions as the pre-
ceding variation for the main plates with flat bars of D'_N steel
rather than D_N steel. A single specimen using a "D_N", "D'_N" com-
bination was also made.

Specimens of Type Z-B and Type Z-C2 (See Figs. 4 and 5) were
fabricated using 3/4-in. thick D_N steel for the main plates with
40-in. lengths and 10 1/2-in. widths at the ends of the flat bars,
and a second variation using 3/4-in. thick ABS-B steel for the
main plates with lengths of 36 in. with 10 1/2-in. widths at the
ends of the flat bars. The flat bars were of 1/2-in. thick D_N
steel or D'_N steel.

Specimens of Type Z-C1 (See Fig. 4) were tested using 3/4-in.

thick D_N steel main plates, and 1/2-in. thick D_N steel side plates. The main plates were 40 in. long and 10 1/2 in. wide at the ends of the flat bars.

Specimens of Type Z-D, Z-E, and Z-BM (See Fig. 5) were fabricated with 3/4-in. thick ABS-B main plates 36 in. long with 10 1/2-in. widths at the ends of the flat bars, and 1/2-in. thick D_N steel or D'_N steel for the flat bars.

The Type Z specimens were fabricated by first reinforcing the 1/2-in. thick flat bars with additional 1/2-in. plate. (See Figs. 2 and 3.) The reinforcing plates were welded to the flat bars with a 3/8-in. fillet around the perimeter of the reinforcing plates. The reinforced flat bars were then welded to the 3/4-in. main plate with a 5/16-in. fillet along the edges and around the ends of the flat bars. After this procedure the end modifications for types other than Z-3 were then flame cut and rough ground.

The 3/4-in. main plates were cut from 6-ft. by 10-ft. plates with axis of loading in the direction of rolling. The plate layouts are shown in Figs. 9 to 12, inclusive. The specimens were given designations which identify them with regard to specimen type, and detail, the plate from which the main plate was cut, and the position within the plate.

For example, the specimen designated as "ZC2-I16", means a Type Z specimen with flat bars bearing the C2 ending, where the main plate was cut from position 16 in Plate I.

Those specimens using D'_N steel for the flat bars are

identified by an asterisk in the tables of Appendix A.

In addition to the specimens described above and listed
in Table I, certain specimens were made for an exploratory
program dealing with the Type Z endings. The specimens were
1/2 the scale shown in Fig. 2 and were fabricated using 3/8-in.
thick hot rolled steel plates for the main plates and 1/2-in.
thick hot rolled steel plates for the side bars. One speci-
men was made of each of the end detail variations shown in
Figs. 2, 4, and 5.